5-1-2011

Regulation of spreading depression events in brain slices by astrocyte metabolism

Jessica L. Seidel

Jessica L. Seidel

Candidate

Biomedical Sciences

Department

This dissertation is approved, and is acceptable in quality and form for publication on microfilm:

C. William Shuttleworth, PhD (Chairperson)

Donald Partridge, PhD

Lee Anna Cunningham, PhD

Oscar Bizzozero, PhD

Regulation of Spreading Depression Events in Brain Slices by Astrocyte Metabolism

By

Jessica Louise Seidel

B.S., Biology, University of Arizona, 2005

Ph.D., Biomedical Sciences, University of New Mexico, 2011

Dissertation

Submitted in Partial Fulfillment of the Requirements for the Degree of

Doctor of Philosophy

Biomedical Sciences

The University of New Mexico

Albuquerque, New Mexico

May 2011

Acknowledgements

I would first like to express my extreme gratitude to my mentor, Dr. Bill Shuttleworth for his faith in me and my project. Thank you for the lessons you have taught me, both about science and life. I appreciate the constant encouragement and never ending support you have provided throughout my project.

I would like to thank the faculty and staff of the Neuroscience Department for their continued support and enthusiasm for my project and for fostering an environment that promotes the development of scientific thought, collaboration, and critical thinking from all members of the department. I would like to specifically thank Mandara for here help with my fellowship application, and Buz for technical support throughout my graduate studies.

I am sincerely grateful to the members of my committee on studies: Dr. Donald Partridge, Dr. Lee Anna Cunningham, and Dr. Oscar Bizzozero, for offering valuable insight and continued support throughout this project. I am thankful for the time and effort invested by each of you to help advance my project throughout the course of these studies.

I thank my lab mates, both past and present, for their thoughtful discussions and invaluable input throughout my project. I am extremely grateful for the encouragement and support you have all provided over the years.

I am grateful to Dr. Gilles Bonvento for the opportunity to collaborate with him for my CNTF studies. He served as an invaluable mentor on the intriguing world of astrocyte biology and has provided critical feedback vital for the progress of my studies.

I would also like to convey my deepest appreciation to my family and friends for their continued understanding and unyielding support that has made this possible.

In addition, I would like to specifically thank Dr. G. Bonvento and Dr. M. Faideau for conducting the bilateral lenti-viral injections of both CNTF and LacZ into murine hippocampus at CEA, I2BM, MIRCen, Fontenay-aux-Roses, France. Mice were then shipped to the University of New Mexico for subsequent studies. I am also grateful to Dr. U. Pannasch for her single cell astrocyte recordings in both CNTF and LacZ preparations at INSERM U840, Collège de France, Paris, France (Figures 3.1D-E, 3.2C, and 3.4B). In addition I would like to thank my mentor Dr. C.W. Shuttleworth for making single cell neuronal recordings in both CNTF and LacZ preparations (Figure 3.3C). Lastly, I am grateful to Dr. A. Brennan for her contribution to the set of NO studies which were conducted when she was at the University of New Mexico (Figure 4.1, 4.2, 4.3A-B).

Regulation of Spreading Depression Events in Brain Slices by Astrocyte Metabolism

By

Jessica Louise Seidel

Abstract of Dissertation

Submitted in Partial Fulfillment of the Requirements for the Degree of

Doctor of Philosophy

Biomedical Sciences

The University of New Mexico

Albuquerque, New Mexico

May 2011

Regulation of Spreading Depression Events in Brain Slices by Astrocyte Metabolism

By

Jessica Lousie Seidel

B.S., Biology, University of Arizona, 2005

Ph.D., Biomedical Sciences, University of New Mexico, 2011

Abstract

Spreading depression (SD) is a severe depolarization of both neurons and astrocytes that can propagate throughout CNS tissue. SD has long been associated with migraine, and recent work has strongly suggested that closely related events are likely to be involved in pathophysiological conditions where they provide a large additional metabolic burden to injured tissues. The major goal of this dissertation was to test the overall hypothesis that manipulation of astrocyte metabolic capacity can modify the initiation and propagation of deleterious spreading depression (SD)-like events. If this were the case, then it

may support targeting these cells in a range of pathological conditions where SD-like events are known to occur.

Work in this dissertation utilized acutely prepared hippocampal brain slice preparations from adult mice to study mechanisms regulating SD initiation and propagation. For the majority of studies, slices were prepared from naïve mice to study functions of normal astrocytes. One set of studies utilized preparations in which astrocytes were activated by bilateral lenti-viral injections of ciliary neurotrophic factor (CNTF) into the hippocampus. SD was generated under either normoxic conditions (using localized microinjections of KCl or block of Na^+/K^+-ATPase activity) or in a model of ischemia (using deprivation of oxygen and glucose). Initiation and propagation of SD and related events was monitored using a combination of extracellular voltage recordings and optical imaging methods. Simultaneous recordings of NAD(P)H autofluorescence and evoked excitatory potentials (fEPSPs) were also used to assess changes in mitochondrial redox potential and neuronal viability.

Initial studies sought to determine the contribution of astrocyte metabolism on the initiation and propagation of SD and related events. Previous work had shown that selective inhibition of astrocyte oxidative metabolism increased SD propagation rate, but little was known about roles of astrocyte glycogen. Pharmacologically preventing glycogen availability significantly increased SD propagation rate and increasing astrocyte glycogen stores resulted in either compete block of SD initiation or, in preparations where SD still occurred, a significant decrease in propagation rate (Chapter 2). Other studies confirmed the

effectiveness of inhibition of astrocyte oxidative metabolism, but showed that targeting glycogen stores may prove more efficacious therapeutically.

Previous work has shown that localized astrocyte activation can be achieved *in vivo* by lenti-viral injections of ciliary neurotrophic factor (CNTF) in rat striatum and lead to neuroprotection. My studies sought to establish a similar model of astrocyte activation suitable for subsequent electrophysiological studies in the well-characterized hippocampal slice preparation. I then used this model to assess the effects of astrocyte activation on SD propagation and initiation. CNTF-infection resulted in sustained astrocyte activation and preparations from these tissues showed profound resistance to SD initiation and propagation under both normoxic and ischemic conditions (Chapter 3). This model may be suitable for many studies of astrocyte activation and these results suggest that targeting astrocyte activation may be useful therapeutically to limit SD.

A final set of studies was conducted to test the hypothesis that an additional metabolic burden in the context of SD, even under normoxic conditions, can lead to irrecoverable neuronal damage. Nitric oxide (NO) has been proposed as a possible treatment to reduce the number of SD-like events following subarachnoid hemorrhage. My studies investigated the effects of manipulation of NO concentrations on the progression and consequences of SD under normoxic conditions. Exogenous NO led to inhibition of mitochondrial respiration, which has been well described previously, and converted recoverable SD events into irreversible depolarizations leading to neuronal damage. These

studies suggest that if NO is to be used therapeutically to limit SD, care must be taken to ensure concentrations do not inhibit oxidative metabolism (Chapter 4).

Overall the studies in this dissertation suggest that strategies which target the maintenance of brain metabolism and normal astrocyte function, including the clearance of extracellular glutamate and K^+, may reduce the incidence of SD and may also limit neuronal injury in pathologic conditions where SD-like events still occur. This work may provide a useful starting point for future studies to determine specific therapeutic interventions including in tissue where astrocyte phenotype may be modified by pathologic processes.

Table of Contents

List of Figures

1. Introduction

1.1 Spreading Depression

1.1.1 The phenomenon of spreading depression

Spreading depression (SD) was first described in 1944 by Aristides Leao in a series of studies originally intended to observe electrical cortical activity occurring during experimental epilepsy. Electrocorticogram (EcOG) responses were recorded from the exposed rabbit cortical surface using a series of differential electrodes. He found that following brief, repetitive electrical stimulation to a region of the cortex, there was a complete abolition of spontaneous electrical activity, which spread slowly in all directions, and involved the whole cortex within 3-6 minutes (Leao, 1944). These events were completely reversible and recovery generally began 5-10 minutes after the depression was initiated, beginning at the point of stimulation (Leao, 1944). In later studies, Leao used direct current (DC)-coupled amplification to record a slow negative voltage shift, which accompanies the depression of spontaneous activity (Leao, 1947). These propagating extracellular voltage changes triggered by SD were large (maximum of 8-15mV). Similar events were also generated by global forebrain ischemia (Leao, 1947). Some key findings from these initial studies were that SD not only affected spontaneous cortical activity, but also inhibited responses to touch, electrical stimulation, and illumination of the retina (Leao, 1944). Importantly, while the mechanisms underlying the spread were initially unclear, Leao suggested that it was likely neuronal and that related events may also be involved in ischemic injury (Leao, 1947).

Figure 1.1

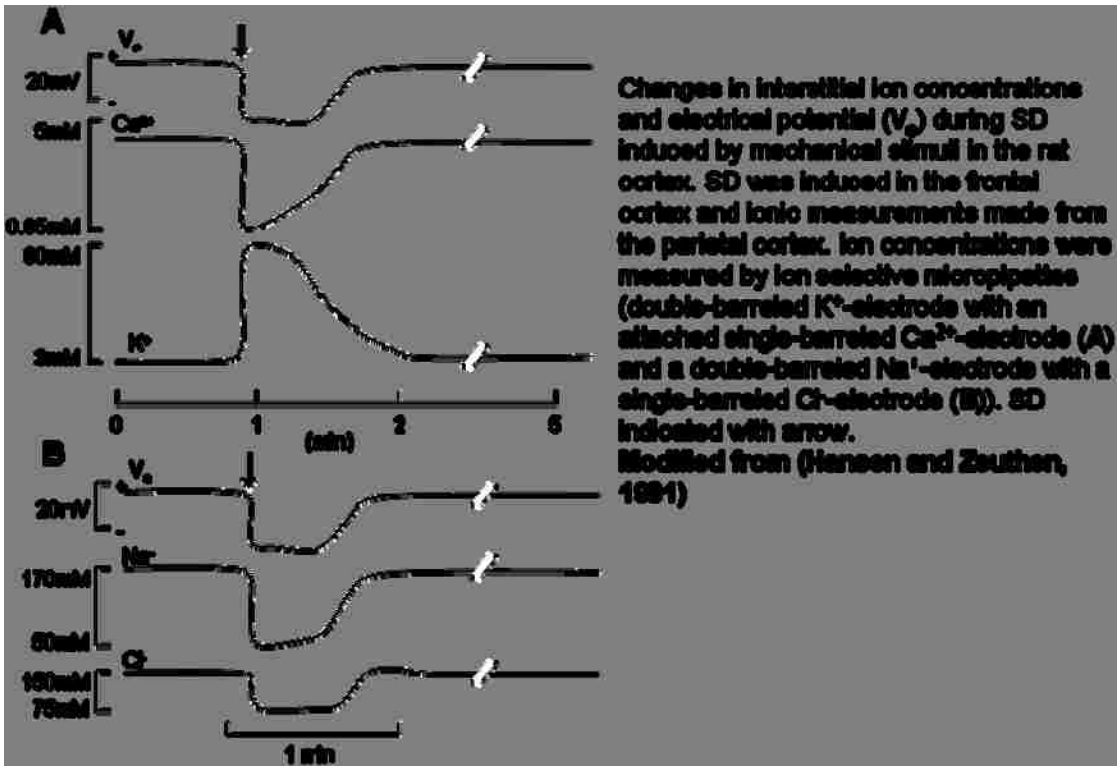

Changes in interstitial ion concentrations and electrical potential (V_e) during SD induced by mechanical stimuli in the rat cortex. SD was induced in the frontal cortex and ionic measurements made from the parietal cortex. Ion concentrations were measured by ion selective micropipettes (double-barreled K^+-electrode with an attached single-barreled Ca^{2+}-electrode (A) and a double-barreled Na^+-electrode with a single-barreled Cl^--electrode (B)). SD indicated with arrow. Modified from (Hansen and Zeuthen, 1981)

The ionic shifts underlying DC potential changes during SD have been extensively characterized using ion-selective microelectrodes and include a very large and rapid increase in extracellular K^+, from normal levels of ~3mM up to 50-60mM (Vyskocil et al., 1972; Mares et al., 1976). It is well established that SD is initiated once $[K^+]_e$ reaches 10-12mM (Vyskocil et al., 1972; Hansen and Zeuthen, 1981; Muller and Somjen, 2000), and the subsequent rapid increase in extracellular K^+ is accompanied by decreases in extracellular Ca^{2+} (from 1.3 to 0.07mM), Na^+ (from 155 to 60mM), and Cl^- (from 130 to 74mM) (Hansen and Zeuthen, 1981) (Figure 1.1) as ions move intracellularly.

1.1.2 Methods for studying SD

1.1.2.1 Induction of SD and related events

Inducing SD *in vivo*

In his initial studies, Leao used a variety of methods to trigger SD in rabbit cortex, and showed not only that high frequency electrical stimulation was effective, but that SD events could be induced with mechanical stimulation, by touching a blunt rod to the cortical surface. Although initial studies were done in rabbit, SD could also be induced in other species as well, including pigeon and cats (Leao, 1944). Since that initial report, many other investigators have used a wide range of stimuli to induce spreading depression-like events including mechanical stimulation such as pressure or puncture, low osmolarity challenges, and a variety of stimulant chemicals (Roitbak and Bobrov, 1975; Lauritzen et al., 1988; Chebabo et al., 1995; Balestrino et al., 1999). Many of these methods are also used to induce seizure discharge, and it is still unclear why one phenomenon may appear instead of the other. A commonly used method today for inducing SD has become the elevation of extracellular K^+ concentrations by either microdialysis, localized microinjections or topical application of KCl (Nedergaard and Hansen, 1988; Herreras et al., 1994; Busch et al., 1996; Takano et al., 2007).

As noted above, events similar to SD have also been shown to occur during global ischemia (Leao, 1947), and many subsequent studies have characterized SD-like events with focal and global ischemia in rodent and non-human primate models (Mies et al., 1993; Nedergaard and Hansen, 1993;

Hossmann, 1996; Strong et al., 1996). These events will be discussed further below (Section 1.3.3).

Studies of SD *in vitro*

The mechanisms underlying SD and related events triggered by ischemia have been studied in detail using cortical and hippocampal brain slice preparations. Using these preparations, stimuli, which induce SD under normoxic conditions (usually using K^+), do not result in observable damage to cells and repetitive SDs may be induced. However, SD-like events induced in *in vitro* ischemia models are irrecoverable and result in neuronal damage if metabolic substrates are not supplied immediately following the depolarization (discussed below, Section 5.4). For the purposes of this dissertation, SD events generated in brain slice by microinjections of K^+, which are recoverable and are induced under normoxic conditions, will be termed "high K^+-SD." Propagating SD-like waves induced to model responses in ischemic conditions can be generated by metabolic substrate removal (oxygen and glucose deprivation; OGD) or pharmacological block of Na^+/K^+-ATPase activity (ouabain). These events will be termed "OGD-SD" and "ouabain-SD," respectively.

1.1.2.2 Recording SD (electrically and optically)

A common method used for recording SD is through the amplification of extracellular direct current (DC) potential changes (Leao, 1947; Herreras and Somjen, 1993). Intracellular recordings have repeatedly shown that, at the onset of SD, neuronal membrane potential transiently approaches zero, and is followed

by a longer-lasting plateau or slowly declining phase (Collewijn and Harreveld, 1966; Czeh et al., 1993; Muller and Somjen, 2000). Because single electrode recordings lack spatiotemporal information, SD propagation rate may be monitored by using electrodes placed at several sites along the exposed cortical surface or brain slice (Leao, 1944; Largo et al., 1997b; Hashimoto et al., 2000). However, imaging is a powerful adjunct method and many *in vivo* studies have utilized techniques associated either with changes in cell volume, tissue autofluorescence, or blood flow to visualize the spread across the brain surface. For example, laser speckle flowmetry (LSF) has recently been applied to *in vivo* studies as a semiquantitative measure of real-time changes in cerebral blood flow associated with SD under both normoxic and ischemic conditions (Dunn et al., 2001; Ayata et al., 2004; Shin et al., 2006; Strong et al., 2007). The studies in this dissertation exploit brain slice preparations to study SD mechanisms regulated by neurons and astrocytes without the additional complexity of blood flow changes. Therefore, the discussion below concentrates on imaging methods applicable for *in vitro* brain slice alone.

A widely used method of imaging used in *in vitro* slice preparations has been recording intrinsic optical signals (IOS). IOS signals are due to changes in light absorption or scattering (by either reflection of refraction) in living tissue, and changes during SD are due mainly to changes in cell volume (Andrew et al., 1999). It is assumed that both neurons and astrocytes contribute to these signals, and IOS imaging has been utilized in brain slice studies where SD was induced by either increasing extracellular K^+ or with models of ischemia (OGD

and ouabain) (Basarsky et al., 1998; Obeidat and Andrew, 1998; Obeidat et al., 2000; Anderson and Andrew, 2002). Cellular swelling leads to increases in light transmittance (LT) while decreased LT may be due to either cell shrinkage or, in the context of injury, decreases in LT may be due to dendritic beading, which will lead to an increase in light scattering (Andrew et al., 1999).

Autofluorescence imaging of NADH has been used to monitor the propagation of SD in both *in vivo* (Strong et al., 1996; Hashimoto et al., 2000; Strong et al., 2000) and *in vitro* slice preparations (Foster et al., 2005; Galeffi et al., 2010). This approach has an important advantage over IOS signals because it provides a measure of mitochondrial redox potential. This is based on the fact that the reduced form NADH fluoresces at 460nm when excited at 360nm (UV range), but the oxidized form (NAD^+) is non-fluorescent. It is assumed that autofluorescence excited at 360nm is due primarily to mitochondrial NADH dynamics and that cytosolic accumulation of NADH is negligible (Chance and Baltscheffsky, 1958; Chance et al., 1962; Blinova et al., 2008). Therefore, changes in autofluorescence can indirectly assess regional oxygen consumption (Takano et al., 2007; Galeffi et al., 2010) in addition to providing visual confirmation of an SD event. During SD induced by topical KCl application (high K^+-SD), bulk NADH changes had a biphasic waveform (Hashimoto et al., 2000; Takano et al., 2007). *In vivo* NADH transients due to SD are more complex in the ischemic brain, due to effects of ischemia on mitochondria alone (Strong et al., 1996; Strong et al., 2000). Under both ischemic and normoxic conditions, autofluorescence signals are likely to be contaminated by some cellular swelling,

and blood flow changes (see Section 5.3). It is currently unknown how significantly cellular swelling may affect NADH autofluorescence measurements in brain slice, and how well these signals can be used to deduce changes in metabolic status. Simultaneous measurements with flavoprotein autofluorescence, which should mirror NADH signals if they are indeed mitochondrial (Shuttleworth, 2010), could help address this issue, and may provide important information about the metabolic competence of tissues following either high K^+ or OGD-SD.

1.1.3 SD initiation and propagation

It is well established that elevations in extracellular K^+ and/or glutamate are key factors responsible for the initiation and propagation of SD. The role of K^+ was first proposed by Bernice Grafstein (1956), who suggested that K^+ released by neurons during intense firing accumulates extracellularly, which, in turn, results in the complete depolarization of these neurons and then adjacent cells; initiating a feed-forward cycle of depolarization (Grafstein, 1956). This hypothesis was based in part on findings that there was a brief period of intense single unit activity prior to the negative DC shift indicative of SD, which may liberate intracellular K^+, and that if this intense spontaneous activity could be inhibited, SD could be prevented (Grafstein, 1956). Since those initial experiments, many studies have verified extracellular K^+ ($[K^+]_e$) elevations associated with the spread of SD, and there is remarkable consistency in threshold concentrations (10-12mM) required for SD initiation and propagation recorded in different laboratories (Vyskocil et al., 1972; Hansen and Zeuthen, 1981; Muller and

Somjen, 2000). Therefore, factors that regulate $[K^+]_e$ are likely to be critical for SD initiation and propagation.

An important role for glutamate was first proposed in 1959 by Anthonie Van Harreveld (Van Harreveld, 1959). In his initial studies, the effects of cortical extracts on crustacean muscle contraction were used to investigate factors underlying SD initiation. The active compound was found to be heat resistant, not oxidized by exposure to air at room temperature for >24hrs, not destroyed by bringing pH to 3 or 12, and was completely absorbed by ion exchange resins (Van Harreveld, 1959). These findings suggested that the compound was likely an amino acid, and indeed, when applied to the rabbit cortex, L-glutamic acid could trigger SD (Van Harreveld, 1959). Many studies have since shown that extracellular glutamate levels increase during SD due to release from both neurons and glia (Szatkowski et al., 1990; Szerb, 1991; Iijima et al., 1992; Fabricius et al., 1993; Davies et al., 1995). Inhibition of NMDA receptors with selective antagonists, such as AP-5 and MK-801, has been shown to block high K^+-SD both *in vivo* and *in vitro* slice preparations (Lauritzen and Hansen, 1992; Busch et al., 1996; Anderson and Andrew, 2002), but it is less effective at blocking SD in the context of ischemia (Lauritzen and Hansen, 1992). However, more recent work has shown that the use of NMDA receptor antagonists, during long-term recordings following focal ischemia *in vivo*, reduced the number of SD-like events (Hartings et al., 2003).

Taken together, these data suggest that glutamate and K^+ are likely to contribute to the spread of SD-like events in both physiological and

pathophysiological conditions. Since astrocytes are major regulators of these two mediators, one goal of the dissertation is to consider the roles of astrocytes in limiting the initiation and progression SD.

1.2 Spreading Depression and Migraine

1.2.1 Medical Impact

Migraine, a primary headache disorder, is a common, recurrent and extremely disabling phenomenon, which affects nearly 30 million people in the United States (Lipton et al., 2001; Steiner, 2005; Ramadan and Olesen, 2006). Migraine is ranked in the top 20 causes of disability worldwide by the World Health Organization and it can be extremely costly; with direct costs ranging from $200-800 per migraine patient and far greater indirect costs ($4,000-5,000) due to patients' inabilities to carry out normal day-to-day functions (Fishman and Black, 1999; Organization, 2001). The most prominent theory for the primary underlying cause of migraine has been inappropriate dilation of cranial vessels; making vasoconstriction the most obvious treatment (Goadsby, 1999). However, recent work suggests that the trigeminal system (TS) is involved; raising the important possibility that migraine is primarily a neuronal disease (Moskowitz, 2008; Tajti et al., 2010).

1.2.2 SD and migraine

The symptoms most frequently reported by migraine patients are pulsatile pain, light and sound sensitivity, nausea, blurred vision or aura, unilateral pain and vomiting (Lipton et al., 2001). Prior to the onset of migraine, one-fifth of

patients suffer from transient neurological symptoms, which are commonly known as aura (Tajti et al., 2010). While migraine auras are generally visual, they may also be manifested as other sensory alterations, including motor and speech deficits (Kelman, 2004). In 1941, Karl Lashley first described the occipital cortex as the origin of a migrating visual aura (Lashly, 1941), and in 1945, Aristides Leao observed a similar rate of spread between his cortical spreading depression measurements and Lashley's aura (Leao and Morrison, 1945). It is generally accepted today that SD is an underlying phenomenon of migraine aura (Milner, 1958; Lauritzen, 1985; Ayata, 2010).

There can be a genetic component to migraine susceptibility, and there are a wide range of identified mutations in familial hemiplegic migraine (FHM) accounting for an increased susceptibility to headaches, particularly those associated with aura (Ophoff et al., 1996; De Fusco et al., 2003; Moskowitz et al., 2004; Vanmolkot et al., 2006). FHM-1 is caused by a mutation in the α1 subunit of the presynaptic P/Q voltage-gated Ca^{2+} channels (VGCCs) that result in changes in glutamate release (Ophoff et al., 1996). FHM-2 results from a mutation on the α2 subunit of the Na^{+}/K^{+}-ATPase and may lead to impaired extracellular glutamate and K^{+} clearance (De Fusco et al., 2003). Lastly, FHM-3 is associated with a missense mutation of the voltage-gated Na^{+} channels that will disrupt the inactivation of excitatory synapses (Dichgans et al., 2005). Excitingly, some FHM mutations have been expressed in transgenic mice, and lead to significant increases in SD susceptibility (van den Maagdenberg et al., 2004; Eikermann-Haerter et al., 2009). Furthermore, SD is also generally

associated with a rapid increase in blood flow (hyperemia) followed by a persistent mild reduction in blood supply (oligemia) (Ayata, 2010). Consistent with a role for SD in migraine, these changes in blood flow that are associated with SD can appear similar to those observed during migraine attacks (Hadjikhani et al., 2001). Together, these studies provide several lines of evidence to support for the hypothesis that SD underlies migraine aura, and for the idea that SD may in fact trigger the onset of migraine headaches (Ayata, 2010).

1.2.3 Current therapeutic strategies

Drug development for the treatment of migraine has proved much more promising that for other pain disorders, and has focused on both acute treatment as well as long-term preventative care. One of the most widely used acute treatments is sumatriptan, a 5-HT receptor agonist, which leads to vasoconstriction and reduces inflammation in the dura matter (Buzzi and Moskowitz, 1990; Goadsby, 1999). Selectivity for 5-$HT_{1B/1D}$ receptors appears to underlie the selectivity of sumatriptan and related drugs for cranial circulation, but the potential deleterious vasoconstrictive side effects on coronary circulation makes the discovery of new therapeutics important (MaassenVanDenBrink et al., 1998). In addition, the relatively short half life (2 hours) of sumatriptan may explain the large percentage of patients who suffer headache recurrence (Fowler et al., 1991; Goadsby, 1999), and sumatriptan is not effective in the treatment of migraine aura (Bates et al., 1994).

For patients who suffer several migraine attacks a month, chronic prophylactic treatment is recommended in an attempt to reduce the frequency and intensity of the headaches, and while this strategy has proved to be moderately effective, new treatments are still required (Ayata et al., 2006). There is a growing body of evidence suggesting SD as a promising target for migraine treatment. Many drugs already utilized for migraine treatment, but with no obvious common mechanism underlying their protective effects, have all been shown to reduce SD events in a dose-dependent manner when administered chronically (Ayata et al., 2006). While these drugs effectively reduce SD incidence, the mechanism(s) underlying this effect are not well understood and finding more selective ways of targeting SD-like events associated with migraine are required.

SD in the context of migraine aura is believed to occur under normoxic conditions, and therefore, the mechanisms underlying these events may be studied using high K^+ to induce the depolarization. Previous work has concentrated on modifying neuronal excitability to treat these disorders, but targeting other cell types may also be useful. Astrocytes may play an important role in preventing the initiation or propagation of SD by clearing extracellular K^+ and/or glutamate. In addition, repetitive SDs are known to induce astrocyte activation (Kraig et al., 1991), which may occur in chronic migraine patients who suffer from recurrent headaches. However, it is currently unknown what functional role these phenotypic changes induced by SD might have.

1.3 Spreading Depression and Stroke Injury

1.3.1 Medical Impact

Stroke is generally defined as events that follow a sudden loss of blood flow to the brain as a result of vascular hemorrhage or occlusion. Each year in the United States, about 795,000 people suffer from a new or recurrent stroke (Lloyd-Jones et al., 2010). In addition, stroke is the third leading cause of death, and it is also recognized as the leading cause of severe, long-term disability (Rosamond et al., 2007; 2009). As many as 30% of all stroke survivors are permanently disabled and 20% of these patients still require institutional care months after the initial insult (Lloyd-Jones et al., 2010). Thus, the average lifetime cost for an individual having suffered an ischemic stroke is $140,048, which includes inpatient care and subsequent rehabilitation necessary for any lasting deficits. When considered with the prevalence in our population, different forms of stroke lead to annual national cost of ~63 billion dollars (Rosamond et al., 2007).

1.3.2 Current therapeutic strategies

Ischemic strokes, due to transient or permanent obstruction of blood supply, are most frequent (~87% of all stroke cases), while intracerebral and subarachnoid hemorrhage strokes account for the remainder (2006; Rosamond et al., 2007; Lloyd-Jones et al., 2010). Thrombolysis became the primary clinical treatment for acute ischemic stroke when tissue plasminogen activator (tPA) was approved by the US Food and Drug Administration in 1996, and over a decade later, it remains the sole pharmacologically approved treatment for ischemic

stroke (Lee et al., 1999; Goldstein, 2007). While in theory tPA could be used as a therapeutic agent for the majority of ischemic stroke cases, due to safety concerns, it is only used rarely in clinical settings. tPA significantly increases the risk of hemorrhage, and can only be used within a short time window (<3 hours) after stroke onset (Alberts, 1998; Alberts et al., 2000), and most patients do not receive intravenous tPA treatment due to arrival to the hospital beyond the approved treatment window (Katzan et al., 2004). An alternative to tPA would be neuroprotective therapies, which aim to preserve brain tissue by reducing the intrinsic vulnerability to ischemia until blood flow returns to the region (Lee et al., 1999; Goldstein, 2007). Such therapies would have the benefit of being potentially useful for both ischemic and hemorrhagic strokes and may have potentially larger windows of time for intervention. The majority of such approaches have focused on limiting the excitotoxic effects of glutamate and calcium overload (O'Collins et al., 2006). However, despite an ever-growing number of clinical trials for neuroprotective agents, which reduce neuronal damage in animal models, none has proved effective in human studies (Dirnagl et al., 1999; O'Collins et al., 2006). This is likely due to a number of unwanted side-effects, which alter normal physiology, including respiratory depression and cardiovascular dysregulation, and may become equally detrimental to patients as the initial stroke injury itself (Dirnagl et al., 1999). Exciting new work suggests that focusing on events similar to SD, which propagate from the infarct core, may be more useful than traditional targets of excitotoxicity mechanism (Hossmann, 1996; Lauritzen et al., 2011) (see below).

As mentioned above, hemorrhagic strokes may be intracerebral (blood accumulates within brain tissue) or subarachnoid (blood accumulates between the skull and brain). Subarachnoid hemorrhages (SAH) make up ~3% of all strokes cases, and the majority arise due to the rupture of a saccular aneurysm, which has developed over the patient's lifespan at the base of the brain (van Gijn and Rinkel, 2001). Patient outcome is generally determined by the initial damage induced by the hemorrhage itself in addition to the commonly occurring complication known as delayed ischemic neurologic deficit (DIND). DIND features narrowing of large cerebral blood vessels known as radiological vasospasm and occurs in 20-40% of patients with a delayed peak onset roughly 7 days after the initial injury (Al-Tamimi et al., 2010; Lauritzen et al., 2011). Vasospasm was initially defined in patients by Arthur Ecker and Paul Riemenschneider in 1951, and although vasospasm appears to be a marker of poor outcome following SAH, there is increasing controversy over whether this phenomenon is correlative rather than causative of DIND (Ecker and Riemenschneider, 1951; Stornelli and French, 1964; Al-Tamimi et al., 2010). As with ischemic stroke injuries, there is currently a lack of effective treatment for DIND following SAH, but (as discussed below) the occurrence of SD-like events following these injuries have been recorded and may be a very useful target for reducing the expansion of SAH injury .

1.3.3 SD and stroke injury

1.3.3.1 Time course of anoxic depolarizations and repetitive SD

During an ischemic stroke, local restriction of blood supply results in the rapid depletion of energy substrates, primarily oxygen and glucose, which are required for the maintenance of ionic and glutamate homeostasis (Martin et al., 1994). This leads to loss of membrane potential and depolarization of both neurons and glia within the region a phenomenon termed “anoxic depolarization” (Somjen, 2001). If there is no vascular re-supply in a region subjected to anoxic depolarization, no substrates are available for repolarization, and little can be done to prevent the rapid necrotic cell death that follows and establishes the infarct core.

The primary mechanism underlying ischemic injury occurring in conjunction with anoxic depolarization was thought to be the excitotoxic accumulation of extracellular glutamate, which is released when neurons depolarize and remains elevated since the energy-dependent process of glutamate clearance by glia is compromised (Dirnagl et al., 1999). In this schema, the mechanisms underlying neuronal damage change over time, but excessive extracellular glutamate leading to neuronal depolarization and intracellular Ca^{2+} overload is likely to initiate the cascade of pathological conditions that follow (Figure 1.2). Increases in intracellular Ca^{2+} then were proposed to lead to the activation of a wide range of signaling molecules that led to the production of free radicals and nitric oxide, which may ultimately contribute to inflammation and glial activation as well as induction of DNA and mitochondrial

damage leading to apoptosis (Dirnagl et al., 1999; Lee et al., 1999; Lipton, 1999). As noted above, efforts have been made to target some of these downstream signaling pathways, but they have not yet led to new viable therapeutic interventions suggesting that excitotoxicity may not be the best target.

Figure 1.2

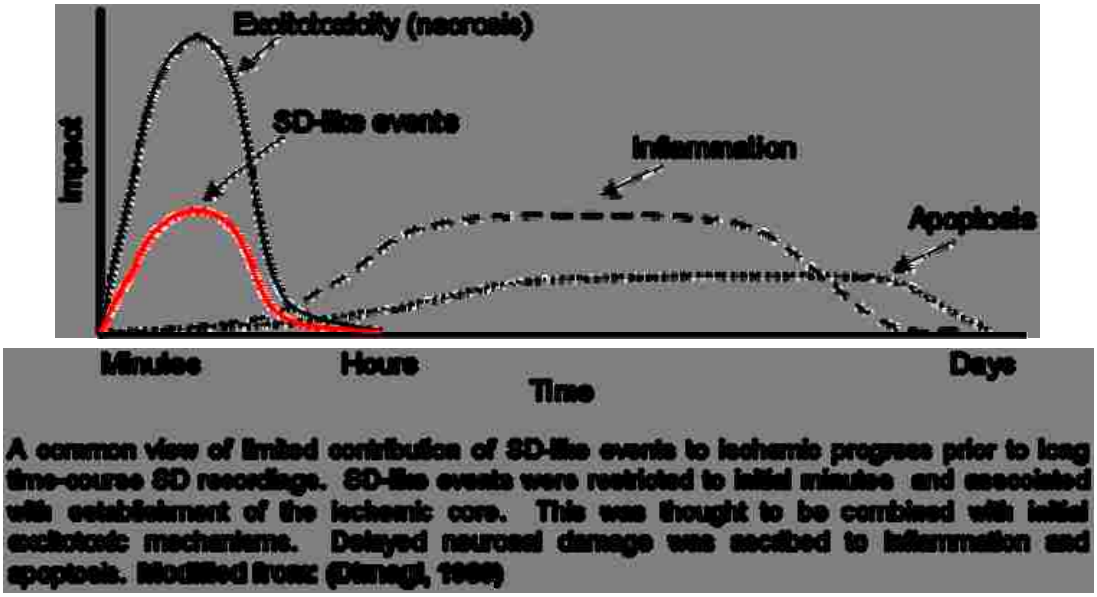

A common view of limited contribution of SD-like events to ischemic progress prior to long time-course SD recordings. SD-like events were restricted to initial minutes and associated with establishment of the ischemic core. This was thought to be combined with initial excitotoxic mechanisms. Delayed neuronal damage was ascribed to inflammation and apoptosis. Modified from: (Dirnagl, 1999)

An important shift in understanding of the progression of stroke injury has come from the realization that excitotoxicity alone may not be a primary contributor to progression of injury. It is recognized that the initial anoxic depolarization described above spreads across the brain surface in much the same way as the phenomenon of SD. Transient increases in extracellular K^+, indicative of SD-like events, have been described following middle cerebral artery occlusion (MCAO) in both the cat and baboon cortex (Branston et al., 1977; Strong et al., 1983). Subsequent work observed repetitive waves of severe depolarization that originate at the edge of infracted regions following *in vivo*

ischemia that spread outwards and these events propagated at a rate of approximately 3mm/min (Nedergaard and Astrup, 1986). As a result, SDs, which occur under the context of ischemia and originate from the ischemic core, have been termed peri-infarct depolarizations (PIDs) (Hossmann, 1996).

PIDs have been studied in a wide range of species including rodent, cat, and non-human primate (Iijima et al., 1992; Strong et al., 2000; Hartings et al., 2003). There is evidence supporting a correlation between the number of PIDs and final infarct volume in *in vivo* MCAO studies (Iijima et al., 1992; Mies et al., 1993; Mies et al., 1994). Glutamate receptor antagonists (MK-801 or NBQX) reduced the number of PIDs and infarct volume, suggesting that these depolarizing events contribute to the expansion of injury in acute studies (Iijima et al., 1992; Mies et al., 1994; Busch et al., 1996). Furthermore, early studies suggested that hypothermia was protective against PIDs and also reduced infarct volume following transient MCAO (Chen et al., 1993). However, historically, there had been little enthusiasm for trying to prevent these depolarizations clinically since they were initially thought to occur only at the very onset of stroke and their relevance in human stroke patients was unknown (Figure 1.2).

In early studies with continuously anesthized animals, the incidence of PIDs may have been significantly underestimated. Inhalational anesthetic drugs, particularly halothane, have been shown to be neuroprotective, slow brain metabolism, and reduce SD frequency (Saito et al., 1997; Kitahara et al., 2001). A recent study has implied that during MCAO, PID incidence may be suppressed by anesthesia, since the SD incidence in the absence of anesthesia was much

higher than in previous results with anesthesia (Hartings et al., 2003). Furthermore, in freely-moving unanesthetized rats monitored for 72 hours after reperfusion, a large number of additional depolarizing events were recorded (Hartings et al., 2003). The number of PIDs correlated with final infarct volumes, particularly those that occurred during a secondary phase (8-18 hours after the insult), and early onset of this secondary phase of PIDs was also predictive of a larger infarct volume (Hartings et al., 2003). These initial long-term recording studies in animals provided an additional motivation for the formation of a collaborative clinical study, whose aim was to measure SD-like events in patients suffering from various acute brain injuries. A primary goal of this multi-center consortium, known as the Cooperative Study on Brain Injury Depolarization (COSBID), has been to determine the relevance of these depolarizations on patient final outcome.

Since its formation in around 2003, COSBID has concentrated on recording SD-like events in human pathologies including traumatic brain injury (TBI) (Strong et al., 2002; Hartings et al., 2009), subarachnoid hemorrhage (SAH) (Dreier et al., 2006; Dreier et al., 2009), intracerebral hemorrhage (Fabricius et al., 2006), and large ischemic strokes (malignant hemispheric stroke) (Dohmen et al., 2008). For these studies, the use of implanted electrode strips in patients who required a craniotomy for lesion evacuation or decompression allowed for long-term (>100hrs) electrocorticographic (ECoG) recordings. Where possible, electrode strips have been placed across the border of infarcts, so that recordings can include signals from irrecoverably damaged

areas, as well as from penumbral and normally perfused regions. To date, these types of measurements have been made in over 200 patients from at least nine centers (Dohmen et al., 2008; Fabricius et al., 2008; Hartings et al., 2008), and there is now compelling evidence to support a role for these SD-like events in the expansion of injury (Lauritzen et al., 2011).

In these COSBID studies, depression of ECoG activity across electrodes was shown to be time-locked with the large negative voltage shift indicative of SD that spreads from one electrode to the next, and limited ECoG recovery has been shown to be associated with prolonged DC shifts (Oliveira-Ferreira et al., 2010). Furthermore, these spreading depolarizations have been shown to cause spreading ischemia in SAH patients causing limited O_2 availability to tissues (Dreier et al., 2009). Consistent with a causative, rather than simply correlative role for SDs in progression of brain injury, interim analysis of collective COSBID data suggests that the occurrence of SD-like events following TBI is a stronger predictor of 6-month patient outcome than any previously established covariate (Lauritzen et al., 2011). Furthermore, similar to what was observed in animal ischemia studies (Hartings et al., 2003), following both TBI and SAH in humans, a recurrent secondary phase of many clustered PID events has been observed in some patients 5-10 days post-injury (Dreier et al., 2006; Hartings et al., 2009). These new findings raise the exciting possibility that targeting PIDs following ischemic injury may be very useful, as this prolonged time course may provide a much larger window of opportunity for therapeutic intervention than the current 3 hr window for tPA treatment.

To date, there are no known blockers of these depolarizing events, but there is evidence that their initiation is dependent on energy availability in both neurons and astrocytes. Therefore, these depolarizations may be an important target with a wide time window for therapeutic intervention (Figure 1.3), and knowing the mechanisms that contribute to energy consumption should be important in the overall assessment of how to prevent continuous depolarizing events.

1.3.3.2 SD and Subarachnoid hemorrhage

Treatments for DIND following SAH, including hemodynamic therapy and nimodipine, have often targeted vasospasm in an attempted to reduce secondary brain injury. Previous studies preformed meta-analysis on results from all randomized trials of prophylactic nimodipine treatment following SAH and found almost a 50% reduction in the risk of DIND, but the mechanism underlying these protective effects has remained unclear (Barker and Ogilvy, 1996). It has recently become well established that SD occurs following SAH in human patients (Dreier et al., 2006; Dreier et al., 2009), and nimodipine can inhibit SD induced by the Na^+/K^+-ATPase inhibitor, ouabain, in hippocampal slice preparations (Dietz et al., 2008) raising the possibility that inhibition of SD can underlie part of the protective effects observed with nimodipine treatments.

Figure 1.3

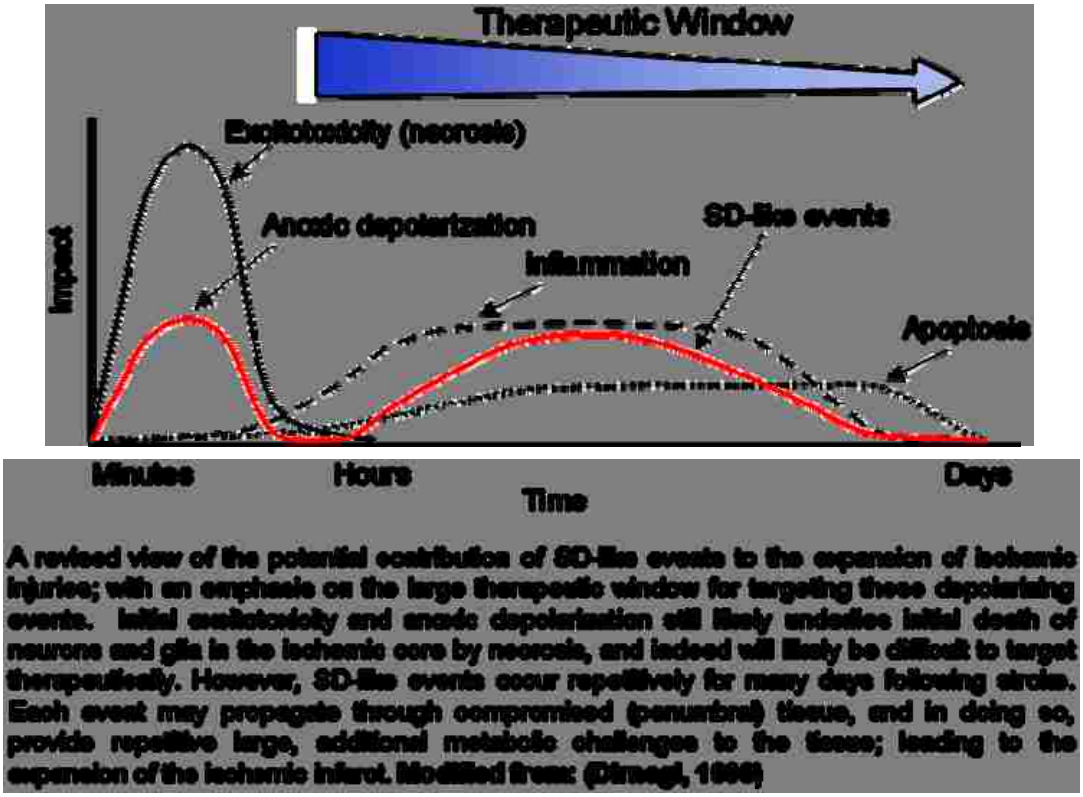

A revised view of the potential contribution of SD-like events to the expansion of ischemic injuries; with an emphasis on the large therapeutic window for targeting these depolarizing events. Initial excitotoxicity and anoxic depolarization still likely underlies initial death of neurons and glia in the ischemic core by necrosis, and indeed will likely be difficult to target therapeutically. However, SD-like events occur repetitively for many days following stroke. Each event may propagate through compromised (penumbral) tissue, and in doing so, provide repetitive large, additional metabolic challenges to the tissue; leading to the expansion of the ischemic infarct. Modified from: (Dirnagl, 1999)

1.3.4 Potential targets for SD intervention

1.3.4.1 Glutamate receptors

From the mechanisms described above, one would predict that approaches to limit glutamate action would be effective for inhibiting SD. There is a relationship between SD, glutamate excitotoxicity, and brain damage that is not fully understood. NMDA or non-NMDA glutamate antagonists, serotonin agonist sumatriptan, as well as the non-selective cation blocker LOE-908 are all drugs that act mainly on preventing the growth of the lesion size in animal models of ischemic injury (Hossmann, 1996; Hartings et al., 2003). As mentioned above, blocking glutamate receptors has been shown to inhibit PIDs and reduce

infarct volume in animal studies (Iijima et al., 1992; Mies et al., 1993; Mies et al., 1994; Busch et al., 1996), and in a recent clinical case study, the use of the NMDA receptor antagonist, ketamine, reduced the incidence of PIDs in two patients following traumatic and spontaneous intracerebral hemorrhage (Sakowitz et al., 2009). However, they were unable to provide clear evidence for a reduction in final infarct volume in this preliminary clinical study. While NMDA antagonists may reduce the number of SD-like events following ischemia, there are a number of undesirable effects that are known to be associated with drugs that target glutamate receptors, including their psychomimetic properties as well as their potential to disrupt normal physiological function (see section 1.3.2); making these receptors a difficult therapeutic target.

There is accumulating evidence that glutamate receptor antagonists provide protection following injury not by preventing excitotoxicity per se (Obrenovitch, 1999), but rather by reducing the number of PIDs (Hossmann, 1996). PIDs will result in the release of glutamate for feed-forward propagation of depolarizations across tissues, but it is likely that the large metabolic burden generated by repetitive PIDs is responsible for death of already compromised tissue (Hossmann, 1996). As reviewed above, complete depolarization of neurons induced by SD requires substantial ATP consumption to restore ionic gradients. In the context of penumbral tissue, where metabolic substrate availability is compromised (Lipton, 1999), massive ionic shifts associated with each PID may not be successfully resolved, and lead to irrecoverable membrane

depolarization. These studies, suggest that selectively targeting metabolic consequences of PIDs may be more effective than targeting NMDA receptors.

1.3.4.2 Nitric oxide

NO has been suggested as a potential therapeutic target for treatment of subarachnoid hemorrhage (SAH). This is due to the vasodilatory effects of NO to alleviate vasospasm, which has been thought to be the major contributor to delayed ischemic neurologic deficits (DIND) (Thomas et al., 1999; Al-Tamimi et al., 2010). The release of hemoglobin by erythrocytes following hemolysis of the subarachnoid clot is thought to induce the vasospasm (Pluta et al., 1998). Hemoglobin binds NO with high affinity (Gibson and Roughton, 1957), and in patients who develop DIND-related vasospasm, significant decreases in NO concentrations were observed over time post-SAH (Sakowitz et al., 2001) suggesting NO scavenging by hemoglobin. Thus adding back exogenous NO has been suggested to compensate for this loss and reverse vasospasm.

Several days following SAH, patients also show significant increases in $[K^+]_e$ that are well-matched with the onset of hemolysis (Ohta et al., 1983) and this raises a possible role for SD-like events in the observed DIND. Indeed, recent studies have shown that SD-like events occur in human patients following SAH and are also associated with DIND (Dreier et al., 2006). Nitric oxide (NO) production is known to increase following SD and inhibition of NO synthesis both *in vitro* and *in vivo* reduces SD threshold (Read et al., 1997; Petzold et al., 2008). Consistent with this idea, replacing endogenous NO with an exogenous donor recovered SD threshold to baseline levels, and led to the suggestion that NO

may be therapeutically protective against SD events in this condition (Petzold et al., 2008). However, NO is also known to inhibit cytochrome oxidase in the electron transport chain, which can result in inhibition of mitochondrial respiration (Brown and Cooper, 1994). Therefore, the addition of exogenous NO may actually be deleterious to the tissue following SAH by further compromising the metabolic capacity of tissue in the presence of repetitive PIDs. This theoretical possibility has not yet been investigated in SD models.

1.3.4.3 Astrocytes

SD and related events affect not only neurons but astrocytes as well. The role of astrocytes in the propagation of SD has been unclear and will be discussed in detail below (Section 1.4.2). Early work suggested that astrocytes might underlie SD initiation, while more recent studies support the idea that glial cells are not responsible for inducing SD and may actually be important for preventing the propagation of the depolarization through tissues. This may be of particular relevance in post-ischemic brain, as astrocytes are more resistant than neurons to ischemic challenges, and furthermore, may change functional phenotype in response to injury (Chen and Swanson, 2003). Therefore, a greater understanding of how astrocytes actually contribute to SD both in normoxic and ischemic conditions is needed; as well as how they might be targeted to mitigate SD and/or its consequences.

1.4 Astrocytes and Spreading Depression

1.4.1 Normal astrocyte physiology

Studies over the past decade have provided substantial new insight into the role of astrocytes within the nervous system. The ratio of glial cells to neurons in the human nervous system is at least 10 to 1 (Kimelberg and Nedergaard, 2010), consistent with crucial roles in signal transduction as well as ionic and metabolic homeostasis (Haydon, 2001). What were once thought of as mere scaffolding for neurons, are now being recognized as dynamic organizers that play significant roles in modifying neuronal activity (Nedergaard et al., 2003; Kimelberg and Nedergaard, 2010). Indeed, it has been suggested that to understand synaptic transmission fully, the synapse must be thought of as a tripartite system rather than simply the interaction between pre and postsynaptic neurons (Newman, 2003). Astrocytes organize into nonoverlapping spatial domains, and each astrocyte may cover more than 100,000 synapses on many different neurons (Bushong et al., 2002). In addition, astrocytes establish large cellular networks by joining hemichannels to form gap junctions, which allow for the transport of metabolites, ions, and potentially other information over large distances (Theis et al., 2005).

Astrocytes are established to be critical for the maintenance of appropriate extracellular K^+, H^+, and glutamate concentrations, and also have emerging roles in providing metabolic support to neurons (by control of cerebral blood flow and additional metabolic substrates), and may even provide antioxidant support to neurons (Chen and Swanson, 2003; Kimelberg and Nedergaard, 2010). When

glutamate is released from presynaptic terminals, it can bind to ionotropic and/or metabotropic receptors on astrocytes, as well as on the better studied postsynaptic neurons. One of the best characterized responses within astrocytes is an increase in intracellular calcium concentration ($[Ca^{2+}]_i$) (Haydon, 2001; Nedergaard et al., 2003; Newman, 2003). This increase in $[Ca^{2+}]_i$ can initiate the release of "gliotransmitters" that may include glutamate, ATP, and D-serine, which can all influence normal neuronal activity (Newman, 2003; Halassa et al., 2007; Hamilton and Attwell, 2010). Glutamate release due to astrocyte stimulation has shown that glial-derived glutamate can potentially modulate synaptic transmission between surrounding neurons (Newman, 2003). There is some debate within the field as to whether astrocytes can actively modify synaptic transmission as a result of Ca^{2+}-dependent gliotransmission (Fiacco et al., 2007; Agulhon et al., 2008). However, astrocytes express all the proteins required for vesicular fusion, and some studies have shown compelling evidence to support vesicular release of glutamate from astrocytes (Parpura et al., 1994; Parpura and Haydon, 2000). Along with releasing glutamate, astrocytes are solely responsible for both the production and release of D-serine in the central nervous system (CNS), a chemical cofactor that must bind along with glutamate in order to allow activation of NMDA receptors (Ouyang et al., 2007).

1.4.1.1 Potassium clearance

Astrocytes are highly permeable to K^+ and their resting membrane potential (V_m) closely follows the K^+ equilibrium potential; suggesting that changes in glial V_m will mimic changes in extracellular K^+ (Orkand et al., 1966;

Amedee et al., 1997). There are large populations of K^+ channels in the plasma membrane of astrocytes, which are generally thought to be active at resting membrane potentials. The inward rectifying K^+ channel, $K_{ir}4.1$, appears to be most important for maintaining the high K^+ permeability of glia (Duffy et al., 1996; Djukic et al., 2007; Chever et al., 2010). Loss of these channels in *in vivo* studies resulted in decreased K^+ permeability and a depolarization of V_m by >20mV (Chever et al., 2010). Astrocytes accumulate K^+ at a much faster rate than do neurons (Walz and Hertz, 1982), and clearance from the extracellular space is achieved by both active and passive uptake (Figure 1.4).

Both intracellular Na^+ and K^+ concentrations are regulated by Na^+/K^+-ATPase activity (Walz and Wuttke, 1999). When extracellular K^+ concentrations rise, some transport of K^+ is ATP-dependent and mediated by the Na^+/K^+-ATPase and $Na^+/K^+/Cl^-$ cotransporter (Kofuji and Newman, 2004). The activity of these pumps and carriers is believed to be linked, since the influx of Na^+ by the $Na^+/K^+/Cl^-$ cotransporter provides the increase in intracellular Na^+ required to drive ATPase activity (Newman, 1995; Walz, 2000). Thus, application of the nonselective Na^+/K^+-ATPase inhibitor, ouabain, in astrocyte culture results in decreased K^+ uptake (Walz and Hinks, 1985), but does not completely eliminate clearance of K^+ by astrocytes because of remaining passive uptake.

Passive uptake, also known as K^+ spatial buffering, is ATP-independent and believed to occur primarily by coupled influx with Cl^- through channels driven by Donnan forces as a result of the uneven distribution of ions across the plasma membrane (Boyle and Conway, 1941; Walz and Hinks, 1985). As mentioned

above, K_{ir} channels are the primary potassium channel on astrocytes and allow K^+ ions to flow more readily in the inward direction (Stanfield et al., 2002). In addition, the large glial network established by gap junctions is necessary to allow the diffusion of K^+ between cells to prevent accumulation of intracellular K^+ to concentrations that would no longer allow uptake (Kofuji and Newman, 2004). Under conditions of SD, the relative contributions of these different transport mechanisms to clear $[K^+]_e$ are not well differentiated. It is possible that during SD, with large $[K^+]_e$ accumulations, ATP-dependent mechanisms may have a significantly larger contribution.

Figure 1.4

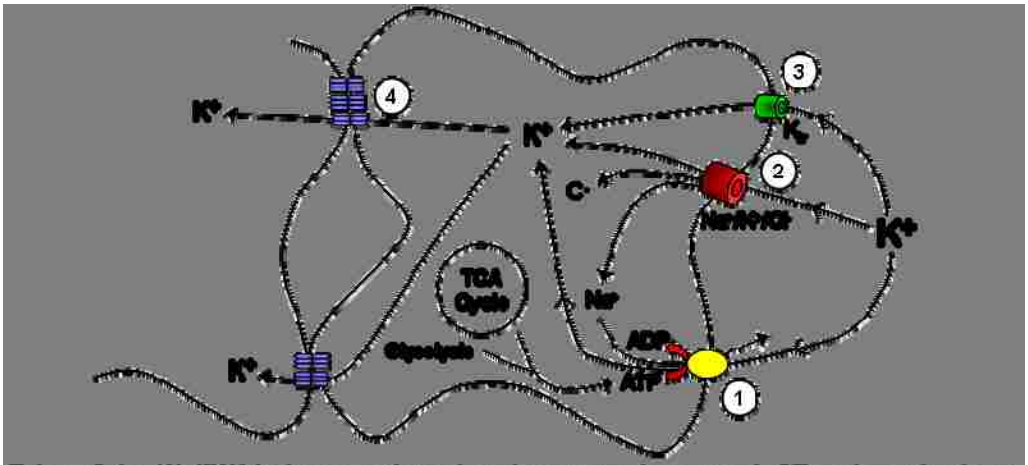

Extracellular K^+ ($[K^+]_e$) clearance by astrocytes occurs by several different mechanisms. The first is activity dependent uptake by the Na^+/K^+/ATPase (1). $[K^+]_e$ is also cleared by the $Na^+/K^+/Cl^-$ cotransporter (2) which is linked to ATPase clearance of K^+ by providing Na^+ for exchange. $[K^+]_e$ is also cleared passively predominantly by inward rectifying (K_{ir}) channels (3). Astrocytes are able to clear large amounts of K^+ from the extracellular space due to their ability to spatially buffer K^+ across a large network created by gap junctional connections (4).

1.4.1.2 Glutamate clearance

Astrocytes are critical for the clearance of glutamate from the extracellular space; a process essential for regulating normal synaptic transmission as well as preventing irreversible excitotoxic injury in the CNS (Swanson et al., 2004). In the

brain, there are three primary glutamate transporters; EAAC1 is primarily neuronal and does not appear to play a large role in the clearance of extracellular glutamate. GLT-1 (also termed EAAT2) and GLAST (also termed EAAT1) are located on astrocytes and are responsible for the majority of glutamate clearance (Schousboe, 1981; Rothstein et al., 1996; Danbolt, 2001). There is a relatively large energetic cost for glutamate co-transport with Na^+ requiring about 1 ATP per glutamate molecule. This is because co-transport with Na^+ requires the maintenance of a large Na^+ gradient across the plasma membrane, which, in turn, requires Na^+/K^+-ATPase pump activity (Figure 1.5). Therefore, either a loss of ionic gradients or ATP depletion results in significantly reduced glutamate uptake by astrocytes (Swanson et al., 1997; Rose et al., 2009).

Within astrocytes, glutamate is converted to glutamine by the astrocyte-specific enzyme glutamine synthetase (GS). Following release into the extracellular space, glutamine can then be taken up by neurons (Martinez-Hernandez et al., 1977), and phosphate-activated glutaminase (PAG) converts glutamine to glutamate for neuronal vesicular repackaging (Kvamme et al., 2001; Bak et al., 2006). Recent studies focusing on the properties of glutamate transporters in both healthy and metabolically compromised astrocytes are providing new insights into glial function during ischemia. Indeed, loss of glutamate uptake by astrocytes can result in elevated extracellular glutamate levels and neurodegeneration (Ouyang et al., 2007; Kimelberg and Nedergaard, 2010).

Figure 1.5

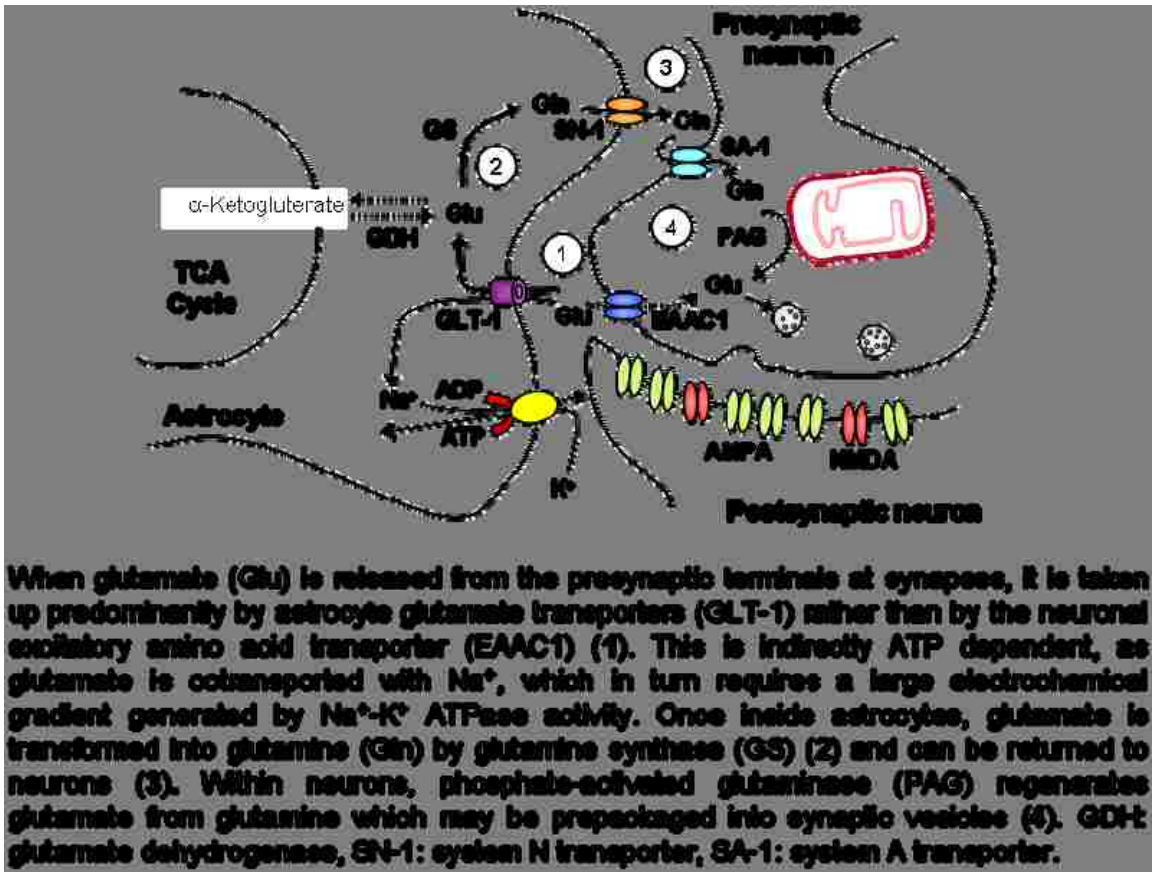

When glutamate (Glu) is released from the presynaptic terminals at synapses, it is taken up predominantly by astrocyte glutamate transporters (GLT-1) rather than by the neuronal excitatory amino acid transporter (EAAC1) (1). This is indirectly ATP dependent, as glutamate is cotransported with Na^+, which in turn requires a large electrochemical gradient generated by Na^+-K^+ ATPase activity. Once inside astrocytes, glutamate is transformed into glutamine (Gln) by glutamine synthase (GS) (2) and can be returned to neurons (3). Within neurons, phosphate-activated glutaminase (PAG) regenerates glutamate from glutamine which may be prepackaged into synaptic vesicles (4). GDH: glutamate dehydrogenase, SN-1: system N transporter, SA-1: system A transporter.

1.4.1.3 Astrocyte metabolism

It is often assumed that anaerobic metabolism is a primary source of ATP production in astrocytes under normal conditions. Consistent with this assumption, the primary source of glycogen, an excellent anaerobic substrate, in the brain is found within astrocytes (Wender et al., 2000; Dugan and Kim-Han, 2004). However, astrocytes have been shown to be abundant in mitochondria, so they are likely also to be capable of aerobic metabolism (Boitier E, 1999; Lovatt et al., 2007). Furthermore, astrocytes have been shown to express similar levels to neurons of enzymes required for a functional TCA cycle, and TCA cycle pathways are active within these cells under normal conditions (Lovatt et al.,

2007). As mentioned above, one primary astrocyte function is clearance of both extracellular glutamate and K^+; both of which can require ATP. Therefore, targeting either glycolytic or oxidative metabolism in astrocytes may reduce extracellular accumulation of these two important mediators and limit SD-like events.

Figure 1.6

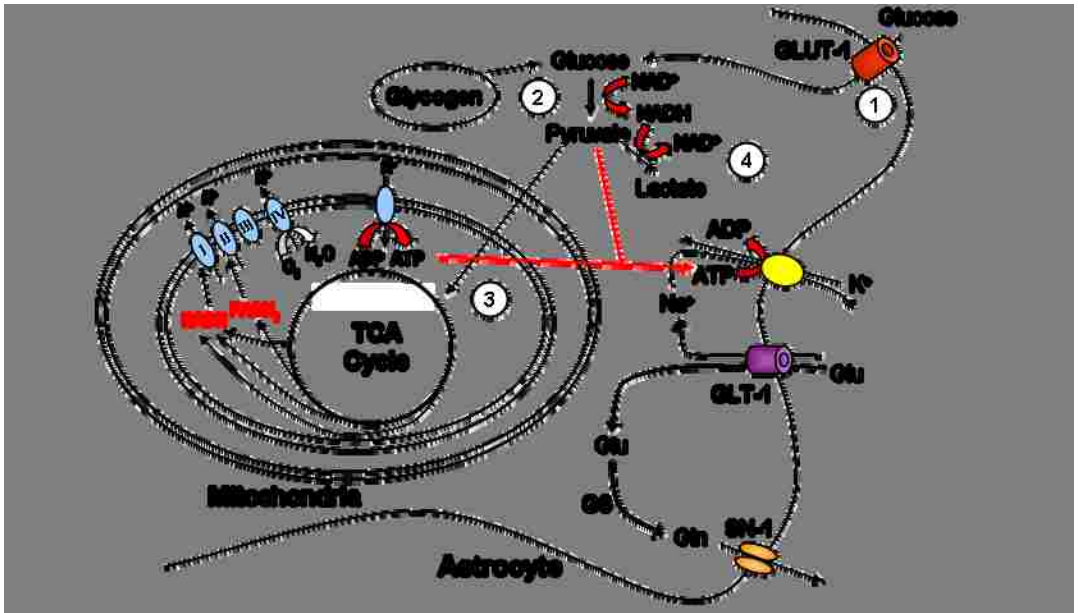

Glucose is transported into astrocytes from the extracellular space by glucose transporter 1 (GLUT-1) (1). Once inside astrocytes, glucose is metabolized into pyruvate via glycolysis yielding 2 ATP (2). Pyruvate may then enter mitochondria for oxidative respiration which yields 34 ATP (3), or it may be converted to lactate to regenerate NAD^+ for maintenance of anaerobic glycolysis (4). NADH: nicotinamide adenine dinucleotide, $FADH_2$: flavin adenine dinucleotide, SN-1: system N transporter, GLT-1: glutamate transporter

1.4.2 Role of Astrocytes in Spreading Depression

Early studies speculated that waves of calcium within astrocytes were responsible for the induction of SD in neurons (Kunkler and Kraig, 1998). However, this idea has been challenged, because SD has been shown to occur even when astrocyte Ca^{2+} waves were abolished (Basarsky et al., 1998; Peters

et al., 2003). Furthermore, astrocytic Ca^{2+} waves occur some time before changes in light transmittance (IOS) associated with SD (Basarsky et al., 1998), and they spread further than both IOS signals and measurable DC-potential shifts (Peters et al., 2003). This suggested that astrocytic Ca^{2+} waves may simply correlate with SD, but are not causative (Somjen, 2001). Recent studies using two-photon imaging techniques of neurons and astrocytes during SD have provided direct evidence showing that astrocytes follow rather than lead SD (Zhou et al., 2010). SD induced in murine cortical slices by perfusion with 40mM KCl, resulted in reversible increases in neuronal volume, acidification, and mitochondrial depolarization, but without observable responses in neighboring astrocytes (Zhou et al., 2010). These studies further suggest that astrocytes play a passive role in response to the wave of neuronal depolarization. While ruling out astrocytes and their Ca^{2+} waves for SD initiation, these findings did not rule out other roles for astrocytes in regulating SD propagation.

Indeed, early work with putative astrocyte gap junction inhibitors completely blocked the propagation of SD in isolated chick retina (Nedergaard et al., 1995). However, in subsequent studies, low concentrations of the same inhibitors resulted in an increase in SD velocity, while high concentrations (similar to those used in the initial studies (Nedergaard et al., 1995)) resulted in an immediate decline in the velocity and even complete block of SD (Martins-Ferreira and Ribeiro, 1995). These observations suggested that at high concentrations, these inhibitors are unlikely to be acting specifically on astrocytic gap junctions and could instead be affecting neuronal hemichannels as well

(Martins-Ferreira and Ribeiro, 1995). A lack of gap junction involvement was also suggested from additional studies using genetic inactivation of astrocyte-specific connexin 43. These preparations showed significantly decreased dye-coupling between astrocytes and 20% acceleration in the velocity of the SD event in the *stratum radiatum* (Theis et al., 2003). This acceleration contrasted with the slowing of SD propagation as would be expected if gap junctional communication were responsible for SD propagation. It is possible that under these experimental conditions, astrocyte networks were no longer able to sufficiently spatially buffer K^+, and $[K^+]_e$ reached threshold (10-12mM) more rapidly during SD stimuli (Theis et al., 2003). These studies, together with those investigating astrocytic Ca^{2+} waves, suggest that astrocyte function may help prevent the spread of neuronal depolarization, but are likely not initiating these events.

A role for astrocyte metabolism in regulating the spread of SD has also been demonstrated with the use of fluorocitrate (FC). FC is a TCA cycle inhibitor with specificity for astrocytes due to selective uptake via the MCT1 monocarboxylate-like transporter. In rat cortex, FC-facilitated SD propagation, suggests that normal astrocyte function is important in the context of these depolarizations (Largo et al., 1997a). Thus, oxidative astrocyte metabolism and consequent facilitation of extracellular K^+ and glutamate clearance may significantly affect SD propagation. As discussed above (Section 1.4.1.3), astrocytes are thought to be primarily glycolytic cells and the primary source of brain glycogen, but it is currently unknown how glycogen may be involved in SD initiation and propagation. Furthermore, astrocytes are known to undergo

significant phenotypic changes following injuries, which are associated with SD-like events, but it is also currently unknown how changes in astrocyte structure and function may affect SD.

1.4.3 Astrocyte Activation

1.4.3.1 General changes in reactive astrocytes

Astrocyte populations are not static and can take on a reactive phenotype following many pathological insults. These include ischemia, brain trauma, infection, and chronic neurodegenerative diseases (Eddleston and Mucke, 1993; Ridet et al., 1997; Kalman, 2004). Similar phenotypes can also be induced experimentally, and these will be discussed below (Section 1.4.3.3). Astrocyte reactivity is characterized by significant hypertrophy of main astrocytic structural processes (Pekny and Nilsson, 2005). Importantly, this thickening of structural elements does not translate to a significant alteration in overall cell volume and each astrocyte maintains its own cellular domain (Wilhelmsson et al., 2006). Glial fibrillary acidic protein (GFAP) is the prototypic marker for astrocyte activation, but other intermediate filament proteins, including vimentin and nestin, are also increased and used to identify reactive astrocytes (Eddleston and Mucke, 1993; Pekny and Nilsson, 2005; Escartin and Bonvento, 2008). While these primary morphological alterations within reactive astrocytes appear to be universal regardless of the inducing stimulus, the range of functional consequences may be quite different and will be discussed in more detail below (Section 1.4.3.2).

Regardless of the inducing stimuli, reactive astrocytes appear to generally increase the expression of cytokines, neuronal growth factors, and calcium-binding protein S100β (Eddleston and Mucke, 1993; Ridet et al., 1997; Escartin and Bonvento, 2008). Release of other factors including (NO) and inflammatory molecules may be potentially toxic and induce neuronal damage, while the release of VEGF, neurotrophic factors, and ATP/adenosine may be neuroprotective (Endoh et al., 1994; Zhang et al., 2000; Hermann et al., 2001; Zhao and Rempe, 2010). Presumably the expression of these different molecules has a wide range of effects, and recent reviews have emphasized that a greater understanding of which molecules are upregulated in reactive astrocytes during different neurological diseases states could be valuable for determining novel targets for therapeutic intervention (Escartin and Bonvento, 2008; Hamby and Sofroniew, 2010). For the remainder of my discussion, I will remain consistent with a recent review, and use the term “reactive astrocytes” to refer to cells following endogenous changes induced by any pathology, while reserving the term “activated astrocytes” to refer to astrocytes modified by exposure to experimental agents in the absence of brain injury (Escartin and Bonvento, 2008).

1.4.3.2 Neuroprotective versus neurodegenerative in ischemia

In the context of ischemia, phenotypic changes within astrocytes are rapidly induced following initial injury, but astrocytes have been shown to remain in this reactive phenotype for more than a month following transient cerebral ischemia; raising the possibility that astrocytes may be relevant as targets for

long term therapy after ischemia (Choi et al., 2010). Reactive astrocytosis following brain injury has long been considered detrimental to neuronal survival due to its apparent association with neurodegeneration (Kalman, 2004). As mentioned above, release of pro-inflammatory factors and NO may induce neuronal damage by causing oxidative stress and disruption of the blood-brain barrier (Chen and Swanson, 2003). In addition, inhibition of axonal regrowth by the formation of a glial scar may also retard recovery following injury (McKeon et al., 1991; Bush et al., 1999).

There is a growing body of work suggesting protective effects of astrocytes following ischemic injury. For example, GFAP/Vimentin double-KO mice have been generated to prevent expression of astrocytes activation, at least as determined by these markers. Following middle cerebral artery occlusion (MCAO) these mice have final infarct volumes three times larger when compared with control littermates, suggesting that reactive astrocytes following ischemia may be neuroprotective (Li et al., 2008). Furthermore, the formation of glial scars following focal lesions may be protective by isolating an area of injury to prevent further expansion of the lesion (Ridet et al., 1997). The production of reactive oxygen species is thought to be one of the underlying causes of ischemic injury, and the primary antioxidant in the brain, glutathione (GSH), is expressed at a higher concentration in astrocytes than neurons (Makar et al., 1994; Chan, 1996; Dringen, 2000). Increased glutathione peroxidase production has been shown in reactive astrocytes, and suggests an increased capacity to protect neurons from nitric oxide (NO) and other oxidative stress (Chen et al., 2001; Shih et al., 2003).

In addition, astrocytes appear to release ATP (through hemichannels) that is then rapidly degraded to adenosine following injury (Lin et al., 2008). Adenosine is known to significantly reduce neuronal activity, an effect, which may in turn preserve energy stores as well as provide neuroprotection from excessive glutamate release (Dunwiddie and Masino, 2001). In addition, adenosine is also known to be a potent vasodilator in hypoxic conditions (Gordon et al., 2008), and increasing local blood flow to increase metabolic substrate delivery may also be a neuroprotective function of adenosine. Lastly, astrocytes express a range of growth factors following injury, which may promote neuronal survival and plasticity as well as angiogenesis (Ridet et al., 1997; Zhang et al., 2000).

It is not yet known whether reactive astrocytes may lead to changes in SD propagation and/or initiation. This is an exciting possibility in the context of ischemic injury, since both reactive astrocytes and SD-like events are have been shown to occur together following the initial injury.

1.4.3.3 Models of astrocyte activation

There are several models currently used to induce astrocyte activation to investigate the functional properties associated with reactive astrocytes without the confounds of neuronal injury. These models aim to target astrocytes specifically while leaving other cell types relatively unaffected. *In vitro* studies in primary cortical astrocyte cultures used cytokines (interleukin-1β (IL-1β) and tumor necrosis factor α (TNFα)) to induce activation, which resulted in enhanced metabolism and increased GSH release (Gavillet et al., 2008). Additional *in vitro* studies have used ciliary neurotrophic factor (CNTF) to induce astrocyte

activation, and in coculture experiments, resulted in a two-fold increase in neuronal survival and a significant enhancement in neurite outgrowth (Albrecht et al., 2002).

Lenti-viral injections with a vector coding for CNTF have been shown to result in sustained and profound activation of astrocytes in the rat striatum (Escartin et al., 2006; Escartin et al., 2007). These preparations show large increases in intermediate filament protein expression within astrocytes including increased GFAP, vimentin, and nestin, as well as an increase in the astrocyte specific connexin 43 (Escartin et al., 2006). Importantly, lenti-viral injections with CNTF did not appear to result in any significant differences in neuronal proteins, including those involved in glutamatergic transmission. Single cell recordings also showed no significant differences in spontaneous activity in glutamatergic neurons when compared with lenti-LacZ controls in rat striatum (Escartin et al., 2006). When exposed to the excitotoxin quinolinate (QA), increases in extracellular glutamate concentrations were significantly lower in CNTF animals, suggesting increased glutamate uptake by astrocytes in CNTF preparations, which could be neuroprotective following ischemic injury (Escartin et al., 2006). However, it is currently unknown whether CNTF-astrocyte activation may affect SD-like events.

Interestingly, very recent work has used high-titer bilateral injections of adeno-associated virus AAV2/5-*Gfa104-eGFP* to induce astrocyte activation (Ortinski et al., 2010). Injections into murine hippocampus led to the overexpression of enhanced green fluorescent protein (eGFP) selectively within

astrocytes, which in turn appeared to induce an activated phenotype (Ortinski et al., 2010). In these mice, activated astrocytes expressed lower levels of glutamine synthetase (GS), and there was a significant reduction in evoked inhibitory postsynaptic currents (eIPSCs) and miniature inhibitory postsynaptic currents (mIPSCs), which could result in neuronal hyperexcitability (Ortinski et al., 2010). While this model may be useful for studies of SD threshold, it is unclear whether this model is truly absent of injury, since astrocyte activation was simply induced by over expression of eGFP, raising the possibility that in this model, astrocytes are potentially reacting to toxic levels of the fluorescent protein. Therefore, a model of astrocyte activation in a preparation suitable for SD studies, but lacking injury is still required to address the possible effects of reactive astrocytes on the phenomenon of SD.

1.5 Goals of this study

The primary goal in these studies was to test the overall hypothesis that manipulation of astrocyte metabolic capacity can modify the initiation and propagation of deleterious spreading depression (SD)-like events in hippocampal brain slice preparations. If this hypothesis is supported, it would suggest that strategies that increase the ability of astrocytes to clear extracellular glutamate and K^+ may reduce the incidence of SD and limit neuronal injury in pathologic conditions where SD-like events still occur.

1.6 Specific Aims

1.6.1 Specific Aim 1

How does modifying astrocyte metabolism contribute to the initiation and propagation of spreading depression (SD) and related events in brain slices?

Experiments utilized a hippocampal slice model in which SD was generated either by using localized microinjections of KCl in normoxic conditions or by oxygen glucose deprivation (OGD), which mimics aspects of ischemic insults. Experiments tested the hypothesis that glycogen depletion or pharmacological inhibition of glycogen availability accelerates the rate of SD in both normoxic and ischemic conditions; similar to effects of selective inhibition of astrocyte oxidative metabolism. Furthermore, these experiments tested whether supplementing glycogen stores in astrocytes can significantly retard SD progression. These experiments were expected to provide suggestions about whether targeting astrocyte glycogen stores might be beneficial to limit SD-like events in pathologic circumstances.

1.6.2 Specific Aim 2

How does astrocyte activation influence SD and related events?

In these studies, I first established and validated a new model of astrocyte activation within the hippocampus, which exploited a recently-described approach using injection of CNTF expressing lenti-virus constructs. I then used this model of long-term astrocyte activation for subsequent electrophysiological studies testing the hypothesis that astrocyte activation can significantly modify

SD initiation and propagation when compared to LacZ injected control preparations. Information from these studies could provide new insights into possible neuroprotective effects of astrocyte activation in injured brain.

1.6.3 Specific Aim 3

How does an additional metabolic burden provided by NO exposure modify SD under normoxic conditions?

Previous work has suggested that exposure to NO may be useful clinically to increase SD threshold. Studies in this aim tested the hypothesis that addition of exogenous NO may also inhibit mitochondrial respiration to such an extent that it provides an additional metabolic burden to tissues during SD. Thus, NO may convert normally non-deleterious SD events (in the context of normoxia) into irrecoverable SD-like events that induce neuronal damage. These studies may provide a caution to the use of NO clinically in the treatment of SD and suggest approaches, which discriminate the protective effects of NO while eliminating its deleterious effects on metabolism.

2. Contribution of astrocyte metabolism to progression of spreading depression and related events in hippocampal slices

J.L. Seidel and C.W. Shuttleworth

Dept. Neurosciences, University of New Mexico School of Medicine, Albuquerque NM 87131

Sumbitted to “Neuroscience”

2.1 Abstract

Spreading depression (SD) is a wave of coordinated cellular depolarization that propagates slowly throughout brain tissue. SD has been associated with migraine aura and related events have been implicated in the enlargement of some brain injuries. Selective disruption of astrocyte oxidative metabolism has previously been shown to increase the propagation rate of SD, but it is currently unknown whether astrocyte glycogen stores make significant contributions to the onset or propagation of SD. We examined SD in acutely-prepared murine hippocampal slices using either localized microinjections of KCl or oxygen and glucose deprivation (OGD) as stimuli. A combination of glycogenolysis inhibitors 1,4-dideoxy-1,4-imino-D-arabinitol (DAB) and 1-deoxynojirimycin (DNJ) increased the propagation rates of both high K^+-SD and OGD-SD. Consistent with these observations, exposure to L-methionine-DL-sulfoximine (MSO) increased slice glycogen levels and decreased OGD-SD propagation rates. Conversely, glycogen availability did not appear to influence the latency to onset of OGD-SD. Effects of glycogen depletion were matched by selective inhibition of astrocyte TCA cycle activity by fluoroacetate (FA). Prolonged exposure to reduced extracellular glucose (2 mM) has been suggested to deplete slice glycogen stores, but significant modification of SD propagation rate was not observed with this treatment. Furthermore, reduced extracellular glucose resulted in significantly decreased latency to onset of OGD-SD. These results suggest that astrocyte glycogen stores contribute to delaying the advancing wavefront of SD, including during severe metabolic challenge of

OGD. Approaches to enhance astrocyte glycogen reserves could be beneficial for delaying or preventing SD in some pathologic conditions.

2.2 Introduction

SD is characterized as a wave of severe depolarization that can propagate throughout CNS tissue and result in suppression of electrical activity, disruption of ion homeostasis, and provide repetitive large metabolic burdens to both neurons and astrocytes (Leao, 1944; Hansen, 1985; Somjen, 2001). If SD is generated in otherwise healthy tissue, neuronal ionic gradients and brain function can be fully restored after SD (Nedergaard and Hansen, 1988), and such recoverable events are believed to be related to migraine aura (Okada et al., 1988; Hadjikhani et al., 2001). However, SD triggered in the context of ischemia, can result in irrecoverable injury if metabolic substrates are not resupplied immediately following SD onset (Rader and Lanthorn, 1989; Tanaka et al., 1997), in both animal models (Nedergaard and Astrup, 1986; Hossmann, 1996; Strong et al., 2000; Hartings et al., 2003) and in human trauma and stroke (Fabricius et al., 2006; Dohmen et al., 2008). Therefore, inhibition of SD-like events following ischemia is being considered a potential therapeutic approach to limit injury progression (Lauritzen et al., 2011), but selective agents are not yet available.

A large body of work has implicated extracellular accumulation of K^+ and/or glutamate in SD initiation and propagation (Somjen, 2001). Under normal conditions, maintenance of both these factors is tightly regulated by astrocyte uptake (Lajtha et al., 1959; Orkand et al., 1966; Rothstein et al., 1996; Kofuji and

Newman, 2004). Selective disruption of astrocyte oxidative metabolism with fluorocitrate (FC) increased the rate of SD propagation (Largo et al., 1997a). Prolonged inhibition of astrocyte oxidative metabolism alone can also be sufficient to initiate SD in hippocampal brain slices under some experimental conditions (Canals et al., 2008); consistent with normal astrocyte function playing a central role in SD by maintaining ionic gradients below threshold levels required for feed-forward cellular depolarization.

Although effects of FC imply a dependence on mitochondrial oxidative metabolism, glycolysis is a major source of ATP production within these cells, and astrocytes are the primary source of glycogen in the brain (Cataldo and Broadwell, 1986; Wender et al., 2000; Brown, 2004). Glycogen stores are known to be depleted *following* SD events (Selman et al., 2004) and inhibition of glycolysis or glycogenolysis in culture results in decreased glutamate uptake by astrocytes (Swanson, 1992; Sickmann et al., 2009), but the possible contributions of astrocyte glycogen stores in the initiation and/or propagation of SD are currently unclear. A previous study has suggested that the latency to single cell anoxic depolarizations in rat hippocampal slices was determined by depletion of astrocytic glycogen (Allen et al., 2005). However, it is not yet known 1) whether the glucose depletion approach used previously did in fact deplete glycogen stores, 2) whether the delay in the onset of a single neuron AD also applies to SD initiation, and 3) whether initiation and/or propagation of coordinated waves of SD are significantly influenced by astrocyte glycogen stores.

In the present study, we have examined these questions by studying SD in murine hippocampal slices. SD was generated either by OGD or by localized high K^+ stimuli, and astrocyte metabolism was disrupted by using fluoroacetate (FA), putative inhibitors of glycogen metabolism, or approaches previously suggested to deplete glucose/glycogen stores prior to SD onset. We conclude that availability of astrocyte glycogen stores does not significantly influence the latency to SD onset generated in ischemia-like conditions. However, SD propagation rates appear to be regulated by astrocyte metabolism, likely by reducing the rate of extracellular K^+ and/or glutamate accumulation within astrocytes at the advancing wave front of SD generated in both normoxic and ischemic-like conditions.

2.3 Materials and Methods

2.3.1 Slice preparation

Male mice (FVB\N) were obtained from Harlan Laboratories (Indianapolis, IN) at 4-6 weeks of age and were housed in standard conditions (12 hr light/dark cycle) for up to 2 weeks prior to euthanasia. Mice were deeply anesthetized with a mixture of ketamine and xylazine (85 and 15 mg/ml, respectively, s.c.) and decapitated. Brains were rapidly removed and placed in ice-cold cutting solution (see below for composition). Coronal sections (250 μm) were cut on a Vibratome (Technical Products International, St. Louis, MO) and slices were subsequently transferred to oxygenated room temperature ACSF (see below). Cutting and recording solutions were both 300-305 mOsm/l. After warming to 34^{o}C for one hour, the ACSF was exchanged again and slices were then held at room-

temperature. Individual slices were then transferred to a recording chamber and superfused with oxygenated ACSF at 2 ml/min at 35^{o}C.

2.3.2 Electrical recording

Extracellular measurements of slow DC shifts characteristic of SD were made using borosilicate glass microelectrodes, filled with ACSF (~5 MΩ) and placed in stratum radiatum ~45 µm below the surface of the slice and approximately 150µm from the pyramidal cell body layer. In some experiments, Schaffer collateral inputs to the CA1 region were stimulated using a bipolar electrode (25 µm tip) placed on the surface of stratum radiatum. Single shocks (80 µs, 0.1-1.5 mA) were applied using a constant-current stimulus isolation unit (Isoflex, AMPI, Israel). Stimulus intensity was chosen based on an input/output curve generated in each slice, to produce responses ~60% of maximal amplitude (0.4-0.55 mA). Signals were amplified (Neurodata IR-283), digitized (Digidata 1322A, Axon Instruments, Union City, CA), and then acquired using Axoscope software (v 8.1, Axon Instruments).

2.3.3 Autofluorescence measurements

NAD(P)H autofluorescence was used to assess the inhibition of slice mitochondrial function during OGD exposures, and also to track the progression of high K^{+}-SD and OGD-SD. This was performed as previously described (Shuttleworth et al., 2003) with minor modifications. In most experiments, 360 nm excitation was delivered via a fiber optic/monochromator system (Polychrome IV; Till Photonics, Grafelfing, Germany) and reflected onto the slice surface using a

dichroic mirror (DMLP 400 nm, Chroma Technology, Brattleboro, VT). Fluorescence emission (>410 nm) was collected with a cooled interline transfer CCD camera (IMAGO, Till Photonics). Image data were background-subtracted to account for camera noise, and presented as the changes in fluorescence intensity/prestimulus fluorescence intensity ($\Delta F/F_o$) from stratum radiatum. All imaging was performed after focusing onto the surface of the slice with a 10X water immersion objective (NA 0.3, Olympus) and fluorescence collected after 2 x 2 binning of the 640 x 480 line image. Single images or image pairs were acquired every 2.5 s.

2.3.4 Tissue glycogen levels

Glycogen measurements were performed following previously-described methods (Cruz and Dienel, 2002). Isolated hippocampal slices were allowed to recover in nACSF for at least 4 hours following slicing, to allow glycogen levels recover (Lipton, 1989) prior to different exposure paradigms. Tissues were then flash-frozen and added to ice-cold 0.3 ml 65% ethanol/phosphate-buffered saline solution and then homogenized and centrifuged at (9000 *g*, 10 minutes). The supernatant was discarded, and the extraction procedure repeated 4-5 more times, before pellets were freeze dried. Samples were then acidified (0.4 ml 0.03 N HCl), boiled (45 min), and then stored at 4^{o}C. Glycogen levels were determined indirectly, after hydrolysis to glucose. Samples were acidified (final concentration of 0.1 M acetate), divided and incubated (2 hours, 37^{o}C) in either the presence or absence of amylo-α-1,4-α-1,6-glucosidase (30 µg/ml). Samples were then centrifuged to remove particulate matter and glucose levels were

analyzed by fluorometry (hexokinase/glucose-6-phosphate dehydrogenase procedure, and responses compared with a glucose standard curve. Tissue levels were within the linear detection range of the assay (Supplementary Figure 2.1), and an approach expected to deplete tissue glycogen (20 min OGD, see (Lipton, 1989)) abolished glycogen signals in slices (-1.18±0.13 nmol/mg protein, n=2, p<.0001) when compared with controls (11.59±0.53 nmol/mg protein, n=7). We used the rough estimate of 150 mg protein per 1 g wet tissue wt to compare our measurement to published work, and found that, while our values were lower (~2 µmol/g wet wt vs. 12.5-5.4 µmol/g wet wt (Cruz and Dienel, 2002)), they were within an order of magnitude of previous work utilizing larger volumes of tissue.

2.3.5 Reagents and Solutions

Except where noted, all drugs and salts were obtained from Sigma Chemical Co (St Louis, MO). ACSF contained, in mM: 126 NaCl, 2 KCl, 1.25 NaH_2PO_4, 1 $MgSO_4$, 26 $NaHCO_3$, 2 $CaCl_2$, and 10 glucose, equilibrated with 95%O_2 / 5%CO_2. Cutting solution contained, in mM: 2 KCl, 1.25 NaH_2PO_4, 6 $MgSO_4$, 26 $NaHCO_3$, 0.2 $CaCl_2$, 10 glucose, 220 sucrose and 0.43 ketamine. For OGD studies, ACSF was modified by replacement of glucose with equimolar sucrose, and equilibration with 95% N_2 / 5% CO_2, rather than 95% O_2 / 5% CO_2. Studies of hypoxia alone, or hypoglycemia alone were performed using ACSF equilibrated with 95% N_2 / 5% CO_2 or replacement of 10 mM glucose by 10 mM sucrose, respectively.

2.3.6 Statistical analysis

Significant differences between group data were evaluated using unpaired Student's t tests or one-way ANOVA. Bonferroni's multiple-comparison test or contrast comparisons were used for *post hoc* analysis in which the effects of multiple treatments were compared against each other. A value of $p<.05$ was considered significant in all cases. Numbers in the study refer to the number of slices, with a maximum of three slices from an individual animal used for each experimental protocol.

2.4 Results

2.4.1 Decreasing glycogen availability increased propagation rate

Normoxic SD was generated by localized microinjections of 1 M KCl and similar events were generated by oxygen-glucose deprivation (OGD) as previously described (Nedergaard and Hansen, 1988; Dietz et al., 2008). Both stimuli produced slow negative DC potential shifts characteristic of SD (Figures 2.1A&B) and the propagation of events across the tissue were monitored using autofluorescence imaging. High K^+-SD generated an initial autofluorescence decrease that was tracked at 2.4±0.1 mm/min across area CA1 (Figure 2.1C). A sustained autofluorescence increase following the transient decrease corresponds to increased oxidative metabolism following the event, as described previously following SD *in vivo* (Hashimoto et al., 2000). During OGD challenges, oxygen deprivation generates a high initial autofluorescence level prior to onset of the SD-like event. OGD-SD propagation was then tracked by prominent autofluorescence decreases (3.25±0.18 mm/min) that appeared more prolonged

than in high K^+ preparations, due to the absence of the substrate-dependent overshoot phase.

To determine whether astrocytic glycogen stores contributed to SD propagation rate, we examined first the effects of pharmacological inhibition of glycogen breakdown using 1,4-dideoxy-1,4-imino-D-arabinitol (DAB, 10 µM) and 1-deoxynojirimycin hydrochloride (DNJ, 10 µM), which inhibit glycogen phosphorylase (GP) and glucosidase respectively (Kuriyama et al., 2008; Walls et al., 2008). As shown in Figure 2.1E-F, pre-exposure to a combination of these agents (15 min) led to a significant increase in propagation rate of both high K^+-SD and OGD-SD. To test whether these exposures were maximally effective, an additional set of studies were conducted with significantly higher exposures to the same inhibitors (100 µM each inhibitor, 75 min exposure) with OGD-SD. Prolonged exposures did not produce any additional increase in OGD-SD propagation rate, (4.1±0.3 vs. 4.2±0.3 mm/min, 100 µM, 75 min vs 10 µM, 15 min, respectively, n=6, p=.83), suggesting adequate penetration and effectiveness of the inhibitors.

2.4.2 Increasing glycogen content slows OGD-SD propagation

To assess the impact of increasing the content of glycogen stores on SD propagation, brain slices were exposed to L-methionine-DL-sulfoximine (MSO, 2 mM; 90-180 minutes), an approach, which has previously been established to significantly increase astrocyte glycogen content in cell cultures (Swanson et al., 1989b). In initial studies, the effectiveness of this approach was evaluated on

glycogen content in isolated hippocampal slices. These MSO exposures significantly increased glycogen content from 11.59±0.53 nmol/mg protein to 13.23±0.44 nmol/mg protein (n=7/8, p=.034).

For high K^+-SD, MSO pre-exposures (90-180 min) did not significantly influence SD propagation rate, when compared with interleaved controls (Figure 2.1E n=6, p=.46). In contrast, OGD-SD was significantly slowed by MSO (Figure 2.1F). As discussed below, MSO exposures prevented the onset of OGD-SD in some preparations, but in those where OGD-SD was generated, the effects on propagation rate appeared dependent on MSO exposure time. Propagation rates approximately halved with 180 minute pre-incubations, compared with interleaved controls (n=3/6, p=.02). Shorter (90 min) MSO incubations appeared to reduce SD propagation rate, but these effects were not significant (n=4/6, p=.16).

When taken together with effects of DAB/DNJ, these data suggest 1) that basal levels of astrocyte glycogen serve to limit the rate of SD and SD-like propagation, and 2) that supplementation of these stores above basal levels selectively decreases the propagation of SD-like events generated by substrate depletion.

2.4.3 Selective inhibition of astrocyte oxidative metabolism

Previous work has established that selective inhibition of astrocyte TCA cycle activity accelerated SD propagation (Largo et al., 1997a). Since glycogen stores are largely (if not entirely) restricted to astrocytes (Cataldo and Broadwell,

1986; Wender et al., 2000), we next examined whether disruption of astrocyte mitochondrial metabolism matched the effects of glycogenolysis inhibitors, under the same experimental conditions. Selective inhibition of astrocyte oxidative metabolism was achieved using fluoroacetate (FA) (Clarke et al., 1970), and compared with interleaved control slices as well as slices pre-exposed to sodium acetate (1 mM), which provided an additional metabolic substrate that could feed directly into the TCA cycle (Waniewski and Martin, 1998). For high K^+ and OGD-SD, FA pre-exposure (FA, 1 mM, 25 min) resulted in a significant acceleration of SD compared to both acetate pre-exposures and control conditions (Figure 2.2A-B, n=6, $p< .01$). This is consistent with prior work inhibiting astrocytic oxidative metabolism (Largo et al., 1997a) and when taken together with the results above, suggests that astrocyte ATP derived from different sources can regulate the spread of SD and related events.

2.4.4 Glucose (rather than glycogen) availability regulates onset of OGD-SD

Based on the significant effects on SD propagation, we next asked whether glycogen stores affect the initiation of SD-like events. OGD-SD occurs after a substantial (11.3±0.5 min) delay following the onset of OGD exposure, and this delay presumably reflects the time taken for depletion of metabolic substrates and cellular ATP, sufficient to result in loss of Na^+/K^+-ATPase activity leading to the induction of a feed-forward SD-like event (Jarvis et al., 2001). High K^+-SD is initiated virtually instantaneously, as the elevation of extracellular K^+ concentration is sufficient to generate SD, without localized metabolic depletion.

Therefore the subsequent studies concentrated on the latency to initiation of SD-like events generated by OGD alone.

Figure 2.3 shows the time course of development and consequences of OGD-SD in a population of slices. Simultaneous autofluorescence measurements and recordings of synaptic potentials were used to assess both mitochondrial redox potential and neuronal viability. Initial NAD(P)H fluorescence increases (contributed to by NADH increases as slice oxidative metabolism is impaired (Chance et al., 1962; Chance, 2004)), reached a plateau at 78.1±2.1% above basline, (Figure 2.3A). The passage of OGD-SD across the field of view was visualized as a transient dark band propagating across CA1 at a rate of 2.4±0.4 mm/min (see Fig 2.1B). In individual slices, this observed propagating wave of NAD(P)H autofluorescence coincided with abolition of postsynaptic fEPSP potentials. Prior to the initiation of SD, there was a brief period of electrical hyperexcitability within the slice that was promptly lost at SD onset, similar to the burst in spontaneous spike firing reported just prior to SD in previous studies (Herreras and Somjen, 1993). This loss of fEPSPs persisted, even after reintroduction of nACSF; suggesting that SD triggered by prolonged metabolic challenge in brain slice results in neuronal damage as previously described (Obeidat et al., 2000).

Consistent with previous reports of substrate dependence for single cell anoxic depolarizations (AD), the onset of SD was dependent on the availability of glucose, rather than oxygen. Slices were pre-exposed to either hypoxia or hypoglycemia for 10 minutes prior to 20 min OGD exposure (Figure 2.3B). While

pre-exposure to hypoxia did not significantly reduce the latency to SD when compared with interleaved controls (n=5/6), hypoglycemia significantly reduced the time to SD onset (n=6, p=.002).

Interestingly, pre-exposure to glycogen breakdown inhibitors DAB and DNJ (10 µM, 15 min), did not result in any decrease in the time to SD when compared to interleaved controls (Figure 2.4, n=6, p=.13). Even prolonged exposures to DAB/DNJ (100 µM, 75 min) did not significantly decrease SD latency to SD when compared with interleaved controls (11.7±0.5 min and 11.5±1.0 min respectively, n=6, p=.87), suggesting that depletion of basal glycogen stores within astrocytes does not contribute to OGD-SD onset. However, significantly increasing glycogen content with prolonged MSO exposures had a time-dependent effect on OGD-SD onset (Figure 2.4). Similar to the time-dependent effects of MSO on propagation rate, preparations subjected to shorter (90 min) 2 mM MSO pre-exposures did not show a significant difference in the time of SD onset when compared with interleaved controls (n=4/6, p=.095), but prolonged pre-exposures (180 min) resulted in a significant delay in the time to SD (n=3/6, p=.008).

2.4.5 2mM glucose pre-exposures

It has previously been suggested that extended (>60 min) exposures to reduced extracellular glucose concentrations (2 mM, rather than 10 mM) may effectively deplete astrocytic glycogen stores in hippocampal slices (Allen et al., 2005). We evaluated this possibility with glycogen measurements and effects on

SD initiation and propagation. There was a trend towards a decrease in total glycogen between samples exposed to 2 mM glucose versus normal ACSF (9.9±0.64 nmol/mg protein and 11.59±0.53 nmol/mg protein respectively, n=7, p=.065) and 2 mM glucose pre-exposures induced SD significantly earlier than the time to SD in interleaved control preparations (Figure 2.5A, n=6, p=.045). However, 2 mM glucose pre-exposed preparations showed no significant increase on the rate of SD across the CA1 when compared with interleaved controls during OGD-SD (Figure 2.5B, n=6, p=.88) or high-K^+ SD (Figure 2.5C, n=4, p=.79). Experiments where slices were pre-exposed to both 2 mM glucose and 10 µM DAB/DNJ (60 min) showed a decrease in SD latency and an increase in SD propagation rate that was not significantly different from pre-exposure to 2 mM glucose or DAB/DNJ alone suggesting there are no additive effects when inhibiting the utilization of glycogen stores prior to OGD (latency: 9.58±0.48 min and 9.68±0.84 min respectively, n=6, p=.92 and propagation: 4.6±0.5 mm/min and 4.7±0.4 mm/min respectively, n=6, p=.42). The contrasting effects of 2 mM glucose pre-exposures with the glycogenolysis inhibitors (see above) suggests that, although this procedure may somewhat deplete glycogen stores, the effects on reducing glucose availability may be much more important for regulating the initiation of SD.

2.5 Discussion

2.5.1 General

This study has addressed the involvement of glycogen stores and astrocytic metabolic function on both the initiation and propagation of SD and

related events in brain slices. Depletion of glucose availability (rather than glycogen stores) appeared more important for determining initial metabolic failure and the onset of SD-like events in experimental oxygen-glucose deprivation studies. In contrast, maintenance of astrocyte metabolism by glycogen stores appeared significant for limiting the rate of SD propagation through tissues in the ischemia model, and also in normoxic conditions. These findings support the possibility that targeting astrocyte glycogen stores could be of benefit in limiting the spread of SD-like events, through peri-infarct tissues in *in vivo* stroke models.

2.5.2 SD propagation rate

Astrocytic uptake of both glutamate and K^+ is likely an important regulator of the propagation of SD and SD-like events. There is evidence that extracellular accumulation of both of these mediators can contribute to the progression of SD (Somjen, 2001), and astrocytic uptake of glutamate (via GLT-1 and GLAST transporters) and K^+ (via K_{ir} channels and $Na^+/K^+/Cl^-$ cotransport) is well established (Walz and Hertz, 1984; Rothstein et al., 1996; Kofuji and Newman, 2004). Previous work using the astrocyte selective TCA cycle inhibitor fluorocitrate (FC) demonstrated the importance of astrocyte oxidative metabolism in setting the rate of SD propagation in rat cortex (Largo et al., 1997a), implying that ATP produced by mitochondrial respiration can be utilized to maintain electrochemical gradients required for transport functions at the advancing SD wavefront. Our results with fluoroacetate (FA) in hippocampal slices were similar, as a significant increase in propagation rate was observed with high K^+-SD in normoxic conditions. Pre-exposure to FA also accelerated the rate of OGD-SD.

Under these ischemia-like conditions, loss of oxygen availability is expected to inhibit utilization of TCA-derived substrates during OGD-exposures, and pre-exposures to FA are likely to accelerate depletion of other metabolic reserves (including astrocyte glycogen) prior to the onset of OGD.

Our results with pharmacological approaches to limit glycogenolysis (DAB/DNJ), suggest that ATP derived from astrocyte glycogen can also significantly contribute to limiting the propagation rate of high K^+-SD and OGD-SD. Inhibitor concentrations utilized for these studies were based on a previous preliminary report in slice preparations (Sadgrove et al., 2008), and no additional effects were observed in a secondary set of studies using higher inhibitor concentrations (100 µM) and more prolonged (75 min) exposures. The effectiveness of this could be due in part to cooperative effects of the inhibitors, as previously suggested (Kuriyama et al., 2008), and is consistent with effective inhibition of glycogenolysis with 10 µM exposures.

In the case of high K^+-SD, two observations suggest that adequate metabolic substrates are available in normoxic conditions to limit SD propagation. Neither supplementation of glycogen stores with MSO, nor provision of an additional substrate for oxidative metabolism (acetate) significantly slowed the propagation of high K^+-SD. In contrast, OGD-SD was significantly slowed by MSO exposures. If depletion of astrocyte metabolic reserves prior to the onset of SD-like events is sufficient to allow more rapid accumulation of extracellular K^+ and/or glutamate, then supplementation of glycogen reserves may be a useful strategy to limit the spread of these events in ischemic tissues. Glycogen is

recognized to be particularly useful in times of severe energy depletion, since it does not require ATP for initiation of glycolysis (Brown, 2004), and there is also the possibility that astrocytes could provide glycogen-derived glucose to neurons (Rossi et al., 2007). It has recently become appreciated that SD-like events can occur repetitively in the ischemic brain in both animal models and humans (Hartings et al., 2003; Dohmen et al., 2008; Lauritzen et al., 2011). Glycogen stores are known to be reduced in ischemic tissues prior to SD onset and also completely depleted by SD-like events in *in vivo* rat brain (Selman et al., 2004). Therefore, these stores could be a particularly useful target to limit the progression and/or metabolic consequences of repetitive depolarizing events.

2.5.3 SD initiation

OGD-SD occurred in all preparations with a delay of ~11 min. We found that both complete (0 mM) and partial (2 mM) removal of glucose prior to OGD decreased the latency to OGD-SD, while removal of O_2 alone had no effect. This implies that the dependence on extracellular glucose for initiation of AD in single cells during similar OGD challenges (Allen et al., 2005), also applies to initiation of propagating SD events. One possibility is that the delay to SD onset is due to the time taken to deplete astrocytes of glycogen stores (Allen et al., 2005). However, the combination of pharmacological and substrate depletion studies completed here suggest that this may not be the case. On the contrary, it appears that depletion of tissue glucose availability (rather than glycogen stores) is responsible for setting the time to OGD-SD onset. It remains to be determined

whether it is depletion of glucose in all cell types or solely in neurons that is most relevant.

Interestingly, increasing glycogen stores within slice preparations during prolonged MSO exposures prior to OGD resulted in a significant increase in the time to SD onset, and in half of the preparations pre-exposed to MSO, OGD-SD events were completely prevented. It is noted that despite the lack of a propagating SD, there were still clear signs of neuronal damage in these preparations. This is not unexpected in extended OGD exposures, when all substrate must eventually be consumed. It is likely that, under these conditions single cell neuronal depolarizations occurred stochastically and astrocytes had sufficient energy substrate to prevent the accumulation of glutamate and/or K^+ to SD threshold levels. It is possible that the effects observed following prolonged MSO exposures could be due to the depletion of vesicular glutamate, since it is known that MSO may also disrupt glutamate-glutamine cycling in hippocampal slice preparations (Laake et al., 1995; Liang et al., 2006). Significant depletion of glutamate could inhibit the onset of SD by preventing extracellular glutamate concentrations from reaching threshold levels. However, if this were underlying the observed effects of MSO on OGD-SD initiation and propagation, similar results would be expected under normoxic high K^+-SD as well. Since no effects of MSO were observed on high K^+-SD threshold or rate of spread, it is suggested that the effects of MSO are not likely due to vesicular depletion. Taken together these results suggest that while basal levels of glycogen may not be able to limit SD initiation during extreme stress conditions such as OGD, pharmacologically

increasing glycogen stores may be able to sufficiently fuel astrocyte function to prevent these depolarizing events in the context of ischemia.

The relevance of these results to in *in vivo* studies is not yet determined, but it is possible that the regulation of SD onset by astrocytes may be even more apparent *in vivo*, since in those preparations astrocyte-mediated buffering and transport of K^+ to vessels may be an additional contributor to reducing SD threshold (Newman et al., 1984; Amedee et al., 1997).

2.5.4 Implications for SD in normoxic and ischemic conditions

In regions where glycogen levels are depleted, SD events may be able to propagate more readily into previously healthy tissue. Prior to each SD event, astrocytes in penumbral tissues, which will have a range of substrate depletion (Lipton, 1999), may have less glycogen available to provide additional substrate required for glutamate and/or K^+ clearance from the extracellular space. Thus, maintenance of glycogen levels within astrocytes may be critical in preventing the spread of SD events through moderately compromised tissue and the stepwise expansion of the core following ischemic injury. It is not yet known how changes in propagation rate may affect the expansion of injury. DC shift duration and SD frequency are well established to correlate injury progression (Dijkhuizen et al., 1999; Lauritzen et al., 2011), but could not be assessed in the current study. Thus, only single SDs could be induced in conditions leading to damage (OGD) and continuous recordings of evoked field potentials limited the ability to reliably measure DC shifts. These parameters would be useful to assess in future

studies. It is noted that even in otherwise healthy tissue, normoxic SD leads to a prolonged decrease in extracellular glucose concentrations, and repetitive depolarizations lead to a stepwise depletion of this substrate *in vivo* (Hashemi et al., 2008). It is not yet known whether this significantly contributes to or may be part of a consequence of glycogen depletion.

As noted above, recent clinical recordings have strongly implicated SD-like events in the progression of stroke injury. The current studies emphasize the importance of astrocyte metabolism in preventing the spread of SD-like events both under normoxic and ischemic conditions, suggesting that these cells may provide a novel therapeutic target for the prevention of SD-like events in clinical settings.

2.5.5 Acknowledgements

We thank Dr. R Dietz for his intellectual contribution to initial hypoxia and hypoglycemia pre-exposure studies. We are grateful to Dr. G Bonvento for his thoughtful discussion and helpful suggestions in these studies.

2.6 Figure Legends

2.6.1 Figure 2.1

Effects of modifying astrocytic glycogen on high K^+-SD and OGD-SD. **(A)** Characteristic negative voltage shift produced by the initiation of SD (arrow) by 1M KCl microinjection **(B)** Similar DC shift potential by OGD exposures. **(C-D)** Visualization of high K^+-SD and OGD-SD propagation using NAD(P)H autofluorescence imaging. Advancing wavefront indicated by arrows (see text for

details). Inset at top left panel is a bright field image of the preparation, followed by 11 consecutive panels showed at 2.5s intervals (numbers indicate the time from SD onset). R: recording electrode, S: KCl delivery electrode. Scale bar: 500µm. **(E)** Rates of high K^+-SD after pre-exposure to either DAB/DNJ combinations (15 min) or MSO (90-180 min). Rates in 10µM DAB/DNJ were significantly faster than interleaved controls, but no difference was observed between 2mM MSO and interleaved controls. **(F)** Rates of OGD-SD were significantly increased by DAB/DNJ, and greatly reduced by prolonged (180min) MSO pre-exposures (n=6, **p<.01 and *p<.05).

2.6.2 Figure 2.2

Effects of fluoroacetate (FA) or acetate on high K^+-SD and OGD-SD. (A) Pre-exposures with 1mM FA significantly increased the rate of high K^+-SD when compared with both control and 1mM acetate pre-exposures. **(B)** FA also significantly increased OGD-SD propagation rates in preparations pre-exposed to 1mM FA when compared with control and 1mM acetate preparations (n=6, *p<.05).

2.6.3 Figure 2.3

Effects of substrate removal on OGD-SD initiation. (A) Mean effects of OGD on NAD(P)H autofluorescence signals and evoked fEPSPs recorded simultaneously in the same preparations. OGD-SD occurred on average at 11.3±0.5 min and propagated at an average rate of 2.5±0.4 mm/min. Prior to onset of OGD-SD, NAD(P)H initially increased due to inhibition of mitochondrial

respiration, stepped down during the progression of OGD-SD, and then continued to decline to levels below the initial baseline, even after restoration of oxygen and glucose. **(B)** Effects of pre-exposures on OGD-SD latency. Slices were pre-exposed to either 10 min hypoxia alone or 10 min zero glucose alone prior to subsequent OGD exposures. OGD-SD latency was significantly reduced by prior glucose reduction, but not pre-exposure to hypoxia (n=6, **p<.01).

2.6.4 Figure 2.4

Effects of modifying astrocyte glycogen on latency to OGD-SD onset. Pre-exposure with glycogenolysis inhibitors, DAB/DNJ (10μM, black bars) did not significantly affect the time to OGD-SD compared with interleaved controls. Pre-exposure with 2mM MSO (striped bars) did not significantly effect the time to SD onset with 90 min pre-exposures, but did result in significant delays to OGD-SD latency following 180 min pre-exposures (n=6, *p<.05).

2.6.5 Figure 2.5

Effects of extended exposures to reduced glucose on OGD-SD and high K^+-SD. Slices were pre-exposed to modified ACSF with 2mM glucose rather than 10mM for ≥60min prior to subsequent OGD exposures. Reduced glucose pre-exposure resulted in significant reduction in OGD-SD latency **(A)**, but had no effect on rates of propagation for either OGD-SD **(B)** or high K^+-SD **(C)** (n=6, *p<.05).

2.6.6 Supplemental Figure 2.1

A glucose standard curve was generated to ensure that all tissue glycogen measurements fell along the detectible range of the curve. Glucose standards ranged from 0.01-100µg/ml. Following all exposure paradigms (with the exception of 20 min OGD which completely depleted glycogen stores) tissue glycogen fell between 3-10µg/ml on the glucose standard curve. All measurements were normalized to protein levels to calculate final glycogen content in nmol glucose/mg protein.

Figure 2.1

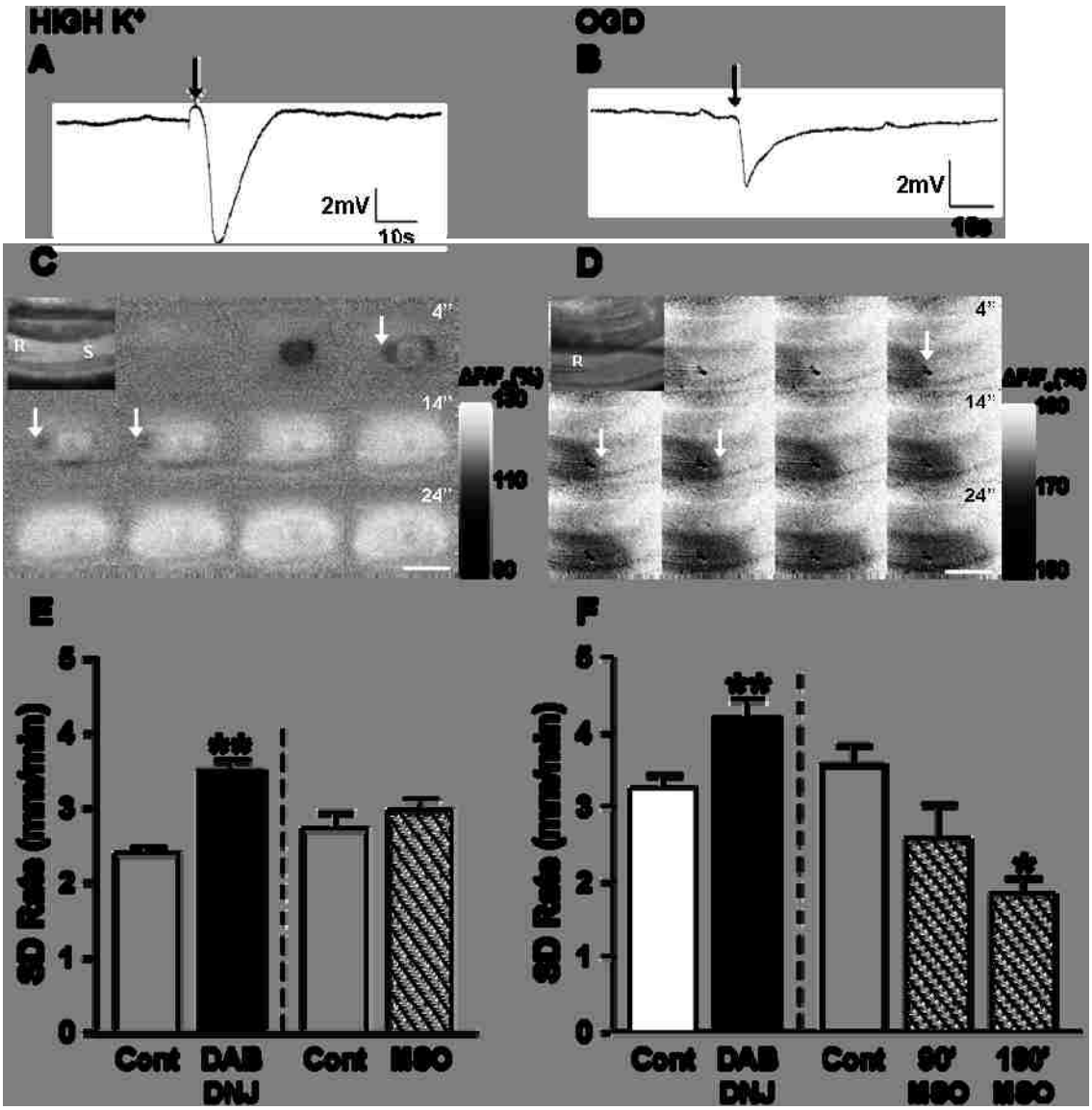

Figure 2.2

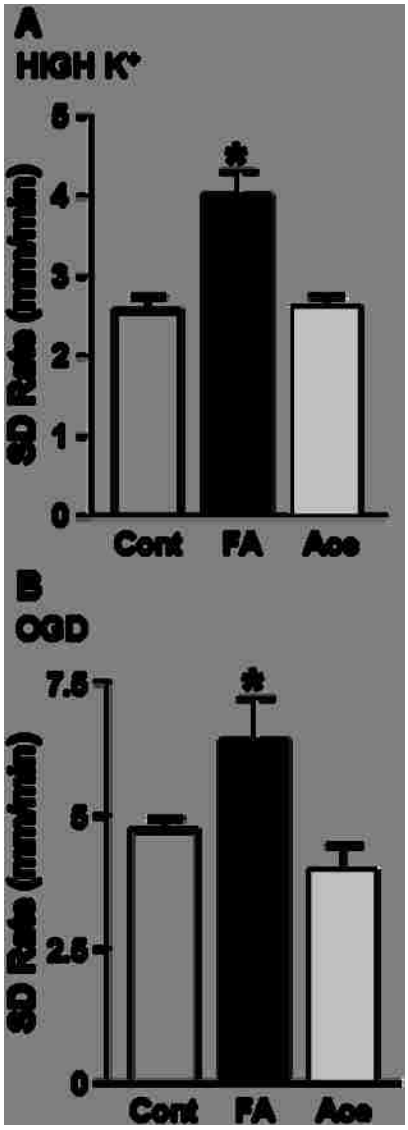

Figure 2.3

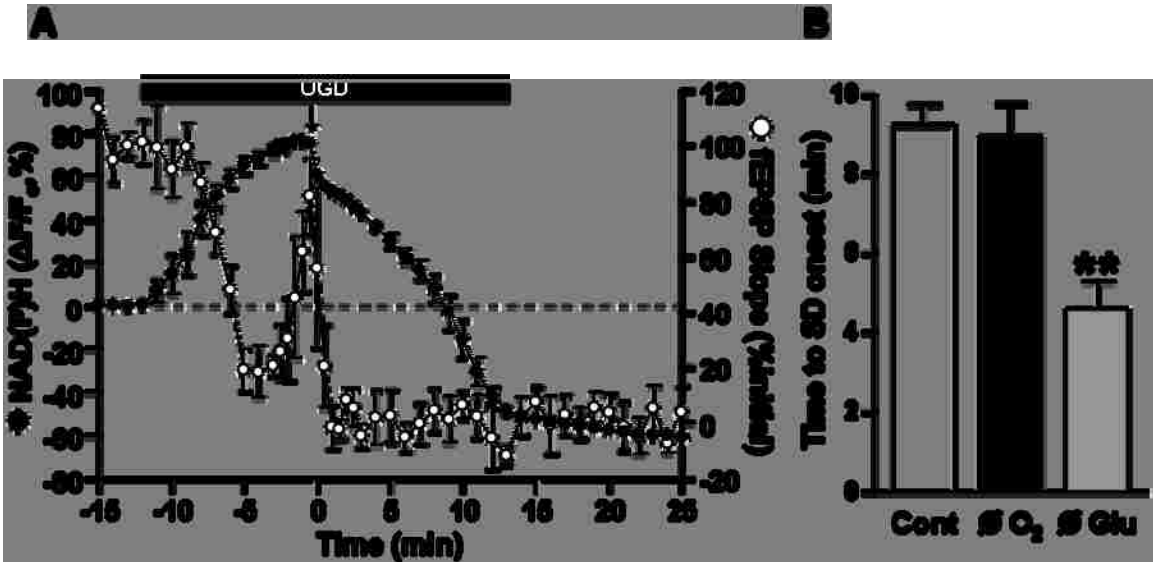

Figure 2.4

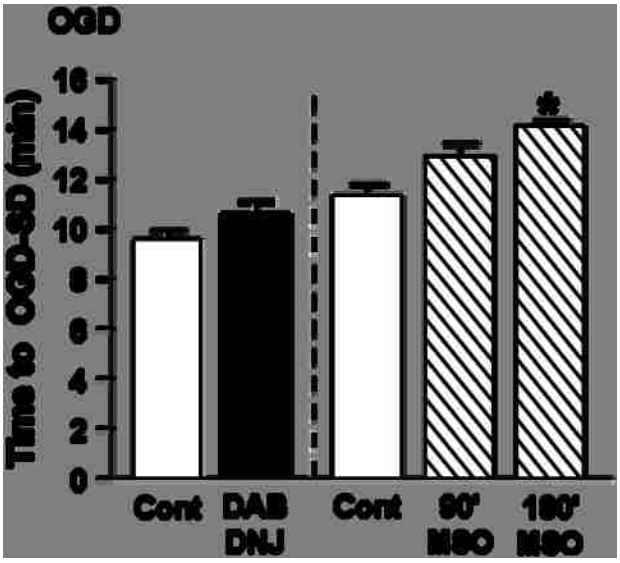

Figure 2.5

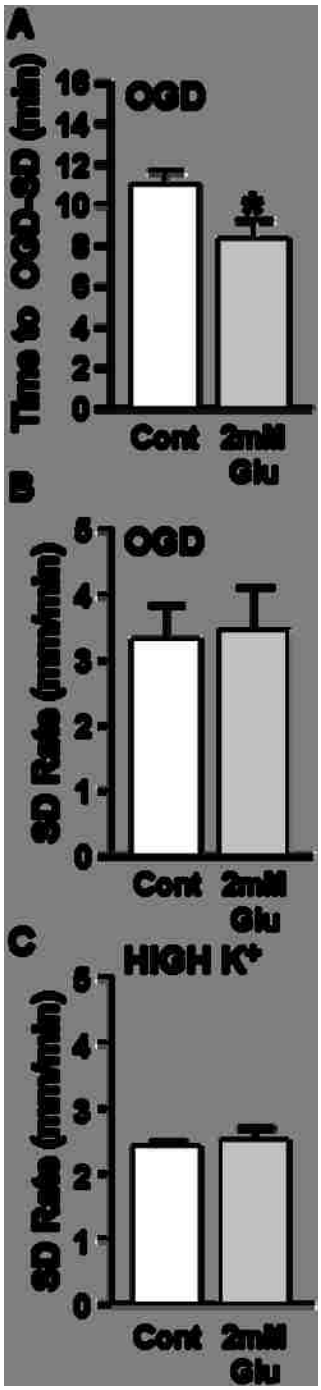

Supplemental Figure 2.1

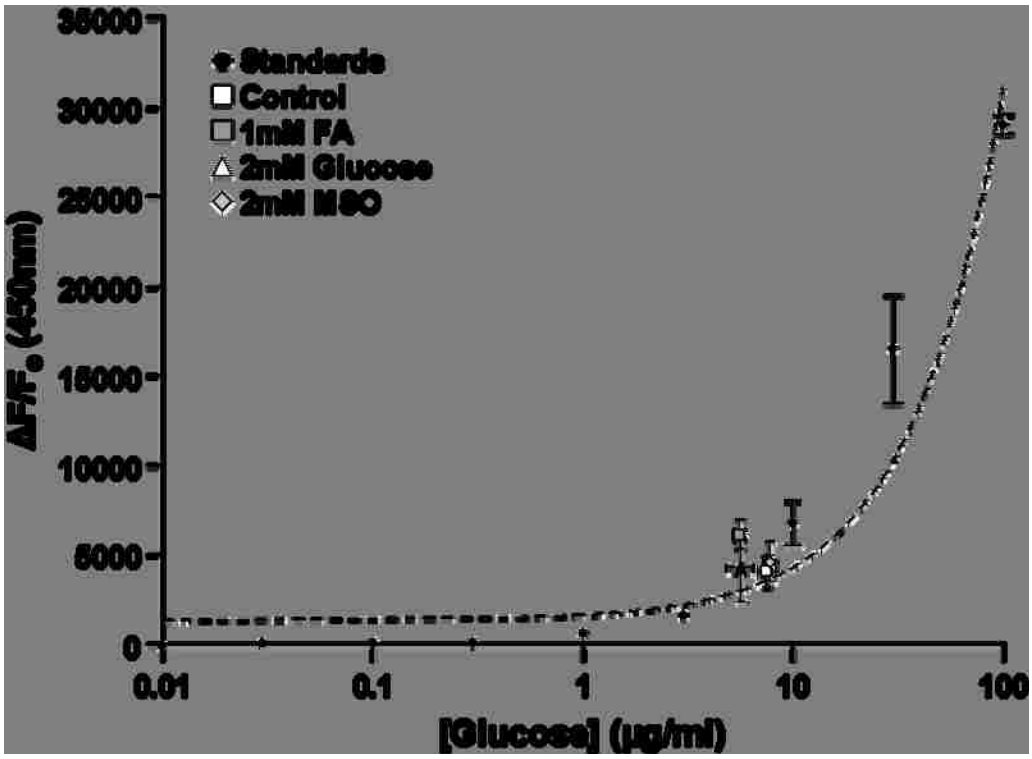

3. Increased threshold for spreading depression-like events in hippocampal slices with CNTF-activated astrocytes

J.L. Seidel[1], M. Faideau[2,3], Ulrike Pannasch[4], G. Bonvento[2,3] & C.W. Shuttleworth[1]

1 Dept. Neurosciences, University of New Mexico School of Medicine, Albuquerque NM 87131

2 CEA, I2BM, MIRCen, Fontenay-aux-Roses, France

3 URA CEA CNRS 2210, Fontenay-aux-Roses, France

4 INSERM U840, Collège de France, Paris, France

Prepared for submission to “PLoS One”

3.1 Abstract

3.1.1 Background

Astrocyte activation is concurrent with many different forms of CNS injury including ischemia, yet the role these cells in the pathophysiology underlying these injuries is not well understood. Previous work has shown that localized activation of astrocytes can be achieved and neuroprotective *in vivo* by constitutive expression and release of ciliary neurotrophic factor (CNTF) in rat striatum using gene transfer. It is not yet known what effects such CNTF exposures have on excitability and potentially noxious stimuli within other regions of the brain. In the present study we examined the effects of CNTF astrocyte activation in murine hippocampal slice preparations.

3.1.2 Methodology / Principal Findings

After injection of a lenti-viral vector encoding CNTF into the hippocampus, activation of astrocytes was verified by the significant upregulation of glial fibrillary acidic protein (GFAP) compared to a control vector encoding LacZ. No significant changes in neuronal density or intrinsic excitability were observed in CA1 neurons, but excitatory postsynaptic potentials (fEPSPs) were significantly reduced in CNTF tissues. This effect was not mediated by a reduction of glutamate release probability or enhanced glutamate clearance by activated astrocytes. The consequences of reduced excitatory transmission were tested on the pathophysiological phenomenon of spreading depression (SD). SD was invariably generated following localized K^+ microinjections in control

preparations, but never obtainable in CNTF preparations with K^+ stimuli. CNTF-injected tissues were capable of generating SD by other stimuli, as demonstrated with the Na^+/K^+-ATPase inhibitor ouabain; although the latency for SD onset was significantly longer and the mean propagation rate significantly slower compared to control.

3.1.3 Conclusions/Significance

These data are consistent with the hypothesis that CNTF lenti-viral injections can lead to strong sustained activation of astrocytes in hippocampus, and this activation is associated with a decrease in excitatory synaptic transmission, which may underlie the increased threshold for SD in these preparations.

3.2 Introduction

It is well appreciated that astrocytes are not a static population of cells, but can undergo substantial changes in structure and function due to a wide range of stimuli. Transformation to an “activated” phenotype has been described following brain injury, and this involves marked upregulation of the structural proteins glial fibrillary acidic protein (GFAP), nestin, and vimentin (Kalman, 2004; Pekny and Nilsson, 2005). Strong increases in astrocyte GFAP labeling have been described in peri-infarct regions in rats following middle cerebral artery occlusion (Chen et al., 1993; Li et al., 1995) and in postmortem tissues from human stroke patients (Zhao et al., 2006), but it is not yet known how activation of astrocytes influences the spread of ischemic damage in these tissues. Whether activated

astrocytes contribute to damage or provide neuroprotection has been difficult to determine; perhaps in part because, while morphological alterations appear to be fairly universal, there is significant heterogeneity in the functional changes associated with astrocyte activation depending on the stimulus (Escartin and Bonvento, 2008).

Recent studies have begun to explore the functional roles of astrocytes with different models of activation. One study utilized high-titer transduction of enhanced green fluorescent protein to achieve an activated phenotype within the hippocampus, resulting in increased excitatory synaptic transmission, attributed to decreased GABA availability due to reduced glutamate-glutamine cycling in astrocytes (Ortinski et al., 2010). It is not yet known whether longer-term (months) activation of astrocytes might also disrupt excitatory transmission, since glutamate pools have also been shown to be sensitive to changes in glutamate-glutamine cycling (Laake et al., 1995; Rae et al., 2003). *In vitro* stimulation with CNTF leads to astrocyte activation (Hudgins and Levison, 1998), and in an alternative approach to achieve longer-term activation of astrocytes, this has been extended to *in vivo* studies by exploiting lenti-viral infection of neurons to constitutively express and release CNTF in the striatum (Escartin et al., 2006; Escartin et al., 2007). The effects of CNTF astrocyte activation within the hippocampus are unknown. These studies sought to determine if this model of astrocyte activation resulted in any changes in neuronal excitability and if any such changes would impact the susceptibility of cells to the pathophysiological phenomenon of spreading depression (SD).

SD is characterized as a wave of severe depolarization that can propagate throughout CNS tissue and result in suppression of electrical activity, disruption of ion homeostasis, and increased energy metabolism in both neurons and astrocytes (Leao, 1944; Hansen, 1985; Somjen, 2001). Previous work has also shown that repetitive SD events alone (in the absence of ischemia or other noxious stimuli) can increase GFAP expression in astrocytes (Kraig et al., 1991; Bonthius and Steward, 1993; Wiggins et al., 2003), but little is currently known of the functional consequences of this activation. We examine here whether lenti-viral infection with CNTF 1) resulted in sustained astrocyte activation, 2) significantly modified neuronal excitability, and 3) was associated with changes in SD threshold within hippocampal slice preparations. The results demonstrate persistent activation of hippocampal astrocytes following lentiviral-mediated gene delivery of CNTF *in vivo* for prolonged periods, with a significant decrease in excitatory neuronal transmission and a coincident large elevation in SD threshold in hippocampal slice studies. These effects raise the possibility that some forms of astrocyte activation may strongly influence the spread of SD events in injured brain tissue that may ultimately lead to neuroprotection.

3.3 Materials and Methods

3.3.1 *In vivo* CNTF expression

Expression and release of CNTF in the mouse hippocampus was achieved by adaptation of a lenti-viral approach recently described for rat striatum (Escartin et al., 2006; Escartin et al., 2007). Self-inactivated lentivirus encoding the human CNTF gene with the export sequence of Ig, were

constructed, purified, and titrated as previously described (de Almeida et al., 2001). Bilateral hippocampal injections (1 µl per hippocampus at 0.1 µl/min) were made in male C57Bl/6 mice, aged 5-7 weeks using the following stereotactic coordinates: anteroposterior -2 mm from bregma; lateral +/-2 mm; ventral 1.3 mm. All experimental procedures were performed in strict accordance with the recommendations of the European Commission (86/609/EEC) concerning the care and use of laboratory animals and animals were used within 21 weeks of age. Throughout the study, an equal number of age-matched control animals were studied. These controls were injected with lentivirus encoding the β-galactosidase gene (LacZ) at the same time as injection of CNTF animals. Equal numbers of CNTF and LacZ experiments were interleaved throughout the course of the study.

Immunohistochemical detection of β-galactosidase was used to determine the distribution of transgene expression in a sample of LacZ control animals (see **Fig 1**). Following perfusion fixation (4% paraformaldehyde), brains were post-fixed overnight, cryoprotected with 30% sucrose and then sectioned at 30 µm thickness using a freezing sliding knife microtome. Floating sections were permeabilized (0.1% Triton X-100), blocked (5% normal donkey serum) and incubated with mouse anti-β-galactosidase antibody (1:100, University of Iowa Developmental Studies Hybridoma Bank, overnight at 4^{o}C) and antigen then localized with FITC-conjugated secondary antibody (1:250; Jackson ImmunoResearch Laboratories, West Grove, PA).

3.3.2 Brain slice preparation

Brain slice preparation was as previously described (Dietz et al., 2008), and followed procedures authorized by the University of New Mexico Animal Care and Use Committee. Briefly, mice were deeply anesthetized with a mixture of ketamine and xylazine, brains removed and cooled in an ice-cold cutting solution (containing, in mM: 2 KCl, 1.25 NaH_2PO_4, 6 $MgSO_4$, 26 $NaHCO_3$, 0.2 $CaCl_2$, 10 glucose, 220 sucrose and 0.43 ketamine), hemisected and then coronal slices cut at 250 or 350 µm using a Vibratome. After recovery for 1 hour at 34°C in ACSF (containing, in mM: 126 NaCl, 2 KCl, 1.25 NaH_2PO_4, 1 $MgSO_4$, 26 $NaHCO_3$, 2 $CaCl_2$, and 10 glucose, equilibrated with 95%O_2 / 5%CO_2), the ACSF was changed again and slices were held at room-temperature (~23°C) until transfer to the recording chamber. Individual slices were then superfused with oxygenated ACSF at 2 ml/min at 35^{o}C and recordings made from the hippocampal CA1 region. For *in vitro* studies, numbers refer to the number of slices, with a maximum of three slices from an individual animal used for each experimental condition.

The degree of astrocyte activation was assessed by GFAP immunohistochemistry in the same slices as used for electrophysiological studies. Slices were not re-sectioned, and extended antibody incubation periods were required for adequate penetration into the slice, using methods previously described (Hoskison and Shuttleworth, 2006). Briefly, slices were fixed (4% paraformaldehyde), blocked (10% normal goat serum) and exposed to mouse anti-GFAP-Cy3 (1:200; 48 hr at 4^{o}C, Sigma Aldrich). After thorough washing,

nuclei were labeled with DAPI (300 nM, 10 min, Invitrogen, Carlsbad, CA) and slices were mounted with Gel Mount and examined using a Zeiss 510 Meta confocal microscope (Carl Zeiss, Thornwood, NY, USA). Astrocyte counts were made of GFAP and DAPI positive soma within the region of interest in the CA1 stratum radiatum, from an image stack (300x300 µm, 20 µm depth) centered above the apex of the upper blade of the dentate gyrus. Identical image acquisition parameters were used for each preparation. In some studies, dendritic density was assessed by using microtubule associated protein-2 (MAP2) immunohistochemistry as previously described (Hoskison and Shuttleworth, 2006). After fixation and washing, thick slices were incubated in anti-MAP2 antibody (AP-20; 1:500, for 48 hr at 4^{o}C), and primary antibody localized by using goat anti-FITC (1:200; 24 hours at 4°C).

3.3.3 Postsynaptic potentials and intracellular recordings

Excitatory post synaptic potentials (fEPSPs) were characterized following stimulation of Schaffer collateral inputs. A bipolar electrode (25 µm tip) was used to apply single shocks (80 µs pulse, 10 s interpulse interval, 0.0-0.32 mA, using a constant-current stimulus isolation unit Isoflex, AMPI, Israel) and fEPSPs were recorded using extracellular glass microelectrodes placed in stratum radiatum, ~150 µm from the pyramidal cell body layer. Recording electrodes were 3-5 MΩ when filled with ACSF. For tests of drug action, the stimulus intensity for test pulses was chosen as 50% of maximal amplitude, based on input/output curves generated in each slice. Paired pulse facilitation was measured at a range of interpulse intervals (50-300 ms). Slopes were measured from 20-80% of the

maximal response and then the ratio of the two fields was determined (fEPSP2/fEPSP1).

Characterization of CA1 membrane properties were made from intracellular recordings using sharp microelectrodes (~100 MΩ Ohm when filled with 3M KCl) as previously described (Shuttleworth and Connor, 2001). Impalements were accepted if neurons required less than 100 pA of negative current injection to maintain stable resting membrane potentials more negative than 65 mV, and injection of depolarizing current pulses produced activation potentials that overshot 0 mV. After stable impalements were achieved, neurons were allowed to recover at least 10 min before characterization of input resistance, action potential threshold and characteristics of action potential trains.

3.3.4 Stimulation and recording spreading depression (SD) in hippocampal slice

SD threshold was determined by using localized microinjections of KCl as described in (Dietz et al., 2008) with minor modifications. A conventional whole-cell patch electrode (tip resistance 3-5 MΩ) was placed 50 µm below the slice surface in stratum radiatum, and microinjections of KCl (1 M) were triggered by brief (10-200 ms) pressure pulses delivered by a PicoPump (SYS-PV830, World Precision Instruments). In other studies, SD was produced by inhibition of Na^+/K^+/ATPase activity by superfusion of the slice with ouabain (100 µM).

SD was characterized as a sharp drop in DC potential (Somjen, 2001), as measured with an extracellular recording electrode placed in stratum radiatum (45 µm below the slice surface, ~300 µm from the KCl ejection electrode).

Recording electrodes were identical to KCl ejection electrodes, but filled with ACSF. Signals were amplified (Neurodata IR-283), digitized (Digitata 1322A, Axon Instruments, Union City, CA) and analyzed using Axoscope software (v 8.1, Axon Instruments).

The propagation of high K^+-SD across slices was monitored by autofluorescence imaging using excitation at 450 nm (150 ms), emission 535±25 nm using a monochromator-based imaging system (Till Photonics) with a cooled interline transfer CCD camera (IMAGO, Till Photonics). Imaging at this wavelength produces a mixed signal during SD. Initial autofluorescence increases provided a measure of initial depolarization and mitochondrial activation (flavoprotein associated), and were used to assess the degree of tissue activation following K^+ application. The spread of large, delayed fluorescence decreases provided a robust measure of swelling associated with spreading SD events (see supplemental data). Studies of ouabain-SD did not require assessment of initial mitochondrial redox changes, and required lower-power observation of both neocortex and hippocampus, and therefore ouabain-SD propagation was tracked by using changes in light transmittance (>575 nm) as previously described (Andrew et al., 1999).

3.3.5 Astrocyte coupling in hippocampal slices

Acute transverse hippocampal slices (300 µm) were prepared as previously described (Rouach et al., 2005) from 12 weeks old C57BL6 mice injected with lenti-LacZ (n=3) or lenti-CNTF (n=3) and were maintained at room

temperature in a storage chamber that was perfused with ACSF containing (in mM): 119 NaCl, 2.5 KCl, 2.5 $CaCl_2$, 1.3 $MgSO_4$, 1 NaH_2PO_4, 26.2 $NaHCO_3$ and 11 glucose, saturated with 95 % O_2 and 5 % CO_2, for at least one hour prior to recording. Slices were transferred to a submerged recording chamber mounted on an Olympus BX51WI microscope equipped for infra red-differential interference (IR-DIC) microscopy and were perfused with ACSF at a rate of 1.5 ml/min at room temperature. Cells in the stratum radiatum were identified as astrocytes based first on morphologic criteria second on electrophysiologic properties (Rouach et al., 2008). Somatic whole-cell recordings were obtained using 5-10 MΩ glass pipettes filled with (in mM): 105 K-gluconate, 30 KCl, 10 HEPES, 10 phosphocreatine, 4 ATP-Mg, 0.3 GTP-Tris, 0.3 EGTA (pH 7.4, 280 mOsm). For intercellular coupling experiments, the internal solution contained biocytin (2 mg/ml), which diffused passively in astrocytes during 20 min in current-clamp mode. Immediately after recording, slices were fixed with 4% paraformaldehyde in PBS for 12 h at 4°C. During biocytin experiments, membrane potential and resistance were measured from patched astrocytes (LacZ: -67.5±3.1 mV (n = 4) and CNTF -70.2±2.7 mV (n = 5); LacZ: 8.4±2.2 MOhm and CNTF: 7.1±2 MOhm respectively). Biocytin was localized by incubating slices in TRITC-conjugated streptavidin (Invitrogen, Carlsbad CA). After several washes, slices were mounted in Fluoromount (Southern Biotechnology) and examined with a confocal laser-scanning microscope (Leica TBCS SP2). Stacks of consecutive confocal images taken at 0.5 µm intervals were acquired using a helium/neon laser at 543 nm and Z projections were

reconstructed using Leica Confocal Software. Manual cell counting was performed with Image J software.

3.3.6 Reagents and Solutions

Except where noted, all drugs and salts were obtained from Sigma Chemical Co. (St Louis, MO). Phosphate buffered saline (PBS) was from Invitrogen (Carlsbad, CA, USA). Antibodies were diluted in PBS supplemented with 2% Triton X-100 (PBST) and including 3% normal goat serum. 8-Cyclopentyl-1,3-dipropylxanthine (DPCPX, 200 μM stock) was dissolved in DMSO and stored at -20^{o}C until use. Ouabain was dissolved in ACSF (100 μM). Neurobiotin (1%) was dissolved in normal intracellular solution containing the following, in mM: 135 K-gluconate, 8 NaCl, 1$MgCl_2$, 10 HEPES, 2Mg^{2+}-ATP.

3.4 Results

3.4.1 CNTF activation of hippocampal astrocytes

Figure 3.1A shows that intrahippocampal stereotaxic injection of the VSV-G pseudotyped lenti-viral vector encoding LacZ resulted in effective transduction of hippocampal neurons as observed with β-galactosidase immunostaining. High β-galacotosidase expression was observed in nerve cell bodies in CA1 and CA2 subregions, the dentate granule cells and hilus, but was not observed in brain regions outside the hippocampus, including the neocortex. A similar distribution of β-galactosidase labeling was observed throughout the rostro-caudal axis of the hippocampus in two animals examined (data not shown).

Injection of CNTF-expressing lenti-viral vector resulted in strong activation of hippocampal astrocytes, as demonstrated by increases in GFAP-like immunoreactivity. Individual astrocytes showed a marked increase in thickness of the main GFAP-positive immunoreactive processes, when compared with LacZ injected controls, and naïve (non-injected) animals (Fig 3.1B). This was assessed in thick brain slices prepared as for electrophysiological analysis (see Methods) and verified throughout the course of the study in preparations from each animal used for electrophysiological recording. Figure 3.1C quantifies the mean area occupied by GFAP fluorescence in 8 CNTF preparations, to demonstrate significant increases compared with LacZ and non-injected controls (n=8,8,7 respectively). Animals used for quantitative analysis were 8-12 weeks post-injection, and in additional studies it was shown that CNTF preparations at 16 weeks post-injection continued to show elevated GFAP expression. Figure 3.1C also plots the average density of astrocytes in the three types of preparation, and shows no significant difference between CNTF, LacZ, and non-injected control preparations (measured in a 300x300x20 µm volume). Together, these results suggest that CNTF expression resulted in localized, long-term activation of astrocytes by transformation of the resident population of astrocytes in the hippocampus, rather than proliferation of progenitor cells. These findings are consistent with previous conclusions from CNTF-lentiviral injections in rat striatum (Escartin et al., 2006; Escartin et al., 2007) and suggest that this approach is useful for subsequent *in vitro* slice studies of the consequences of hippocampal astrocyte activation on spreading depression (SD).

Astrocyte coupling was compared in LacZ and CNTF preparations since previous work has shown that disruption of gap junctional networks can both increase and decrease SD propagation (Nedergaard et al., 1995; Theis et al., 2003). Dye coupling in astrocyte networks was determined by injection of biocytin into a single astrocyte and counting the number of coupled cells based on diffusion of the tracer, but no significant difference in the degree of coupling was observed between the two types of tissues (27.9±4.4 vs. 26.0±3.5 coupled cells n=8 for LacZ and n=9 for CNTF).

3.4.2 Effects on neuronal structure and excitability

Previous reports of astrocyte activation resulted in decreased GABAergic transmission within the hippocampus (Ortinski et al., 2010), we examined whether glutamate-mediated synaptic transmission was modified in CNTF tissues. Excitatory postsynaptic potential (fEPSPs) recorded in area CA1 were significantly decreased in CNTF preparations, throughout the range of stimulus intensities tested (Figure 3.2A, LacZ n=7, CNTF n=6). Normalization of fEPSPs to maximal responses in each preparation showed that the stimulus intensity required for half-maximal responses was not significantly different (LacZ: 146±6 µA and CNTF: 149±4 µA), implying a significant difference in efficacy, rather than sensitivity. Single cell recordings from CA1 pyramidal neurons also showed a significant difference in fEPSCs in CNTF preparations when compared with LacZ controls (Figure 3.2B).

It was possible that CNTF lenti-viral injections could be significantly altering neurons in some way that could account for the decrease in excitatory transmission, so we next examined the arrangement of CA1 pyramidal neurons and found that CNTF expression did not lead to readily demonstrable changes in the packing density or structure of CA1 neurons. Estimates of CA1 pyramidal cell number were made from DAPI counts of nuclei in stratum pyramidale of confocal stacks (10 µm thickness) and showed no significant difference between CNTF and LacZ controls (Figure 3.3A, 9160±331 cells/mm^2 and 8920±838 cells/mm2 respectively, n=5, p=.797). The density of apical dendritic projections (as calculated from MAP-2 immunoreactive processes in 20x150x10 µm confocal stacks centered 200 µm from stratum pyramidale) also showed no significant differences between CNTF and LacZ preparations (Figure 3.3B, 11905±2926 dendrites/mm^3 and 10068±923 dendrites/mm^3 respectively, n=5, p=.566).

Intrinsic membrane properties of CA1 neurons (assessed from intracellular recordings) were also not significantly different between the CNTF and LacZ groups. When tested at a resting membrane potential of -65 mV, input resistances were almost identical (87.5±10.8 and 92.7±10.84 MΩ for LacZ and CNTF, respectively; n=10 and 12, p=0.74) and depolarizing current pulses (100-500 pA) produced very similar trains of action potentials (no significant difference in number of events, p=0.24) and degrees of spike frequency adaptation during long stimuli (Figure 3.3C).

There are several possible mechanisms, which may underlie the decrease in fEPSP observed. We first addressed the possibility that CNTF preparations

had reduced presynaptic glutamate release. In order to test this hypothesis, paired-pulse facilitation (PPF) was performed at a range of interpulse intervals (Figure 3.4A, 50-300 ms, n=6). We found no significant differences between LacZ and CNTF preparations suggesting that differences in initial presynaptic glutamate release probability are unlikely to underlie differences in the amplitude of evoked synaptic potentials. Another possible mechanism underlying the decrease in fEPSPs could be an increase in activated astrocytes ability to clear glutamate from the synaptic cleft. To test this hypothesis, single cell recordings were made from astrocytes in both CNTF and LacZ preparations. No significant differences were observed in GLT-1 currents when normalized to the fEPSC amplitude (Figure 3.4B) suggesting astrocytes in CNTF preparations are not able to remove glutamate more effectively from the synapse and decreasing availability to the post synaptic cells. We next tested whether the reduced fEPSP slope could be due to increased presynaptic adenosine A1 receptors activation in CNTF tissues. Astrocytes are likely a primary source for extracellular adenosine accumulation (Halassa et al., 2009) and presynaptic A1 receptor activation effectively inhibits glutamate release and may contribute to neuroprotection (e.g. Dunwiddie and Masino, 2001; Martin et al., 2007; Canals et al., 2008). However the difference in synaptic efficacy between CNTF and LacZ tissues was not resolved by blocking adenosine A1 receptor activation using the selective A1 receptor antagonist 8-cyclopentyl-1,3-dipropylxanthine (DPCPX, 200 nM). DPCPX increased fEPSP slopes in both CNTF and LacZ preparations at the half-maximal stimulus intensity (Figure 3.4C, (86±7% and 106±2% increase in CNTF

and LacZ preparations respectively, n=5 for both). However, fEPSPs were still significantly smaller in CNTF preparations when DPCPX was present when compared with control LacZ preparations. These results imply that differences in adenosine accumulation are not sufficient to explain the change in synaptic efficacy in CNTF preparations and are consistent with the conclusion of PPF studies that initial glutamate release probability is not reduced in CNTF tissues. Changes in synaptic transmission could be a result of decreased glutamate-glutamine recycling or changes in postsynaptic receptors.

3.4.3 Increased SD threshold in CNTF preparations

The decrease in synaptic transmission could have many downstream mechanisms. We chose to investigate the possible effects on the pathological phenomenon of SD since glutamate receptor activation can contribute to the spread of SD (Somjen, 2001). SD was reliably triggered by localized microinjections of KCl in all LacZ preparations. Localized KCl pulses of progressively increasing duration were used to estimate the threshold for onset of these all-or-none events, and they revealed a threshold from 30-100 ms in LacZ preparations (n=18). SDs were recorded as a sharp negative shift in extracellular DC potential at a recording site ~300 μm from the KCl injection site (Figure 3.5A). The propagation of SD in LacZ preparations was readily monitored by large autofluorescence decreases that propagated across the CA1 region (Figure 3.5B). In the LacZ preparations these signals spread at least as far as the edge of the field of view (~1300 μm in 7/11 preparations) with average propagation rate in LacZ preparations was 3.85±0.21 mm/min (n=18). In the case

of LacZ preparations, SDs generated by KCl microinjection were fully recoverable, and could be evoked repetitively at 10 minute intervals in these slices.

In contrast, K^+ injections never induced SD in slice preparations from CNTF-injected mice. No DC shift was recorded (Figure 3.5C, Fig 3.6A) over the range of stimuli that were effective in LacZ tissues, and even when the K^+ stimulus was increased by using much longer pulses (500 ms Fig 3.6B), no propagating event was observed optically (Fig 3.5D) or recorded with extracellular electrodes. Previous reports have shown that modest $[K^+]_e$ (8 mM) increases can significantly reduce the threshold for SD in tissue resistant to the propagating wave by increasing neuronal excitability (Funke et al., 2009). However, when extracellular K^+ levels were raised to 8 mM (from 2 mM) SD still could not be induced in CNTF preparations (data not shown, n=2). The lack of spreading events in all CNTF preparations was confirmed by analysis of the spread of delayed autofluorescence decreases that occurred after K^+ ejection. These relatively sustained autofluorescence decreases are a consequence of tissue swelling that accompanies tissue depolarization. After they became established within 10 s of the K^+ stimulus, there was no further spread of the signals. The fluorescence decreases are therefore likely to represent the consequences of passive spread of K^+ from the stimulating electrode.

Comparison of initial components of autofluorescence transients also suggested that the lack of high K^+-SD in CNTF preparations was not due to differences in effective depolarization of the tissue surrounding the stimulating

electrode. Initial autofluorescence (E_x 450 nm) increases following KCl ejection are matched by NAD(P)H autofluorescence (E_x 360 nm) decreases, and therefore provide an indication of mitochondrial redox potential changes in stimulated tissue (Shuttleworth et al., 2003). Consistent with similar initial activation, we found no significant difference in initial autofluorescence transients between LacZ and CNTF preparations (7.2±0.6% and 7.9±1.1% respectively at 100 ms K^+ pulse, p=.49).

3.4.4 Increased threshold, rather than inability to generate SD

To determine whether CNTF-activation of astrocytes resulted in a generalized inability to generate SD in slice preparations or alternatively whether there was a more selective increase in high K^+-SD threshold, we examined responses to extended exposures of slices to ouabain (100 µM). Ouabain inhibits Na^+/K^+-ATPase activity and is known to be an effective stimulus of SD in hippocampal slices (Basarsky et al., 1998; Dietz et al., 2008). In LacZ preparations, SDs were induced in all preparations 3.9±0.3 min after ouabain reached the bath and propagated at a rate of 4.08±0.96 mm/min (Figure 3.7A, n=5). SD was also generated in all CNTF preparations, although the latency to SD onset was significantly longer (5.42±0.32 min) and the mean propagation rate was significantly slower (Figure 3.7B, 2.28±1.26 mm/min, n=6, p=.002). As an internal control, we simultaneously measured SD in the adjacent neocortex (using intrinsic optical imaging for these low power imaging studies, see Methods). Ouabain-SD propagation rates in neocortex were not significantly different between CNTF and LacZ slices (3.62±0.60 mm/min and 3.78±0.69

mm/min respectively, n=6,5, p=0.69), consistent with the hypothesis that differences in ouabain SD were selectively related to CNTF-activated astrocytes in hippocampus.

3.5 Discussion

The main conclusions from this study are 1) that a CNTF expression model can be used to successfully produce strong sustained activation of astrocytes in the hippocampus, suitable for subsequent slice electrophysiological studies, 2) excitatory transmission within CNTF preparations is significantly decreased and may be due to reduced glutamate-glutamine cycling and 3) SD threshold is substantially elevated in tissues with activated astrocytes. These findings are consistent with the hypothesis that astrocyte activation may contribute to neuroprotection in some neurological or neurodegenerative disorders where SD is known to contribute to the expansion of injury.

3.5.1 CNTF model for astrocyte activation

In mature astrocytes, CNTF triggers a cascade of intracellular events involving the JAK-STAT pathway that leads to the generation of an activated phenotype (Bonni et al., 1997; Hudgins and Levison, 1998). CNTF is normally expressed by astrocytes in the mature brain, with little (if any) neuronal expression. Our experimental model involves transduction of neurons with a CNTF expression system, so that the factor is now expressed in these cells. Because the CNTF construct includes an immunoglobulin export sequence, it does not accumulate within neurons, but is released in the extracellular space

(up to 1ng/mg protein, see (de Almeida et al., 2001). All cell types within the CNS express the CNTFRα, making it possible that some of the effects observed in this model may not be astrocyte specific. Studies both *in vitro* and *in vivo* tested the effect of CNTF on hippocampal neurons during both excitotoxic and ischemic injury respectively, and showed that the neurotrophic factor provided significant neuroprotection during both types of injury (Wen et al., 1995; Semkova et al., 1999). However, these studies were unable to determine whether these neuroprotective effects were mediated by specific changes within neurons and/or astrocytes. CNTF may also act as a pro-survival factor by restricting apoptotic cell death in oligodendrocytes, which suggests a possible protective role for CNTF in inflammatory demylinating diseases such as multiple sclerosis (Louis et al., 1993; Cagnon and Braissant, 2009). Our results demonstrate robust and sustained activation of murine hippocampal astrocytes by CNTF, as has been described previously following injection of the same lenti-viral construct into rat striatum (Escartin et al., 2006; Escartin et al., 2007; Beurrier et al., 2010). Because hippocampal slices are so widely used for electrophysiological studies, this model could be useful to assess functional consequences of astrocyte activation on many aspects of neuronal-glial interactions. This model may also be particularly relevant when discussing ischemic injury since previous work has shown an increase in both CNTF and CNTFRα expression following transient occlusion (Lin et al., 1998). More generally, these studies provide a model for modifying gene expression *in vivo* that may then be translated to a commonly used *in vitro* model. *In vivo* lenti-viral injections into the hippocampus allow for

constitutive, long term expression of a gene of choice, which could then be used for *in vitro* hippocampal slice studies.

3.5.2 Consequences of CNTF exposure on astrocyte and synaptic function

Increased GFAP immunolabeling is a well-established anatomical hallmark of astrocyte activation following a range of stimuli (Kalman, 2004; Pekny and Nilsson, 2005), yet the associated functional changes are not well characterized and are likely to be different depending on the inducing stimulus. There is an ongoing debate about the contribution of astrocyte activation to neuronal survival or to cell death following CNS injury. On the one hand, astrocytes may exacerbate injury by secreting pro-inflammatory factors and forming a glial scar, which can prevent regrowth of neuronal processes (Swanson et al., 2004). However, there is also increasing evidence supporting the hypothesis that astrocytes promote neuronal survival following injury (Sendtner et al., 1994; Li et al., 2007), and experiments where activation is inhibited in mice subjected to MCAO resulted in infarct sizes three times larger than in littermate controls (Li et al., 2008). Importantly, astrocytes have been shown to remain in this activated phenotype more than a month following transient cerebral ischemia (5 min); making these cells a useful target for therapeutics following ischemic injury (Choi et al., 2010).

We found a significant decrease in synaptic efficacy in studies of stimulation of glutamatergic inputs from Shaffer collateral fibers to CA1 pyramidal neurons. Paired pulse facilitation studies suggested that this effect was not due

to a decrease in the initial probability of transmitter release. The possibility of decreased vesicular release was further tested using the A1 receptor antagonist, DPCPX. One of the many ways in which astrocytes modulate synaptic activity is by the release of adenosine at the synapse to decrease presynaptic release of glutamate (Dunwiddie and Masino, 2001; Pascual et al., 2005). However, addition of DPCPX did not restore CNTF fEPSPs to similar levels as LacZ preparations, which provides additional support to the PPF data suggesting that decreased synaptic efficacy was not a result of decreased probability of vesicular release. Recent work has evaluated a range of functional consequences linked to astrocytes activation by CNTF in the striatum. CNTF over-expression produced a redistribution of astrocytic glutamate transporters, GLAST and GLT-1, into raft functional membrane microdomains, which are believed to be important for efficient glutamate uptake (Escartin et al., 2006). However, our single cell recordings from astrocytes suggest that enhanced glutamate uptake is likely not to contribute significantly to the decreased excitatory transmission or resistance to SD of CNTF-exposed tissues.

We hypothesize that the changes observed in synaptic transmission are due to decreased glutamate-glutamine cycling within astrocytes resulting in decreased glutamate within presynaptic neurons. Previous work in hippocampal slice culture has shown significant decreases in glutamate in pre-synaptic terminals when glutamate-glutamine cycling is inhibited within astrocytes (Laake et al., 1995). As mentioned above, a recent study showed decreased GABAergic transmission in preparations where activated astrocytes had reduced glutamate-

glutamine cycling (Ortinski et al., 2010). Inhibitory transmission was restored following brief bath application of exogenous glutamine at a high concentration (10 mM). However, it has been shown that at physiological levels (0.5 mM), prolonged glutamine exposures showed no significant effects on synaptic transmission and at higher concentrations (2-5 mM) prolonged exposures resulted in an attenuation of synaptic transmission and the induction of SD in some preparations at 34°C (An et al., 2008). In other experiments conducted at room temperature, SD was not induced after prolonged glutamine exposures at 4 mM (Kam and Nicoll, 2007). Due to the wide variability in conclusions made from exogenous glutamine exposures, the apparent importance of glutamine may depend on the specific experimental method since metabolic demands, anatomical relationship, and other factors may determine the degree of a neuronal populations' dependence on the glutamate-glutamine cycle (Kam and Nicoll, 2007; An et al., 2008). It does appear that GABA neurotransmitter pools depend on astrocyte-derived glutamine for GABA synthesis to a greater extent than glutamatergic synapses, which could depend more on direct reuptake and/or have a greater cytoplasmic reserve pool (Fricke et al., 2007; Ortinski et al., 2010).

In the context of ischemia, differences between sensitivities of glutamatergic and GABAergic transmission to glutamine may have a profound effect on the progression of post-stroke injury. This initial phase of excitotoxicity and hyperexcitability (due to GABA depletion), may precede a delayed decrease in excitatory transmission in the days following the initial infarct. Importantly, such

a decrease in excitatory transmission may underlie the resistance to SD we observe in CNTF slice preparations (see below).

3.5.3 Changes in SD threshold

SD threshold is determined by progressively increasing the intensity of electrical or K^+ stimulation to the brain surface or brain slice. In our studies, we characterized the threshold for SD using graded, localized KCl microinjections, delivered by pressure pulses of increasing duration from a conventional patch electrode. Rapid and localized extracellular K^+ elevations are expected to depolarize a population of cells, and subsequent glutamate and/or K^+ release from these cells is thought to underlie the feed-forward propagation of the SD event (Kager et al., 2000; Somjen, 2001). Once initiated, SD then progressed slowly (~3-5 mm/min) from the injection site, and if generated in otherwise healthy tissue, the depolarizing event is fully recoverable (Nedergaard and Hansen, 1988). While SD threshold could be readily determined in each LacZ control slice (generally between 30-100 ms pulse duration), SD could never be induced with KCl in CNTF preparations, even with very prolonged K^+ stimuli and elevations in extracellular K^+ concentrations (8 mM). This striking difference was not due to differences in the K^+ microinjection, since the same delivery electrodes were utilized for paired CNTF and LacZ studies on individual recording days, and autofluorescence studies of mitochondrial activation indicated similar degrees of slice activation at the K^+ ejection site (Supplemental data). These observations suggested instead that there was a greatly increased threshold for SD initiation with the K^+ stimulus, or possibly a complete inability of CNTF preparations to

allow propagation of SD waves. Previous studies have shown an increase in connexin 43 expression with CNTF infection in rat striatum (Escartin et al., 2006) which could increase astrocyte gap junctional coupling. However, we found no significant differences in astrocyte coupling in the present studies suggesting that differences in K^+ buffering within the astrocytic network, or other consequences of changes in coupling between astrocyte are not major contributors to effects of CNTF. It is possible that increased connexin 43 expression could result in an increase in hemichannels on astrocytic membranes, which could potentially increase the ability of a single astrocyte to clear local K^+ even if there is not an enhancement in the ability to siphon it to neighboring astrocytes. This could be important under *in vivo* conditions where astrocytes can connect with the local vasculature and clear K^+ into the bloodstream, but this would not explain the effects on SD threshold in slice preparations shown here.

Subsequent experiments with bath application of ouabain revealed that CNTF tissues do retain the ability to generate SD, albeit with a significantly longer latency to onset and significantly slower propagation rate than was observed in LacZ controls. By confirming that CNTF tissues retain appropriate structural and functional properties required for SD, this observation provides a useful control for the high K^+ studies. In addition, the fact that ouabain triggers SD by a very different mechanism (inhibition of Na^+/K^+-ATPase) provides insight into possible mechanisms by which CNTF limits SD. The concentration of ouabain used here is expected to inhibit the major Na^+/K^+-ATPase isoforms found in both neurons and astrocytes (α3 and α2, respectively) (Watts et al.,

1991), and has previously been shown to reliably generate SD in hippocampal slices (Haglund and Schwartzkroin, 1990; Basarsky et al., 1998; Balestrino et al., 1999; Dietz et al., 2008). Inhibition of Na^+/K^+-ATPase in neurons will lead to rapid depolarization and extracellular K^+ and glutamate elevations. The main difference between ouabain and high K^+ stimuli is that ouabain will also lead to a significant impairment in Na^+-dependent glutamate uptake by astrocytes as a consequence of Na^+/K^+-ATPase inhibition. However, a decrease in the overall glutamate pool (as suggested by our fEPSP results) in CNTF tissues could be sufficient to prevent the propagation of high K^+-SD and would explain the increased latency and slower propagation of ouabain-SD.

3.5.4 Activation of astrocytes by SD and ischemia

A number of studies have described astrocyte activation following SD, as demonstrated by strong increases in GFAP immunolabeling in the affected tissue (Kraig et al., 1991; Wiggins et al., 2003). This association between SD and astrocyte activation has been demonstrated most clearly in studies of repetitive application of K^+ in otherwise healthy brains. Activation occurred within 6 hours of induced SD events and persisted for at least one week post-SD (Kraig et al., 1991; Bonthius and Steward, 1993; Wiggins et al., 2003). There have been few studies of the consequences of astrocyte activation following SD, but it is noteworthy that a recent preliminary report describes a progressive increase in SD threshold when rats are repetitively challenged by SD (Sukhotinksky et al., 2008) as well as studies where preconditioning with SD showed a correlation between reduced cortical infarct volume following MCAO and increase in GFAP

expression (Matsushima et al., 1998). Our results raise the possibility that astrocyte activation itself could underlie SD threshold increases, when animals are subjected to repetitive SD *in vivo*.

Recent work has provided increasing support for the hypothesis that repetitive SD events are common following animal and human stroke (Hartings et al., 2003; Dohmen et al., 2008), and that the metabolic consequences of SD contribute to the enlargement of stroke injuries (Iijima et al., 1992; Busch et al., 1996). It is not yet known whether SD events associated with ischemia contribute to the well-described activation of astrocytes in peri-infarct regions in animal models of stroke (Chen et al., 1993; Li et al., 1995) or in postmortem tissues from human stroke patients (Zhao et al., 2006). However our observations of greatly elevated SD threshold in tissues with CNTF-activated astrocytes suggest that periinfarct activated astrocytes could serve to limit the spread of SD into healthy brain tissue following stroke. As noted above, decreases in glutamate-glutamine cycling may contribute to elevated SD thresholds, and it will be of interest to examine these and other mechanisms in future studies, in particular, using *in vivo* ischemia models. The present results in slice do provide evidence consistent with an important supportive role for astrocytes, and suggests that maintaining normal astrocytic function in compromised tissue may be valuable for preventing repetitive depolarizing events, which contribute to the expansion of neuronal injury.

3.5.5 Acknowledgements

We thank Isamu Aiba for assistance with some of the intracellular recordings and analysis, and Dr. T. VanderJagt for whole-cell neurobiotin loading of neurons.

3.6 Figure Legends

3.6.1 Figure 3.1

Astrocyte activation within murine hippocampus. A. Representative distribution of β-galactosidase immunohistochemistry demonstrates that intrahippocampal lentivirus injections lead to infection localized within the hippocampus, and high power confocal images of the CA1 and dentate gyrus showing localization to neuronal cell bodies (30 µm cryostat section, scale bar: 1mm and 100 µm respectively). **B.** GFAP immunohistochemistry: Low power confocal projections (20 µm thick) were used to quantify changes in either total astrocyte number or simply increases in GFAP expression within resident astroscytes in hippocampal slice preparations (250 µm sections) from mice injected with lenti-CNTF versus lenti-LacZ as well as none injected controls (top panel, n=8/8/7). Representative high power confocal images (20 µm thick) show increased GFAP within single astrocytes from CNTF hippocampal slices versus LacZ and controls (bottom panel). (GFAP: red, DAPI: blue, Scale bars: top panel 100 µm, bottom panel 50 µm). **C.** Quantification of area expressing GFAP and total astrocyte density. There was a significant increase in GFAP expression in CNTF preparations when compared with both LacZ and non-injected controls ($F(2,22)=5.049$, $*p=.017$, One-way ANOVA with Tukey's post-hoc test), but no

significant difference in total number of astrocytes (F(2,22)=.968, p=.40, One-way ANOVA with Tukey's post-hoc test). **D.** Representative low-power images from slice preparations where single astrocytes were loaded with biocytin to assess astrocytic coupling (scale bar: 150 µm). When the number of coupled cells were counted, there were no significant differences in astrocyte coupling between LacZ and CNTF preparations (t(15)=.335, p=.74, independent t-test).

3.6.2 Figure 3.2

CNTF astrocytes activation results in reduced synaptic efficacy. A. Input-output curves were generated from the slope of fEPSP at increasing currents (0.0-0.3 mA, 0.02 mA interval) (left) and representative fEPSPs at half maximal amplitude are shown (right). There was a significant decrease in the slope of the fEPSPs in CNTF hippocampal slices when compared to LacZs (n=6 and n=7 respectively, F(2,10)=4.32, *p<.05). **B.** Single cell recordings were made from pyramidal neurons within the CA1 cell layer. CNTF preparations showed a significant decrease in fEPSCs when normalized to the pre-synaptic fiber volley.

3.6.3 Figure 3.3

Effects of CNTF lentiviral injections on pyramidal neurons within the hippocampus. A-B. Confocal stacks (10 µm thick) processed for MAP-2 (green) to determine dendritic density within the *sr* and the nuclear stain DAPI (blue) to determine neuronal density within the CA1 pyramidal cell layer. Representative images from the *sp* show similar neuronal density between LacZ and CNTF preparations (scale bar: 20 µm) and low-power images of the entire CA1 region

show no demonstrable changes in dendritic density (region centered 200um from stratum pyramidale, scale bar: 50 µm). **C.** Intrinsic membrane properties of neurons were also not significantly different between CNTF and LacZ controls.

3.6.4 Figure 3.4

Reduced fEPSPs not due to decreased probability of presynaptic glutamate release or increased glutamate clearance by astrocytes. A. Paired pulse facilitation (PPF) was measured at a range of interpulse intervals (50-300 ms), and no significant differences were observed between CNTF and LacZ preparations suggesting that the decrease in fEPSP slope was not a result of decreased presynaptic vesicular glutamate release ($F(4,40)=.289$, $p=.884$, repeated measures ANOVA, n=6). **B.** Single cell recordings from astrocytes determined that there was no significant difference in glutamate current through the GLT-1 transporter in LacZ and CNTF preparations**. C-D.** Input-output curves were generated in preparations both pre- and post- exposures to the A1 receptor antagonist (DPCPX, 200 nM) to determine if the decrease in synaptic efficacy in CNTF preparations was adenosine dependent (C) and representative fEPSPs at half maximal amplitude are shown both pre- and post-DPCPX (D). Bath application of DPCPX significantly increased fEPSPs in both CNTF and LacZ preparations (at half maximal stimulus intensity (0.14 mA), $F(1,8) = 5.94$, $p=.04$, repeated measures ANOVA, n=5), but CNTF fEPSPs were still significantly smaller that LacZ preparations ($F(1,8)= 6.42$, $*p<.05$, repeated measures ANOVA, n=5).

3.6.5 Figure 3.5

Inhibition of SD in slices with CNTF-activated astrocytes. A. Representative DC recordings from LacZ preparations during 50 ms, 100 ms, and 200 ms KCl microinjections with 10 min intervals between stimuli. Recordings (R) were taken ~300 µm from the KCl injection site (S) as shown in bright field images in top corner of montages (B). **B.** Representative montage of 450 nm autofluorescence during the 100 ms KCl microinjection (shown electrically in A) from the LacZ preparation which resulted in the propagation of SD across the preparation beyond the field of view (~1300 µm). **C.** Representative DC recording from a CNTF preparation where KCl microinjections up to 200 ms in duration did not result in SD. **D.** Representative 450 nm autofluorscence recording during the 100 ms KCl microinjection from the CNTF preparation where the initial passive depolarization due to the exogenous KCl application occurred, but no propagating SD event.

3.6.6 Figure 3.6

A. SD threshold determined with high K^+ microinjections (1M KCl). In LacZ slices SDs were induced in all preparations by the longest K^+ microinjection (200 ms) (n=18/18). The same stimuli did not generate an SD in any CNTF preparations (n=0/18). **B.** Distance of the final tissue depolarization in CNTF preparations versus the initial passive depolarization due to the spread of exogenous K^+. CNTF preparations showed no significant differences between the passive K^+ depolarization (white triangles) and the final response (white

boxes), providing further support for the lack of SD in CNTF preparations (n=12, dashed line represents the average distance of the view frame).

3.6.7 Figure 3.7

During 100 µM ouabain exposures, both electrical recordings and intrinsic optical signals were used to measure SD in the *sr* of the CA1. **A.** Although SD could be induced in all CNTF preparations (n=6), the latency to SD was significantly longer when compared to LacZ controls (n=5) ($t(14)=4.19$, $p=.001$, independent t-test). **B.** The rate of propagation was also significantly slower in CNTF preparations when compared to LacZ slices ($t(14)=-3.89$, $p=.002$, independent t-test).

3.6.8 Supplemental Figure 3.1

NAD(P)H autofluorescence has been widely used to visualize the spread of SD and similar events *in vivo* and in brain slice (Strong et al., 2000; Shuttleworth et al., 2003; Takano et al., 2007). We chose to near-simultaneously optically measure both NAD(P)H and AF_{450} in order to better understand the biphasic NAD(P)H response which results in an initial rapid oxidizing event followed by a slower "overshoot" that is confounded by swelling. **A.** Representative NAD(P)H and AF_{450} kinetics from a LacZ preparation where SD occurred. The initial rapid oxidizing event (AF_{450}) could not be used to measure the propagation of SD since it was no longer visible in most preparations by 300 µm away from the stimulating electrode (black trace (stimulating electrode) versus green trace (300 µm)). Additionally, changes in the NAD(P)H "overshoot"

phase were difficult to distinguish over baseline due to swelling (blue and red traces). However, the slower AF_{450} response was amplified by the optical artifact of swelling (black and green traces). **B.** Population data from LacZ preparations (n=7) determined that, as suggested by the representative traces in A, the initial AF_{450} oxidizing response decreased in intensity rapidly and was overcome by the swelling response in almost all preparations (black bars), while the slower response showed a stable intensity across the entire slice (white bars), and is easy to visualize due to the additive effects of the swelling response.

3.6.9 Supplemental Figure 3.2

K^+ spread versus SD in a LacZ preparation. **A.** DC electrical recording 50 µM from stimulating electrode of both a sub-threshold depolarizing event and an SD event. At 50ms there was a negative voltage shift, but it lacked the characteristic saddle shape indicative of SD which was observed with the 100 ms K^+ microinjection. **B.** AF_{450} at 50 ms showed the local passive depolarization due to the K^+ microinjection while when SD was induced with the 100 ms microinjection, the AF_{450} decrease propagates across the slice.

Figure 3.1

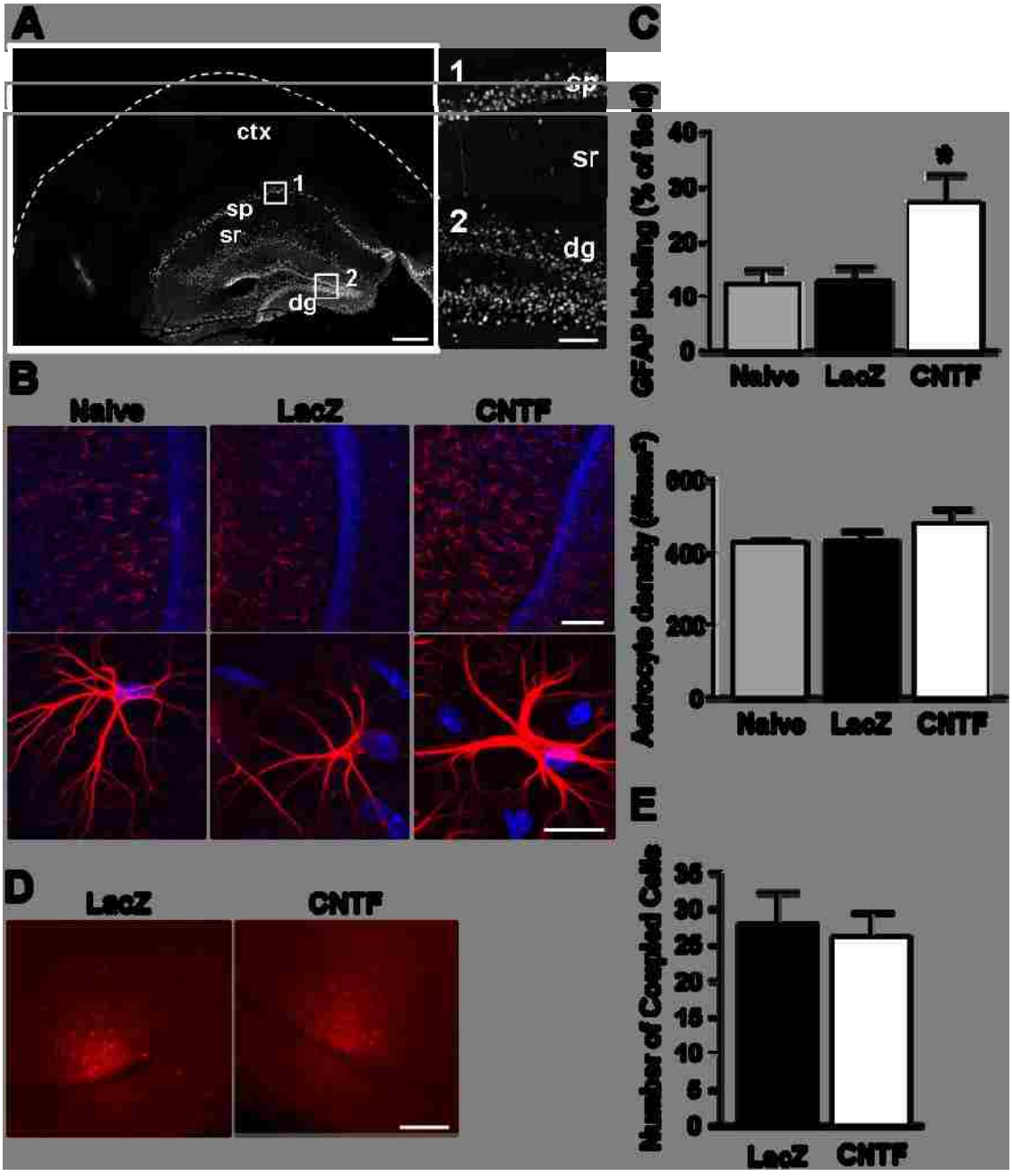

Figure 3.2

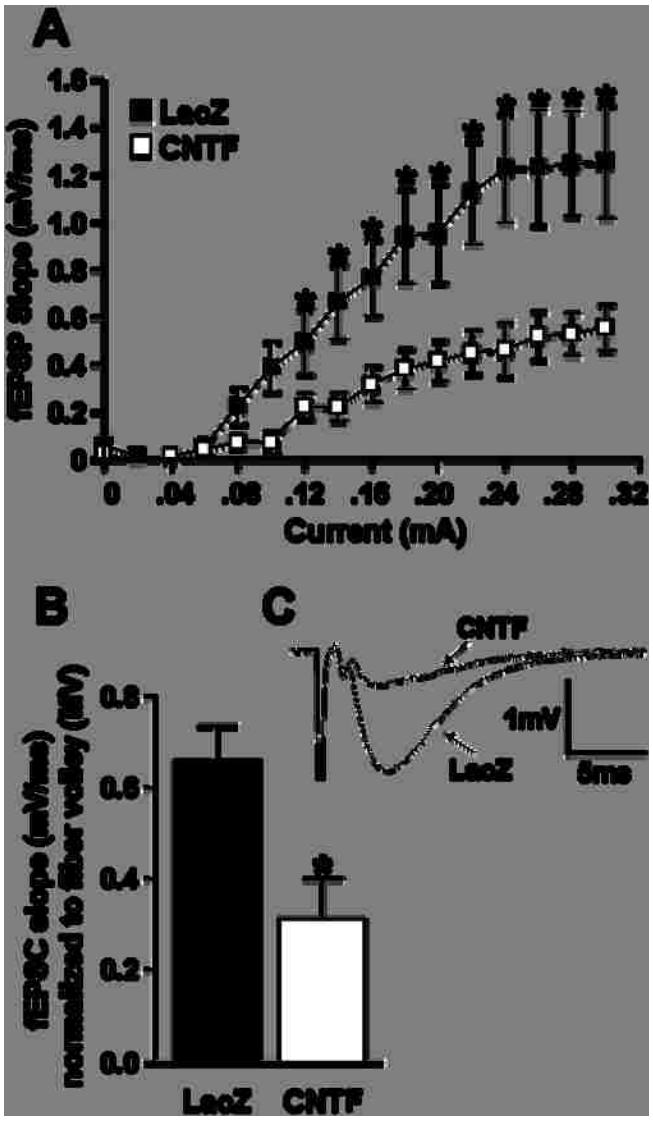

Figure 3.3

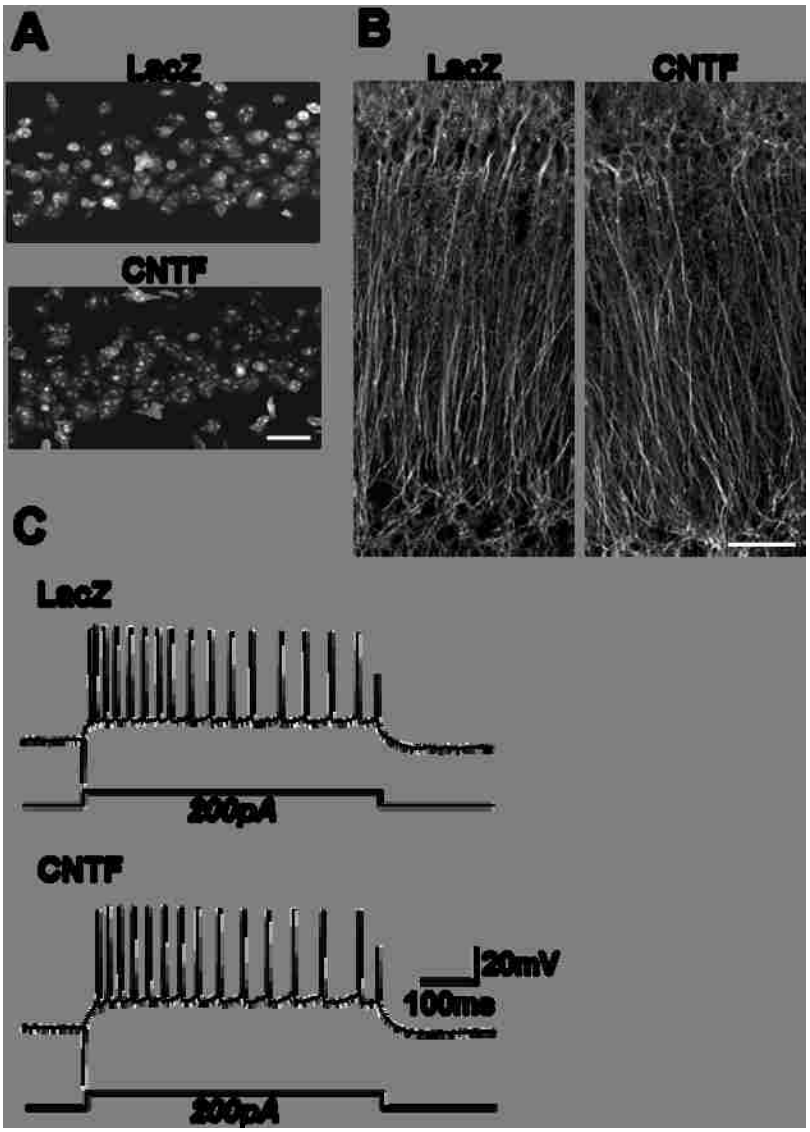

Figure 3.4

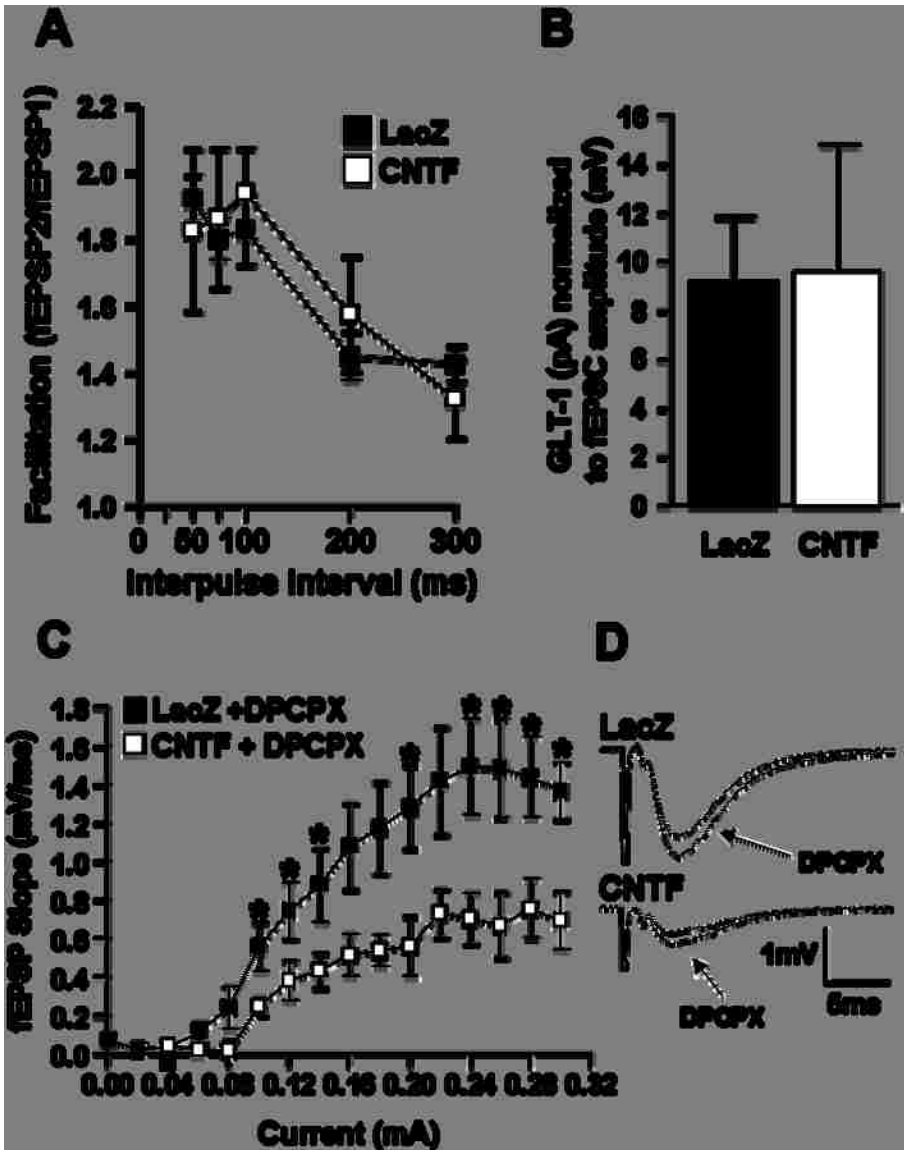

Figure 3.5

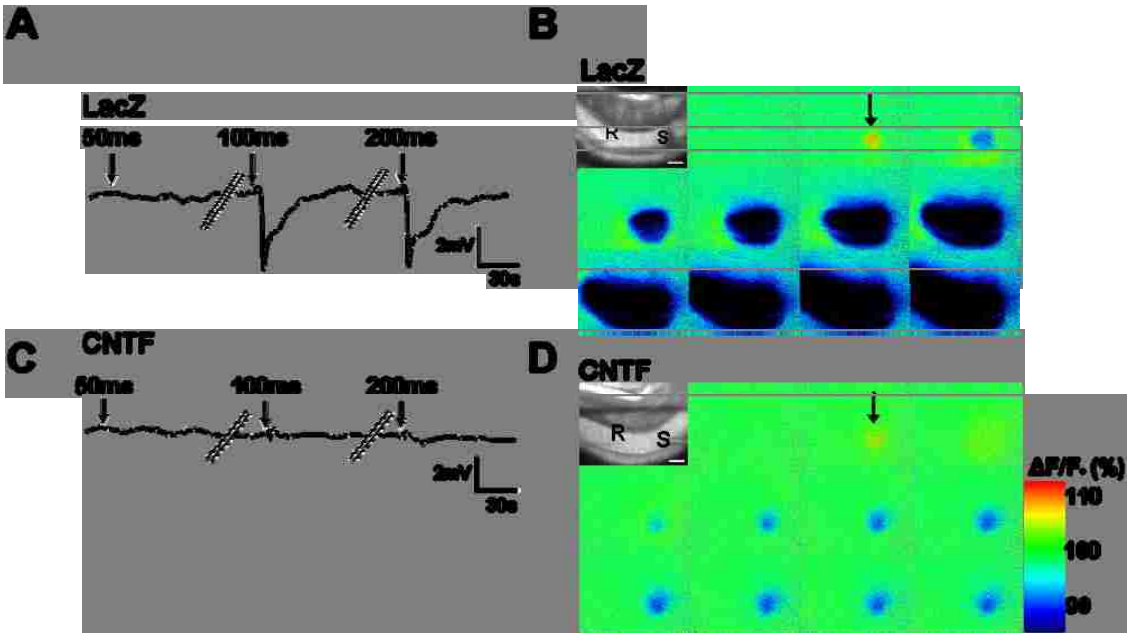

Figure 3.6

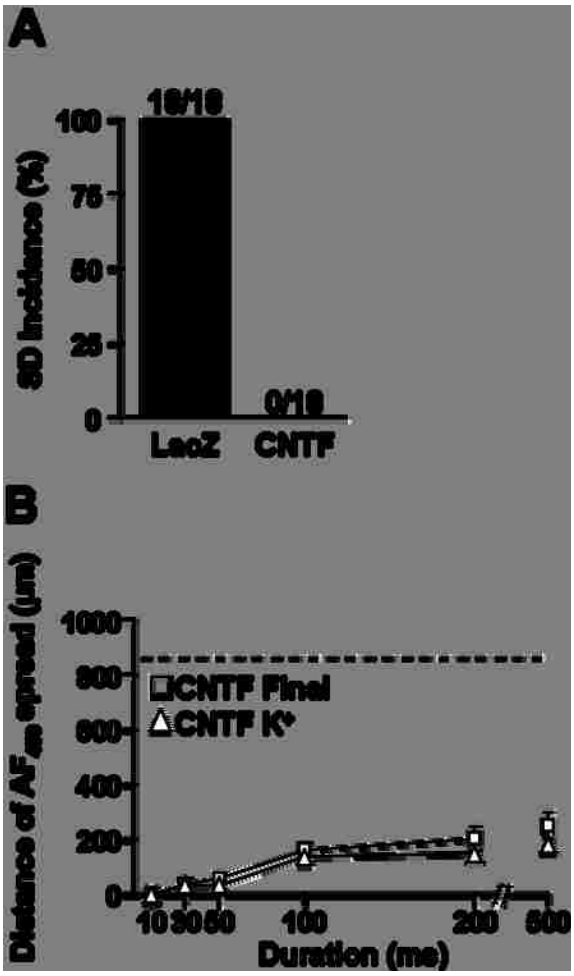

Figure 3.7

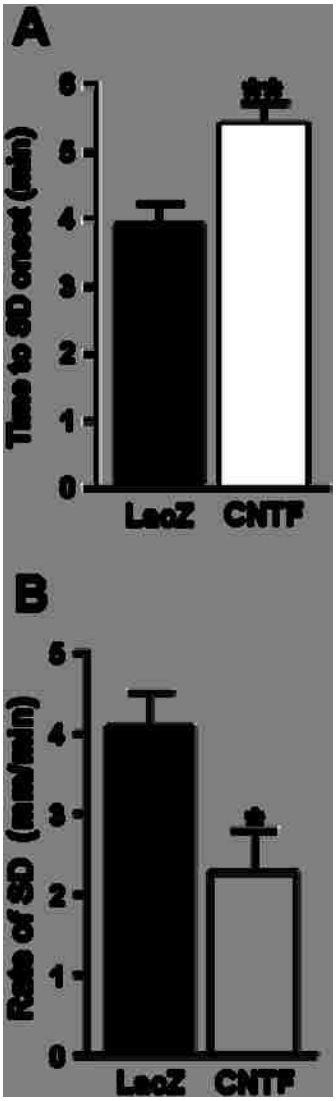

Supplemental Figure 3.1

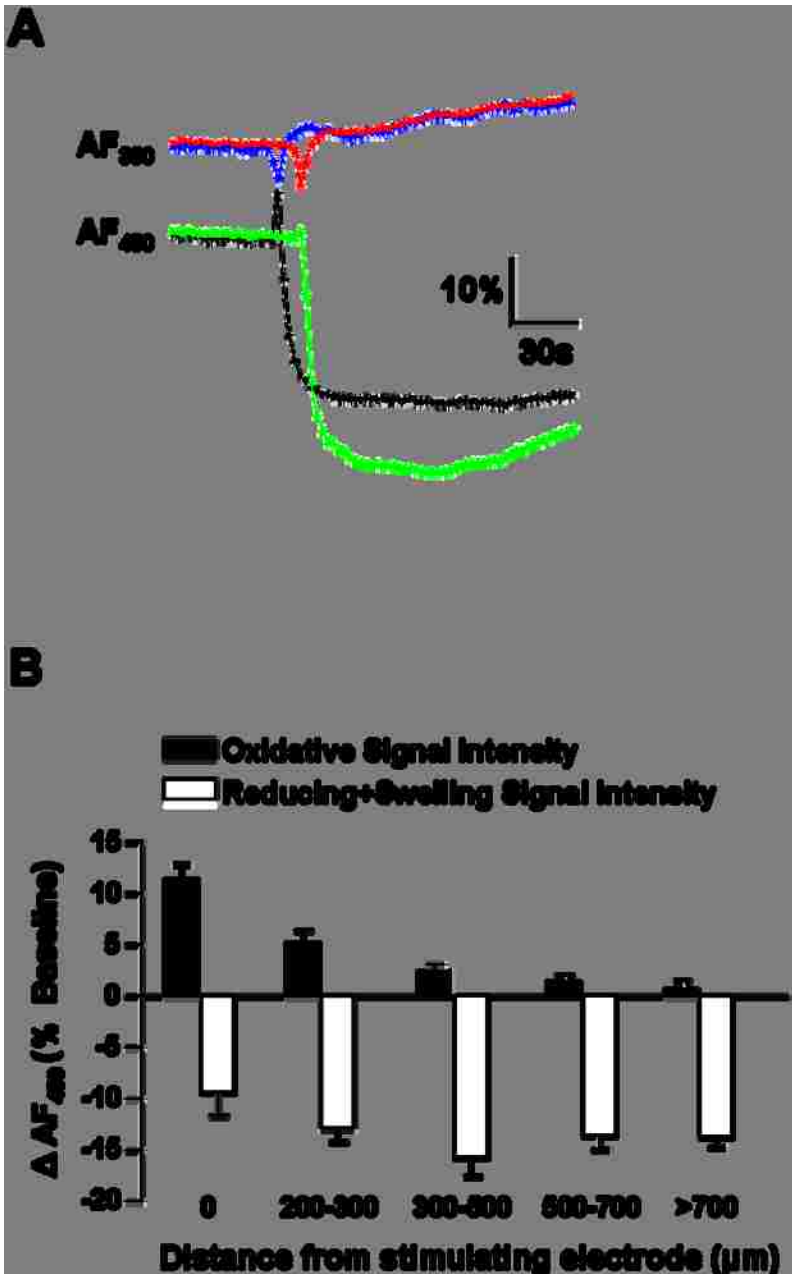

Supplemental Figure 3.2

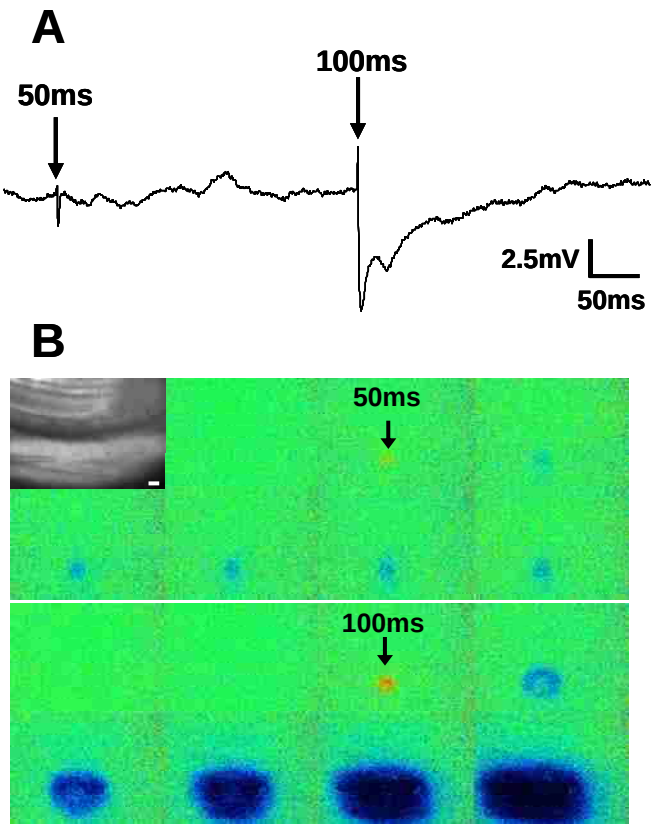

4. Evaluation of the effects of nitric oxide on spreading depression and metabolism in hippocampal brain slice

J.L. Seidel, A.M. Brennan, M.R. Williamson, Y. Zhu, J.A. Connor, C.W. Shuttleworth

Dept. Neurosciences, University of New Mexico School of Medicine, Albuquerque NM 87131

Prepared for submission to “Neuroscience Letters”

4.1 Abstract

Previous reports have suggested that nitric oxide (NO) may provide protection following some forms of ischemic brain injury by limiting the number of spreading depression (SD) events that occur. Levels of NO are known to increase following SD and may increase SD threshold. However, NO is also known to inhibit respiration, suggesting that excessive NO exposure may induce an additional metabolic burden to compromised tissues. The present study evaluates the effects of NO on SD progression and consequences in acutely prepared murine hippocampal slices. Selective inhibition of nitric oxide synthase (NOS) resulted in a significant increase in rates of SD induced by localized KCl microinjections. Addition of an NO donor 2-(N, N-Diethylamino)-diazenolate 2-oxide (DEA/NO, 100-300 μM) also resulted in a significant increase in SD propagation rates. NAD(P)H and flavoprotein autofluorescence measurements during DEA/NO exposures demonstrated inhibition of mitochondrial respiration similar to that produced by sodium cyanide. NO-dependent metabolic inhibition appeared to be cGMP-independent and presumably due to direct inhibition of cytochrome oxidase. Exogenous NO resulted in a loss of synaptic transmission which occurred coincident with metabolic inhibition and was attenuated by A1 receptor antagonists. Under normal conditions, SD was recoverable and synaptic transmission returned to baseline levels after SD. However, in the presence of DEA/NO, SD led to irrecoverable suppression of synaptic potentials, likely due to the inability of neurons to restore ionic homeostasis. These results suggest that while basal NO levels may be protective, excessive NO exposures can provide

an additional metabolic burden, sufficient to transform a benign response into a deleterious one.

4.1.1 Research highlights

1. Inhibition of NO production increased SD propagation rate in murine hippocampal slices. 2. Addition of exogenous NO increased SD propagation rate, and transformed normoxic SD into a non-recoverable event. 3. Deleterious effects of exogenous NO are likely due to inhibition of mitochondrial respiration.

4.1.2 Keywords

Hippocampal slice, spreading depression, nitric oxide

4.1.3 Abbreviations

nACSF: normal artificial cerebral spinal fluid, SD: spreading depression, NO: nitric oxide, DEA/NO: 2-(N, N-Diethylamino)-diazenolate 2-oxide,NAD(P)H: Nicotinamide adenine dinucleotide, L-NNA: N_{ω}-Nitro-L-arginine, fEPSP: post-synaptic field potential.

4.2 Introduction

Spreading depression (SD) is characterized as the rapid depolarization of both neurons and glia in an “all-or-none” fashion (Somjen, 2001). SD-like events, known as peri-infarct depolarizations (PIDs), are known to occur following a wide range of ischemic insults and contribute to the subsequent expansion of infarct volume (Mies et al., 1993; Busch et al., 1996). It has been shown in animal studies that these events occur for many hours following initial ischemic injuries

(Hartings et al., 2003), and recent work has shown that PIDs occur in humans following traumatic brain injury (TBI), subarachnoid hemorrhage (SAH), and stroke (Dreier et al., 2006; Fabricius et al., 2006; Dohmen et al., 2008; Dreier et al., 2009). For these reasons, there is a significant interest in finding new ways to target and minimize the number of these depolarizing events and improve patient outcome (Lauritzen et al., 2011).

Previous studies have shown that spreading depression events lead to increased expression of inducible nitric oxide synthase (iNOS) and synthesis of its product nitric oxide (NO) (Read et al., 1997; Petzold et al., 2008; Viggiano et al., 2008). NO production can regulate SD and inhibition of basal NO synthesis results in decreased SD threshold and delayed recovery of the negative DC shift (Wang et al., 2003; Petzold et al., 2008). These prior studies suggested that increasing NO availability following ischemic injuries may be useful clinically to prevent SD during a period of delayed ischemic neurologic deficits following SAH (Petzold et al., 2008). For this strategy to be effective the concentration of NO available will likely be important, since the role of NO in neuronal cell death and survival is complex.

It is well established that NO can inhibit cytochrome oxidase activity (by competing with oxygen for binding) and can significantly reduce neuronal ATP production (Brown and Cooper, 1994; Brookes et al., 1999). Astrocytes, which are considered primarily glycolytic cells, are relatively resistant to the toxic effects of NO on mitochondrial function, unless glucose is removed from the media (Almeida et al., 2001).

The main question addressed in this study was whether basal endogenous or exogenous NO applications could limit the propagation and influence the consequences of SD. The effects of both removal and addition of NO were examined in hippocampal slice preparations, and SD was induced by localized 1M KCl microinjections. We conclude that while basal levels of NO may limit SD events, exposures to excessive exogenous NO concentrations significantly accelerate SD and worsen outcomes in brain tissue. These effects may limit NO exposures that can be used clinically to modulate SD threshold.

4.3 Materials and Methods

4.3.1 Slice preparation

Male mice (C57Bl/6) were obtained from Jackson Laboratories (Bar Harbor, ME) or Harlan (Indianapolis, IN) at 4-6 weeks of age and were housed in standard conditions (12hr/12hr light/dark cycle) for up to two weeks before euthanasia. All experiments were performed in accordance with approved protocols from the University of New Mexico Laboratory Animal Care and Use Committee. Numbers in the study refer to numbers of slices, with a maximum of two slices obtained from an individual experimental animal used for each protocol. Mice were deeply anesthetized with a mixture of ketamine and xylazine (85 mg/ml and 15 mg/ml, respectively; 150 ml s.c.) and then decapitated. Brains were removed and placed in ice cold cutting solution (see below for composition). 350 μm coronal sections were cut using a Vibratome (Technical Products International, St Louis MO) and slices were transferred into room-temperature ACSF (see below). Cutting and recording solutions were both 300-305 mOsmol/l.

After warming to 34^{o}C and holding for 1 hour, ACSF was changed again, and slices were held at room temperature until used for recording. Individual slices were transferred to the recording chamber, and were perfused with warmed (34^{o}C), oxygenated ACSF at 2 ml/min.

4.3.2 Autofluorescence imaging

NAD(P)H autofluorescence was imaged as previously described (Shuttleworth et al., 2003). Briefly, UV excitation (360 nm) was delivered via a fiber optic - monochrometer system (Polychrome IV; Till Photonics) and reflected onto the slice surface using a dichroic mirror (Chroma, DMLP 400 nm). Fluorescence emission (>410 nm) was collected using a cooled, interline-transfer CCD camera (IMAGO, Till Photonics, Germany). Changes in flavoprotein (FP) autofluorescence were monitored using excitation at 450 nm, and emission detected using a 535 (50 BW) interference filter. In some experiments, near-simultaneous NAD(P)H / FAD imaging was performed by switching filter cubes at 0.4 Hz. In both cases, imaging was performed after focusing onto the surface of slices, using either 10X or 40X water immersion objectives (Olympus, NA 0.3 and 0.8 respectively), and collected after 2x2 binning of the 640x480 line image. After binning, individual pixels corresponded to areas of 2.6 μm^2 and 0.64 μm^2 for 10X and 40X objectives, respectively. For analysis, image data were filtered using 3x3 pixel averaging and presented as the change in fluorescence intensity/prestimulus fluorescence intensity ($\Delta F/F_o$).

4.3.3 Recording of Postsynaptic Potentials

Schaffer collateral inputs to the CA1 region were stimulated using a concentric bipolar electrode (25 µm tip) placed on the surface of stratum radiatum. Single shocks (80 µs, 0.1-1.5 mA) were applied using a constant-current stimulus isolation unit (Isoflex, AMPI, Isreal). Extracellular field recordings of excitatory postsynaptic potentials (fEPSPs) were made using glass microelectrodes (4-8 MΩ) filled with ACSF. Electrodes were placed in stratum radiatum of CA1, approximately 150 µm from the pyramidal cell body layer. Stimulus intensity was chosen based on an input/output curve generated in each slice, to produce responses >60% of maximal amplitude (0.6-1.0 mA). Signals were amplified (Neurodata IR-283), digitized (Digidata 1322A, Axon Instruments, Union City, CA), and then acquired using Clampex software (v 9.2, Axon Instruments).

4.3.4 Stimulation of spreading depression events

Spreading depression (SD) was induced using localized microinjections of KCl as described in (Dietz et al., 2008) with minor modifications. A conventional whole-cell patch electrode (tip resistance 4-8 MΩ) was placed ~50 µm below the slice surface in stratum radiatum, and miroinjections triggered by brief (10-200 ms) pressure pulses delivered by a PicoPump (SYS-PV830, World Precision Instruments). SD resulted in the loss of fEPSPs and the propagation of SD across the tissue was monitored using autofluorescence imaging (see methods above).

4.3.5 Reagents and Solutions

Except where noted, all drugs and salts were obtained from Sigma Chemical Co (St Louis, MO). ACSF contained, in mM: 126 NaCl, 2 KCl, 1.25 NaH_2PO_4, 1 $MgSO_4$, 26 $NaHCO_3$, 2 $CaCl_2$, and 10 glucose, equilibrated with 95%O_2 / 5%CO_2. Cutting solution contained, in mM: 3 KCl, 1.25 NaH_2PO_4, 6 $MgSO_4$, 26 $NaHCO_3$, 0.2 $CaCl_2$, 10 glucose, 220 sucrose and 0.43 ketamine. NaCN stock was made fresh daily at 1 M concentration based on previous work (Gerich et al., 2006). DEA/NO was prepared as reported previously (Bon and Garthwaite, 2001). Briefly, 100 mM DEA-NO was dissolved in 10 mM NaOH and stored frozen for <24 h before use. DEA/NO was then dissolved in ACSF to its final concentration (100 µM) immediately before use.

4.3.6 Statistical analysis

Significant differences between group data were evaluated using unpaired Student's t tests or one-way ANOVA. Bonferroni's multiple-comparison test or contrasts were used for post hoc analysis in which the effects of multiple treatments were compared with each other. A value of $p<.05$ was considered significant in all cases.

4.4 Results

4.4.1 Effects of modifying NO availability on SD

Initial experiments set out to determine whether there were changes in SD threshold with the manipulation of endogenous NO as previously reported in rat cortical slices (Petzold et al., 2008). To block NO synthesis, slices were pre-

exposed to the NOS inhibitor N_{ω}-Nitro-L-arginine (L-NNA, 1 mM, 15 min) prior to KCl challenges, and these responses were compared to control responses with preparations exposed to an excess of endogenous NOS substrate L-arginine (0.5 mM). SD threshold is usually determined by progressively increasing the intensity of electrical stimulation or K^+ concentration applied to the brain surface or brain slice (Ayata et al., 2000; van den Maagdenberg et al., 2004; Ayata et al., 2006). For the current studies, we characterized SD threshold using graded localized KCl microinjections, delivered by increasing durations of pressure ejection from a conventional patch electrode (10-200 ms). NOS inhibition did not obviously change SD threshold, with 100 ms duration stimuli initiated SD in all slices (data not shown). Inhibition of NO synthesis did significantly increase SD propagation rate (Figure 4.1A); consistent with previous observations in rat slices (Petzold et al., 2008).

To test the hypothesis that the addition of exogenous NO may provide neuroprotection and decrease SD propagation, slices were pre-exposed to an NO donor for 10 minutes prior to SD induction with KCl microinjection. Excitatory postsynaptic potentials were monitored throughout these experiments, to assess the impact on neuronal viability. We chose to utilize 2-(N, N-Diethylamino)-diazenolate 2-oxide (DEA/NO) since its release of authentic NO has been well characterized, including in hippocampal slices (Keefer et al., 1996; Feelisch, 1998; Bon and Garthwaite, 2001, 2003; Hopper et al., 2004). Figure 4.1B shows representative recordings of evoked excitatory synaptic potentials in L-arginine controls (open circles) and DEA/NO pre-exposed preparations (filled circles),

before and after the onset of high K^+-SD (arrow). As discussed in detail below (Figure 4.4), DEA/NO itself led to a robust suppression of fEPSP slope, but it did not prevent the initiation or propagation of SD. In fact, SD propagation rate was increased in DEA/NO (Figure 4.1C). Importantly, under control conditions, SD resulted in only a transient depression of evoked synaptic activity, which generally recovered within ~10 min as neurons restored ionic homeostasis. Thus, in control preparations, fEPSPs recovered to 81.01±19.75% baseline levels (Figure 4.1C, n=5). In contrast, in preparations pre-exposed to DEA/NO, SD never recovered and the loss of synaptic activity at SD onset persisted suggesting neuronal damage (-1.97±2.03% recovery, n=5). Therefore, while basal levels of NO may be important for setting SD threshold and propagation rate, excessive NO may be detrimental to tissue subjected to SD.

4.4.2 Effects of exogenous NO on neuronal function

It is well established that NO can inhibit oxidative metabolism by competing with oxygen at cytochrome oxidase within the electron transport chain (Brown and Cooper, 1994; Cleeter et al., 1994; Giulivi, 1998). Near simultaneous NAD(P)H and flavoprotein autofluorescence were used to monitor the effects of 100 µM DEA/NO on oxidative metabolism. DEA/NO exposures resulted in sustained increase in NAD(P)H autofluorescence, which was mirrored by flavoprotein autofluorescence decrease (Figure 4.2A, n=6). These effects were mimicked by the respiratory chain inhibitor sodium cyanide (NaCN, 100 µM), which inhibits oxidative metabolism in a concentration-dependent manner (Figure 4.2B-C). Direct effects of NO on mitochondrial respiration are cGMP

independent. In these preparations, inhibition of cGMP synthesis with 1H-[1,2,4]oxadiazolo-[4,3-α]quinoxalin-1-one (ODQ, 100 μM) are consistent with this conclusion, since small cGMP increases in NAD(P)H autofluorescence were not matched by flavoprotein autofluorescence decreases (Figure 4.3), implying a cytosolic origin.

It is possible that endogenous NO production may provide a significant contribution to autofluorescence measurements. Thus, the NO binding of cytochrome oxidase might be close to saturated, making the effects of exogenous NO smaller. However, neither L-NNA (1mM) nor L-arginine (0.5 mM) resulted in significant changes in NAD(P)H autofluorescence (data not shown), consistent with there being little contribution of endogenous NO to resting NAD(P)H autofluorescence.

As noted above, DEA/NO exposures resulted in reversible reduction of fEPSPs (Figure 4.4A-B). It has been described previously in rat hippocampus that NO triggers adenosine accumulation and inhibition of synaptic potentials, and that selective A1 receptor antagonists can prevent the loss of fEPSPs induced by application of the NO donor S-nitroso-acetylpenicillamine (SNAP) (Broome et al., 1994; Saransaari and Oja, 2004). The adenosine dependence of the loss of fEPSPs in our studies was confirmed by pre-exposing preparations to the A1 receptor antagonist 8-cyclopentyl-1,3-dipropylxanthine (DPCPX, 200 nM) prior to 10 minute DEA/NO. Under these conditions, fEPSPs were not significantly decreased due to DEA/NO (Figure 4.4C).

4.5 Discussion

These studies have shown that, consistent with previous work, loss of endogenous NO alters SD events. Our studies were unable to delineate a difference in SD threshold, but there was a significant increase in the rate of SD propagation across the tissue with the inhibition of NO production. Interestingly, we found that the addition of exogenous NO also resulted in an increase in the spread of SD across the tissue and led to neuronal damage measured by fEPSP recovery. Our data are consistent with the possibility that these effects are likely due to the inhibitory effects of NO on mitochondrial respiration. Therefore, while NO may be neuroprotective against SD-like events following some ischemic injuries (discussed in (Petzold et al., 2008)), effectiveness may be quite concentration dependent, and these additional deleterious effects should be taken into consideration when discussing the therapeutic potential of NO.

As mentioned above, previous studies have found a significant decrease in SD threshold both *in vivo* and *in vitro* slice preparations with the inhibition of NO production (Wang et al., 2003; Petzold et al., 2008). The lack of effects on threshold in the current studies is likely due to a difference in the methods of elevating extracellular potassium in the preparation. In the current studies, extracellular potassium was increased within a small localized region of the slice preparations by micro-injection of 1 M KCl; making the overall change in $[K^+]_e$ dependent on the duration of the micro-injection. Previous studies have evaluated SD-threshold by increasing $[K^+]_e$ in the superfusing solution (Petzold et al., 2008; Zhou et al., 2010). The later method likely allows for changes in

extracellular potassium over a wider range of concentrations while the method employed in these studies may not provide the gradual increases required to determine subtle changes in SD threshold.

We did observe a significant increase in the rate of SD propagation across the tissue with NOS inhibitor exposures; suggesting that endogenous NO can provide protection against the spread of SD. The mechanisms underlying these protective effects have been examined both *in vivo* and *in vitro.* Vascular effects of NO are well established (Moncada and Higgs, 1993). Within the context of SD, NO production is known to increase following depolarization and may be critical for the preservation of a cerebral blood flow (CBF) response to hypercapnia that follows (Fabricius et al., 1995; Scheckenbach et al., 2006; Petzold et al., 2008). However, NO can act on neurons as well, and the effects of NO on SD threshold in previous studies, were not solely due to modifications of CBF, but believed to be predominantly direct effects of NO on neuronal P/Q-type voltage gated calcium channels and NMDA receptors to reduce neuronal excitability (Petzold et al., 2008). Therefore, changes in NO concentrations will modify both vascular and neuronal factors, each of which will likely affect the initiation, propagation, and consequences of SD-like events. The addition of exogenous NO together with NOS inhibitors results in a recovery of SD threshold to levels not significantly different from control conditions; leading to the suggestion that the addition of exogenous NO or inhibition of NO-lowering mechanisms could provide a possible therapeutic treatment for delayed ischemic neurological deficits (Petzold et al., 2008). However, the addition of exogenous L-arginine, which leads to an

increase in NO synthesis, facilitated the propagation of SD in previous studies (Maia et al., 2009). In our studies, the addition of exogenous NO alone, without the inhibition of endogenous NO synthesis, also resulted in an increased rate of SD propagation across the tissue and appeared to be neurodegenerative; likely due to the fact that NO can compete with oxygen at cytochrome oxidase and inhibit mitochondrial respiration (Brown and Cooper, 1994; Cleeter et al., 1994). It is estimated that 100-300 μM DEA/NO should produce local NO concentrations in the 100 nM range in brain slices, which should be enough to partially inhibit mitochondrial respiration and higher DEA/NO should not give a proportional rise in NO concentration, because of loss of NO by reaction with O_2 (Bon and Garthwaite, 2001). DEA/NO dissociates rapidly with a half life of ~6 minutes at 30^{o}C to release the NO radical from DEA (Bon and Garthwaite, 2001). The effects of the liberated DEA were not explicitly tested in these studies. However, the effects observed with DEA/NO exposures were consistent with previously observed effects of NO. Thus, inhibition of mitochondrial respiration was confirmed in our preparations with autofluorescence imaging showing similar inhibition to that of 100 μM CN. The NO donor also resulted in the reversible loss of fEPSPs which was confirmed to be adenosine dependent by the addition of the A1 receptor antagonist DPCPX. In preparations pre-exposed to DEA/NO prior to SD, there was the adenosine-dependent loss of fEPSPs prior to SD events that did not recover even after a twenty minute wash-out period of DEA/NO. In control conditions, SD events resulted in a loss of fEPSPs that recovered back to baseline over time. The lack of recovery in DEA/NO slices

even after wash-out of the drug suggests that under these conditions, SD results in neuronal damage.

4.5.1 Conclusions

These results show that basal concentrations of NO are likely to provide protection against SD events, and that either a decrease or increase from basal levels may facilitate the spread of these depolarizing waves through tissue. Increasing NO significantly above basal concentrations may prove to be especially detrimental, since our results suggest that it can transform normally-recoverable SD events into terminal depolarizations. Strategies, which target NO as a potential therapeutic target against SD, will require tight regulation to ensure exogenous NO concentrations stay within basal ranges, or alternative agents that reduce P/Q-type calcium channel and NMDA receptor activity without inhibition of mitochondrial respiration must be utilized.

4.6 Figure Legends

4.6.1 Figure 4.1

Effects of changing NO availability on SD progression and consequences. A. Inhibition of NOS production with L-NNA (100 µM, 20 min) prior to induction of SD significantly increased SD propagation rate (n=6, p=.0082). **B.** Representative examples of field potential recordings before and after generation of SD (arrow) by localized KCl microinjections. In control tissues (open circles), SD resulted in only transient loss of synaptic activity that recovered over the course of ~15 minutes to baseline levels (n=4, p=.406).

Interleaved slices were exposed to DEA/NO for 10 min prior to SD onset (black bar, filled circles). Under these conditions, fEPSPs were suppressed by DEA/NO alone. If SD were not induced, fEPSPs would recover following DEA/NO washout (see Figure 4.4). However, SD in the presence of DEA/NO led to irrecoverable loss of fEPSPs (n=6). **C.** Addition of the NO donor DEA/NO 10 minutes prior to SD induction did not inhibit SD onset, and significantly increased in SD propagation rate (n=6, p=.0095).

4.6.2 Figure 4.2

Effects of exogenous NO on mitochondrial function measured by changes in NAD(P)H and flavoprotein autofluorescence. A. DEA/NO resulted in a significant increases in NAD(P)H autofluorescence that were matched by flavoprotein decreases, consistent with inhibition of oxidative metabolism (n=6). **B-C.** The effects of DEA/NO on NAD(P)H and flavoprotein were mimicked by the complex IV inhibitor NaCN in a concentration dependent manner (n=6).

4.6.3 Figure 4.3

Effects of a selective cGMP inhibitor. Inhibition of soluble guanylate cyclase with ODQ (100 µM) resulted in an increase in NAD(P)H autofluorescence which was not matched by flavoprotein decreases, due to cytosolic rather than mitochondrial consequences. This is consisted with the conclusion that NO effects on mitochondrial respiration are likely cGMP independent and due to direct inhibition of cytochrome oxidase.

4.6.4 Figure 4.4

DEA/NO results in a transient, fully-reversible loss in fEPSPs that is adenosine dependent. A. Representative traces during baseline, 10 minutes DEA/NO, and washout (n=6). **B.** Population data for 10 minute DEA/NO exposures. **C.** Slices were pre-exposed for 20 minutes with the A1 receptor antagonist, DPCPX (200 nM), prior to wash in of DEA/NO. DPCPX completely prevented the loss of fEPSPs when compared with preparations exposed to DEA/NO alone (n=4).

Figure 4.1

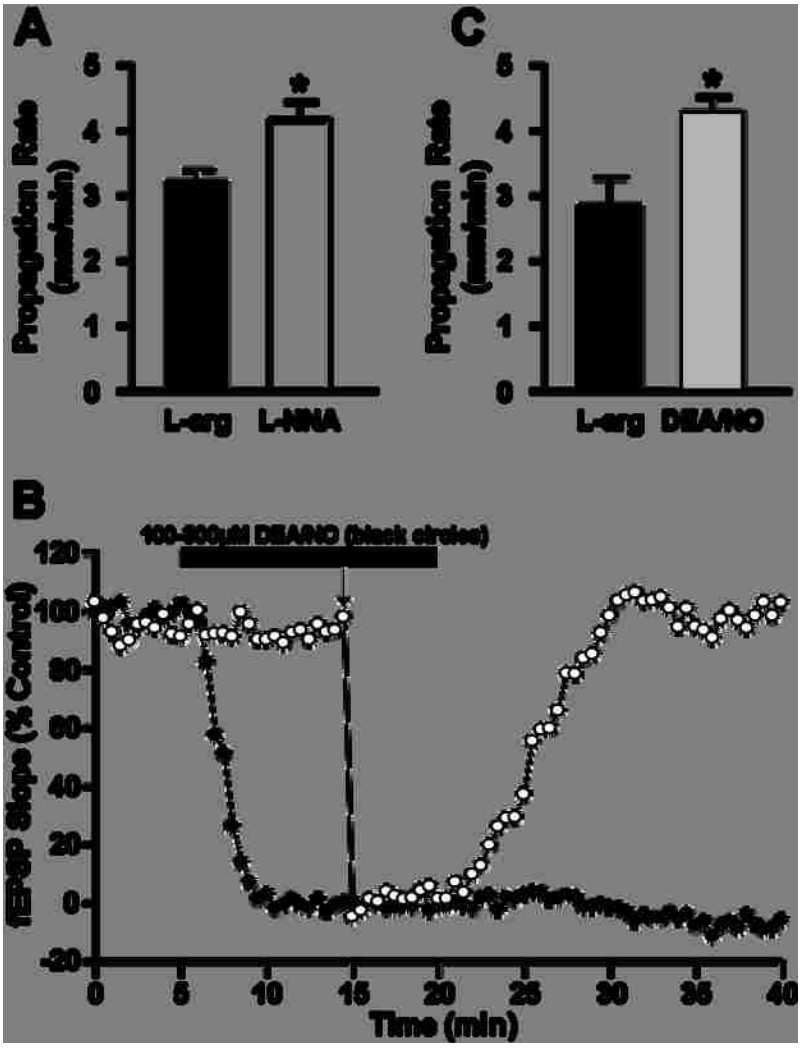

Figure 4.2

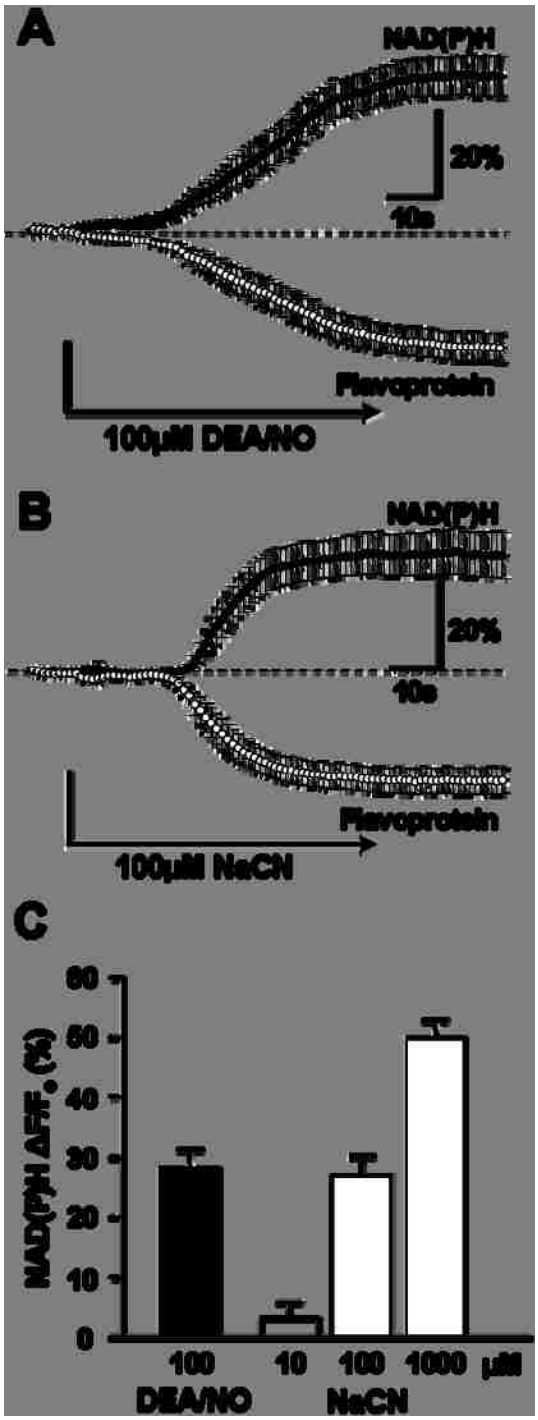

Figure 4.3

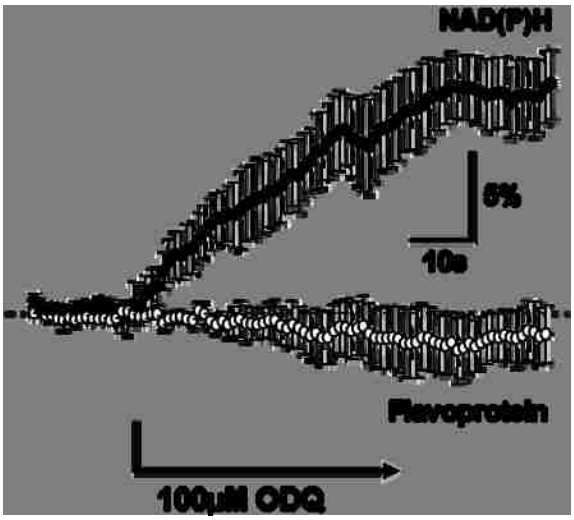

Figure 4.4

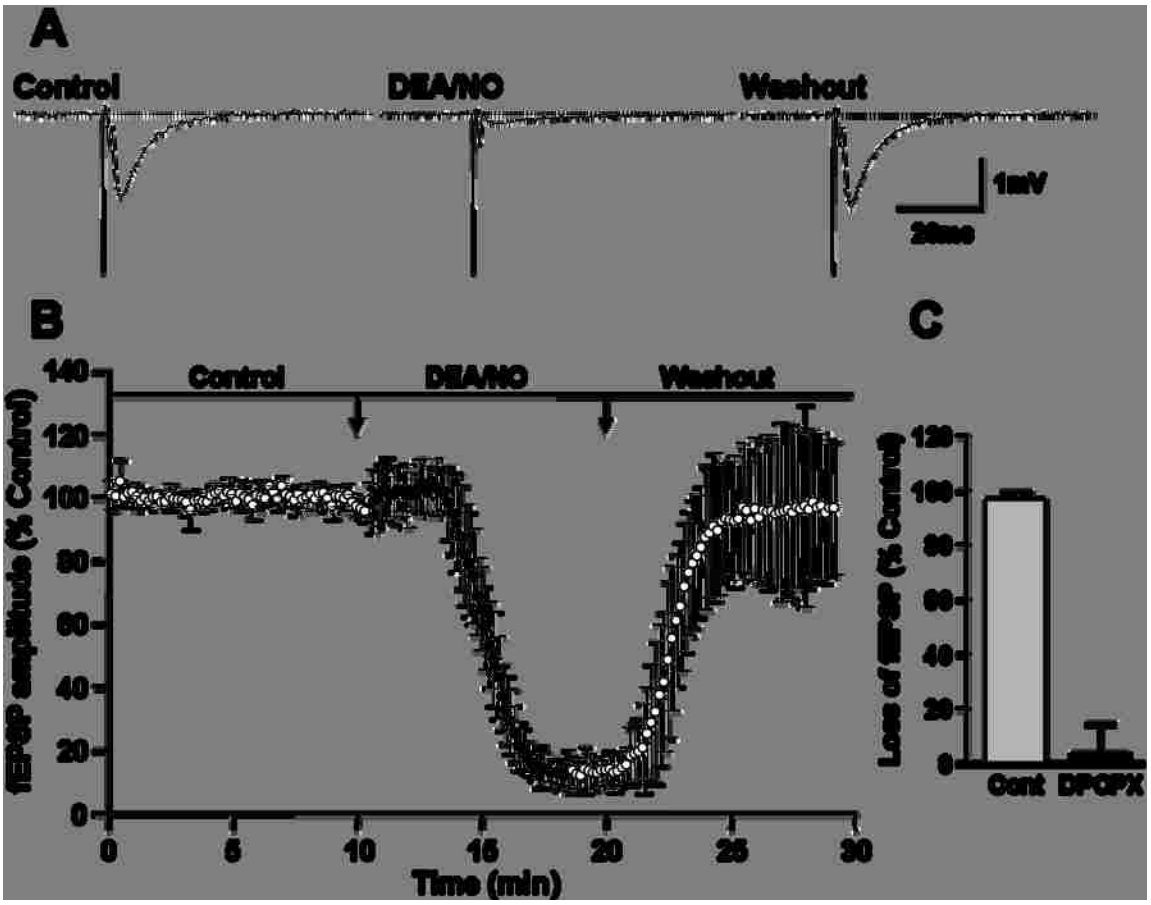

5. General Discussion

5.1 Introduction

Studies in this dissertation examined basic mechanisms contributing to regulation of spreading depression (SD) in brain slices. In recent years, a combination of animal and clinical recordings has raised the exciting possibility that SD and related events can contribute to the expansion of brain injury. Understanding better the basic mechanisms involved using reduced brain slice preparations should be helpful to the development of novel specific therapeutic interventions targeting SD-like events.

Previous work has evaluated roles of astrocytes in SD initiation, but concluded that depolarization of these cells follows the progression of SD rather than lead it. However, astrocytes are well-positioned to regulate the spread of SD by uptake of both extracellular K^+ and glutamate. Indeed, it has been shown previously that selective inhibition of astrocyte metabolic function (with fluorocitrate), leads to more rapid SD propagation. However, I found that providing additional oxidative substrate for astrocytes did not significantly slow the rate in either normoxic or ischemic conditions, implying that targeting astrocyte oxidative metabolism may not be a useful therapeutic strategy. My studies have gone on to show that manipulation of astrocyte glycogen stores does significantly modify SD propagation. In preparations where astrocytic glycogen stores were significantly enhanced, SD propagation across the tissue significantly slowed or inhibited all together in ischemic condition. This work suggests that targeting astrocyte glycolytic substrates, particularly glycogen, may

be useful for reducing the incidence of SD-like events in the context of brain injury.

Previous work has studied the roles of reactive astrocytes in brain injury and historically, these studies have emphasized deleterious roles underlying these phenotypic changes within astrocytes. However, an emerging view is that reactive astrocytes could be neuroprotective and contribute to limiting spread of injury and promote recovery. In my studies I have developed a new model of astrocytes activation to test the effects of this phenotypic change on SD initiation and propagation. My studies provide exciting evidence consistent with the possibility that activation of these cells could be protective by limiting the onset of SD and related events in the context of ischemia.

Previous work has studied the possible protective effects of nitric oxide (NO) in the context of delayed neurological deficits associated with subarachnoid hemorrhage (SAH). Those studies suggested that NO may act directly on NMDA receptors and P/Q-type voltage gated Ca^{2+} channels to reduce neuronal excitability and increase SD threshold. My studies emphasize the possible deleterious effects of NO due to inhibition of mitochondrial respiration, and suggest that other therapeutic agents which may target the protective effects of NO without inhibition of oxidative metabolism are required.

5.2 Propagation of SD

5.2.1 SD Propagation

Extensive work has previously established that the propagation of spreading depression relies on feed-forward accumulation of glutamate and/or K^+ in the extracellular space (see Section 1.1.3). As discussed above (Section 1.4.1), the clearance of both these mediators is regulated by astrocytes and consumes ATP. It is generally accepted that SD and related depolarizing events progress across tissues in the general range of 3-6 mm/min (Somjen, 2001). Previous studies using rat hippocampal slice preparations compared propagation rates between normoxic SD (induced with microinjections of KCl) and hypoxic SD (induced by replacing 95% O_2 with 95% N_2) (Aitken et al., 1998). Based on the duration and amplitudes of IOS and electrical signals between the two stimuli, they concluded that there was no significant difference in the SD propagation rate between the conditions, although hypoxic SD trended towards a faster propagation (Aitken et al., 1998).

My studies utilizing high K^+ and OGD-SD showed a clear difference in propagation rates, with OGD exposures in slice preparations resulting in significantly more rapid SD propagation rates than high K^+-SD. During OGD, removal of metabolic substrates from the entire preparation results in slow depolarization of all neurons as extracellular K^+ levels rise toward SD threshold levels (Vyskocil et al., 1972; Hansen and Zeuthen, 1981). Thus, it is possible that the faster propagation rate during OGD is a result of the fact that neurons ahead of the advancing SD wavefront are moderately depolarized by K^+. Ischemic

glutamate accumulation could also contribute. Under ischemic conditions large increases in extracellular glutamate, attributed mainly to the reversal of neuronal glutamate transporters, likely contribute to initial anoxic depolarizations (Szatkowski et al., 1990; Rossi et al., 2000). Increased extracellular K^+ can stimulate the reversal of glutamate uptake (Szatkowski et al., 1990), and since increases in extracellular K^+ occur during OGD conditions, it is possible that reversal of glutamate transporters could contribute to the increased rate of OGD-SD compared with normoxic responses. However, the relative importance of reversed glutamate transport to OGD-SD propagation is not yet known.

Another intriguing possibility is that, during OGD, astrocytes lose metabolic capacity to limit glutamate and/or K^+ clearance ahead of the advancing wavefront. During high K^+-SD, threshold levels of extracellular K^+ (10-12 mM) and glutamate (~34-40 µM) are required at the front of the depolarization (Hansen and Zeuthen, 1981; Fabricius et al., 1993; Scheller, 1993; Iijima et al., 1998; Muller and Somjen, 2000). Normally-functioning astrocytes are expected to retard both extracellular K^+ and glutamate accumulation (see Section 1.4.1). In contrast, in the context of OGD, astrocyte ATP levels may be severely depleted, and accumulation of K^+ and glutamate to threshold levels may thus be more rapid at the front edge of the depolarization, which could lead to a more rapid spread of SD across tissues. This idea is supported by the effects of selective astrocyte metabolism discussed below (Sections 5.2.2 and 5.2.3).

5.2.2 Astrocyte glycogen stores and SD propagation

5.2.2.1 Astrocyte metabolism

As discussed above (Section 1.4.1.3), astrocytes appear to utilize both mitochondria and glycolysis for ATP production. However, astrocytes are often considered to be primarily glycolytic cells, and indeed, previous work has shown that even in the complete absence of oxygen, glycolysis can produce sufficient ATP to maintain normal astrocyte glutamate uptake (Swanson, 1992; Swanson et al., 1994). This implies a strong Pasteur Effect, as the rates of glycolysis must be dramatically increased during anoxia (Krebs, 1972).

Glycolysis can be fueled during severe energetic demands by glycogen. Brain glycogen stores are found almost exclusively in astrocytes (Cataldo and Broadwell, 1986; Wender et al., 2000; Brown, 2004), and are thought to be rapidly metabolized when cellular energy demands increase (Brown et al., 2003). Glycogen mobilization is regulated by phosphorylation and allosteric binding of AMP to glycogen phosphorylase, which results in hydrolysis to glucose-6-phosphate (Brown, 2004). Metabolism of glycogen is energy efficient since glucose-6-phosphate enters glycolysis after the initial ATP-dependent phosphorylation required for glucose metabolism (Brown, 2004). From these considerations it is not surprising that previous work has shown depletion of glycogen stores by SD (Selman et al., 2004). Consistent with this, in my studies, 20 minute OGD exposures (which always generated OGD-SD) resulted in complete depletion of glycogen from brain slices.

As will be discussed below, my studies also suggest a significant role for glycogen stores in the regulation of SD propagation; a finding that may be useful for future approaches to limit SD in pathological conditions.

5.2.2.2 Preventing glycogenolysis and SD propagation

In my *in vitro* studies, inhibition of glycogenolysis was obtained by brief (15 minute) pre-exposures to a combination of inhibitors (DAB and DNJ). Inhibiting the metabolism of glycogen in astrocytes resulted in a significant increase in the propagation rate of both high K^+ and OGD-SD. These results suggest that the ability of astrocytes to clear glutamate and/or K^+ from the extracellular space was compromised by inhibition of glycogenolysis. Furthermore, utilization of rapidly metabolized glycogen stores likely contributes to limiting the rate of SD propagation in both normoxic and ischemic conditions.

An important consideration for these studies was whether glycogenolysis inhibitors reached effective concentrations in astrocytes *in situ.* It was not possible to test the inhibition of glycogen breakdown in brain slices directly using the glycogen assay described above (Section 2.3.4). In this assay, endogenous glucose was initially removed from the samples before hydrolysis of tissue glycogen by amyloglucosidase (Cruz and Dienel, 2002). The presence of glycogenolysis inhibitors would prevent the activity of exogenous amyloglucosidase, which was essential for the assay. The choice of both the duration and the dosage of these inhibitors was thus based on previous hippocampal slice studies showing effects on field EPSPs (Sadgrove et al., 2008). It is noted that previous studies in rat optic nerve have shown that longer

exposures (60 min) to higher DAB concentrations (300-1000 μM) were required for complete inhibition of glycogen phosphorylase (GP) (Walls et al., 2008). However, optic nerves are tightly wrapped in myelin and penetration of DAB is likely better in hippocampal slices used in the present studies. In addition, the co-incubation of DAB with DNJ likely greatly potentiated its effects. This assumption is based on previous studies in rat hepatocyte cultures, which have shown that the inhibitory effects of DAB were significantly enhanced by the addition of 100 μM DNJ (Kuriyama et al., 2008). However, due to concerns that my initial choice of drug concentrations may not have been sufficient for complete inhibition of glycogenolysis, I conducted a secondary set of studies where slice preparations were exposed to a combination of DAB and DNJ at relatively higher concentrations (100 μM) for more extended periods of time (75 min). There was no additional effect of the glycogenolysis inhibitors when compared to my initial studies with shorter exposures at lower concentrations (Section 2.4). These findings support the assumption that glycogen metabolism was effectively impaired with my initial exposure paradigm.

5.2.2.3 Increasing glycogen content

To increase glycogen concentrations within astrocytes, I utilized L-methionine-DL-sulfoximine (MSO, 2 mM). MSO was first identified as the convulsant formed in bleached wheat flour (Bentley et al., 1950), and it has since been shown to increase brain glycogen, although the mechanisms underlying this effect are not well understood (Folbergrova, 1973; Swanson et al., 1989b; Swanson et al., 1990). Other methods have previously been employed to

increase astrocyte glycogen stores, including increased glucose, insulin, and insulin-like growth factor (IGF) (Dringen and Hamprecht, 1992). However, MSO was chosen for these experiments based on previous work in primary astrocyte cultures where 24 hour exposures to MSO (1 mM) resulted in a 300% increase in astrocyte glycogen (Swanson et al., 1989b). It is known that MSO is not taken up as readily in slice preparations (Folbergrova, 1973), so confirming an increase in glycogen was important for the design and interpretation of my electrophysiological studies. I found prolonged 2 mM MSO exposures resulted in a significant increase in slice glycogen stores. The magnitude of increased glycogen was much smaller the previously reported in astrocyte cell cultures studies (Swanson et al., 1989b), which may be due to a number of significant differences in experimental methods. Firstly, utilizing astrocyte cultures permitted 24 hour drug exposures, and such extended treatments are not possible with acutely-prepared brain slices, which were viable for only approximately 8-10 hours. Therefore, my pre-exposure paradigm required balancing the time required to have a significant effect of MSO on glycogen stores, with the diminishing health of slice preparations throughout a given experimental day. It is also possible that astrocytes derived from neonatal tissues and maintained in confluent cultures may have a greater capacity to increase glycogen stores than mature astrocytes that are integrated into functioning hippocampal networks.

In my studies, three hour MSO (2 mM) exposures were required for a significant increase in slice glycogen content, and this was accompanied by a decrease in OGD-SD propagation rate, but had no effect on high K^+-SD. The

significant slowing of OGD-SD is likely a result of a strong Pasteur Effect, which could lead to a significant increase in the rate of glycolysis to increase ATP availability and support the clearance of both extracellular glutamate and K^+ by astrocytes. The lack of effect of MSO on high K^+-SD may be a result of the fact that under normoxic conditions, there are sufficient metabolic substrates (including glycogen) available to astrocytes and provision of excess substrates may not provide an additional benefit. This general conclusion is also supported by the lack of effect of additional substrate for oxidative metabolism on high K^+-SD propagation rate (discussed Section 5.2.3).

The chemical structure of MSO strongly resembles glutamate and this compound is a known convulsant (see above); likely because it mimics the neurotransmitter at the synaptic cleft. MSO is also known to inhibit glutamine synthetase (GS) activity within astrocytes (Cloix and Hevor, 2009) which could reduce glutamate recycling. Indeed, hippocampal slice culture studies have shown that MSO exposures lead to significant decreases in glutamate in nerve terminals while increasing both glutamate and glutamine in astrocytes (Laake et al., 1995). MSO also has significant effects on inhibitory transmission; leading to a decrease in evoked inhibitory postsynaptic currents (eIPSC) (Liang et al., 2006). Thus, seizure activity resulting from MSO exposures may be due not only to diminished capacity for astrocytes to clear extracellular glutamate, but decreased inhibitory GABA tone as well. Increases in glycogen stores within astrocytes are known to precede the convulsive period induced by MSO exposures suggesting that this increase in metabolic substrate is not a response

to the seizure activity, but may actually serve to delay seizure onset (Cloix and Hevor, 2009). It is possible the the decreased SD propagation rate observed during OGD could be the result of diminished synaptic glutamate. However, the same effects were not observed under normoxic conditions during high K^+-SD suggesting that there is a metabolic component mediating the observed effects rather than a change in synaptic glutamate concentrations.

Overall, these studies with both inhibitors and a potentiator of glycogen utilization suggest that astrocytic glycogen stores slow the rate of SD in both normoxic and ischemic conditions. This raises the interesting possibility that targeting astrocyte glycogen could be a useful strategy when trying to limit the spread of these depolarizing events in clinical conditions.

5.2.3 Astrocyte oxidative metabolism and SD propagation

5.2.3.1 Selective inhibition of astrocyte oxidative metabolism

The effect of selective inhibition of astrocyte oxidative metabolism (with 1mM fluorocitrate) on SD propagation rate has been shown previously in *in vivo* rat cortex (Largo et al., 1997a). Selective metabolic inhibition with either fluorocitrate (FC) or fluoroacetate (FA) is a result of by preferential uptake by the monocarboxylate-like transporters isoform on astrocytes, MCT1 (Waniewski and Martin, 1998), and subsequent block of the TCA enzyme aconitase. In my studies, I confirmed the facilitatory effects of FA on SD propagation in hippocampal slices. Interestingly, inhibition of astrocyte oxidative metabolism with FA had a comparable effect on increases in SD propagation rate for both

high K^+ and OGD-SD when compared with effects of glycogenolysis inhibition. The effect on SD propagation in these FA studies were larger than those described *in vivo* by Largo (Largo et al., 1997a). It is possible that by utilizing *in vitro* slice preparations, I was able to more effectively deliver FA uniformly from above and below a thin tissue slice, while in *in vivo* preparations, where FC was delivered by microdialysis, a homogeneous distribution of the drug over the whole SD field was likely very difficult.

In the present studies, I was also interested in the possible effects of FA pre-exposures on glycogen levels within hippocampal slices. I expected that inhibition of oxidative metabolism may result in a decrease in glycogen within astrocytes due to increased glucose consumption as a result of the Pasteur Effect (Krebs, 1972). However, I found that FA exposures did not significantly deplete glycogen concentrations. It is possible that glycogen stores within slice preparations are already low, which is supported by the lower levels of total glycogen measured in my preparations when compared with that measured from whole brain homogenate and cell culture (Swanson et al., 1989a; Swanson and Choi, 1993; Cruz and Dienel, 2002). In addition, previous studies have reported that slice glycogen falls dramatically immediately after cutting during the hour incubation period at 36^{o}C, and recovers over the next 3 hours (Lipton, 1989). I was careful to allow my preparations sufficient time to recover after cutting, to ensure that glycogen levels had returned to baseline levels. Given these considerations, it seems possible that anaerobic glucose consumption through glycolysis can be sufficient to fuel ATP production within astrocytes. Therefore, it

is possible that in the presence of 10 mM glucose, FA-induced inhibition of astrocyte oxidative metabolism may increase the glycolytic rate of these cells, leading to increased glucose uptake that may flux through glycogen stores. Previous work provides evidence that brain glycogen is not static and glucose that enters astrocytes may go through glycolysis or glycogenolysis depending on neuronal activity (Shulman et al., 2001). Therefore, although selective inhibition of astrocyte TCA cycle activity in the presence of 10 mM glucose does not appear to deplete glycogen stores, increased glucose may flux first through glycogen stores prior to glycolysis.

5.2.3.2 Non-selective inhibition of oxidative metabolism and SD propagation

In contrast to FA, non-selective inhibition of oxidative metabolism in both neurons and astrocytes can be achieved by agents such as sodium cyanide, which easily enters all cells and results in effective inhibition of mitochondrial respiration by inhibition of cyctochrome oxidase (complex IV). This was demonstrated in my studies with inverted signals generated by near simultaneous NAD(P)H and flavoprotein (FP) imaging (Figure 4.1). However, cyanide is an irreversible toxin, and not of clinical utility for therapeutic intervention for SD. In this dissertation, I instead chose to examine the effects of nitric oxide (NO) as another non-selective inhibitor of cytochrome oxidase, since this agent has been suggested to be useful in adjunct therapy for SAH in relation to SD (see below). I chose to utilize the nitric oxide (NO) donor 2-(N,N-Diethylamino)-diazenolate 2-oxide (DEA/NO) to inhibit oxidative metabolism. NO

can inhibit cytochrome oxidase activity by competing with oxygen for binding, resulting in reduced ATP in brain mitochondria and an increase in anaerobic glycolysis (Brown and Cooper, 1994; Brookes et al., 1999). My studies show effective inhibition of mitochondrial respiration by DEA/NO in brain slices (Figure 4.1), again as assessed by near simultaneous autofluorescence imaging of NAD(P)H and FP (discussed below). The effects of DEA/NO were concentration-dependent, and comparable with the well-established inhibitor cyanide.

SD leads to increases in inducible nitric oxide synthase (iNOS) and its product NO (Read et al., 1997; Petzold et al., 2008; Viggiano et al., 2008). In my studies, addition of DEA/NO resulted in a significant increase in the rate of high K^+-SD propagation. It was possible that the inhibition of either neuronal or astrocyte oxidative metabolism by NO could underlie these effects. NO exposures could result in moderate neuronal depolarization at the advancing wavefront. In addition, as discussed above, exogenous NO may inhibit astrocyte oxidative metabolism prior to high K^+-SD onset, and thus result in decreased astrocyte clearance of extracellular K^+ and glutamate. This latter mechanism is consistent with the results observed with selective inhibition of astrocyte metabolism with FA discussed above (Section 5.2.3.2).

The effect of exogenous NO on SD in my studies is different from what had been described previously with rat brain slices (Petzold et al., 2008). In those studies, inhibition of nitric oxide synthase (NOS), decreased SD threshold, and subsequent addition of exogenous NO, returned SD threshold to normal levels. NO is believed to be neuroprotective by interacting with presynaptic P/Q voltage

gated calcium channels (VGCCs) to decrease glutamate release as well as inhibiting postsynaptic NMDA receptors to reduce postsynaptic action (Read et al., 1997; Petzold et al., 2008); both of which would be expected to be neuroprotective by decreasing excitatory transmission. It is likely that in my DEA/NO studies exogenous NO reached higher concentrations than in those previous studies, where exogenous NO was co-applied with a NOS inhibitor. Therefore, to determine if the protective effects of NO observed previously (Petzold et al., 2008) could potentially be exploited to limit SD events, future studies using an NO donor such as S-Nitrosoglutathione (GSNO), which should not inhibit cyctochrome oxidase activity, are required.

5.2.3.3 Selective increases in astrocyte oxidative metabolic substrate

To test the hypothesis that increasing astrocyte oxidative metabolism would decrease the rate of SD propagation, slices were pre-exposed to acetate. Like FA, acetate is selectively transported into astrocytes due to the preferential uptake by the astrocytic monocarboxylate-like transporters isoform, MCT1 (Waniewski and Martin, 1998). Previous *in vivo* studies using radiolabeled acetate found a significant increase in astrocyte metabolism and acetate utilization in penumbral tissue during reperfusion following 120 min MCAO (Haberg et al., 2006) suggesting that astrocytes can readily take up acetate and utilize it as an oxidative substrate. In my studies, acetate pre-exposures had no significant effect on SD propagation rates under normoxic (high K^+) conditions. This implies that hippocampal slice preparations have adequate metabolic substrates during normoxic (high K^+) SD, which is consistent with my 2mM MSO

results with this stimulus (see above). The fact that OGD-SD was not slowed by acetate was not unexpected. Acetate cannot be metabolized under anoxic conditions, since removal of oxygen will inhibit electron transport chain activity and prevent the production of ATP from mitochondrial respiration. Taken together, these studies suggest that under both normal and ischemic conditions, providing astrocytes with additional glycolytic (rather than oxidative) substrates may be useful to limit the spread of SD, especially in ischemic conditions.

5.2.4 Effects of astrocyte activation

5.2.4.1 Long-term astrocyte activation in hippocampus

As discussed in the introduction (Section 1.4.3), astrocyte activation may lead to a range of phenotypic changes, including changes in metabolism, which can significantly modify astrocyte function. I set out to develop a model of astrocyte activation within the hippocampus, which could be utilized for *in vitro* slice studies of SD. Astrocyte activation was assessed using the classical marker of activation, glial fibrillary acidic protein (GFAP) (Pekny and Nilsson, 2005). For these studies, I required a method, which resulted in sustained activation, but without the confounding factors of brain injury. Therefore, I chose to use an approach previously established in studies of rat striatum where astrocyte activation was induced by lenti-viral injections with a vector that encodes ciliary neurotrophic factor (CNTF) (Escartin et al., 2006; Escartin et al., 2007). As discussed earlier (Section 3.5), an export sequence was included to allow release from neurons and stimulation of astrocyte CNTF receptors. There was a significant increase in immunohistochemical staining of GFAP in CNTF-infected

preparations when compared with LacZ controls, and this activated phenotype persisted and was observed in mice up to 10 months of age. Importantly, this significant increase in GFAP was due to increased expression within the resident population of astrocytes and not due to progenitor cell proliferation (Section 3.4).

There were no observable differences in the overall health of the animals infected with CNTF compared with LacZ control animals. Immunohistochemistry was preformed to assess both dendritic structure and neuronal density within the CA1 pyramidal cell layer in CNTF preparations compared with LacZ controls. MAP2 immunostaining showed no significant differences in dendritic structure within the CA1 stratum radiatum as a result of astrocytes activation. Nuclear DAPI staining for neuronal density also showed no significant difference between CNTF and LacZ preparations. Therefore, CNTF-lenti-viral injections resulted in profound activation of astrocytes with no significant changes to pyramidal neuron morphology, suggesting that this model of astrocyte activation within the hippocampus may be useful when studying a variety of neurodegenerative diseases where astrocyte activation occurs.

In initial studies, I set out to use each animal as their own control, and CNTF lenti-viral vectors were initially injected into the hippocampus in a single hemisphere, and β-galactosidase (LacZ) lenti-viral control vectors were injected in to the contralateral hemisphere. These unilateral injections of CNTF vectors resulted in profound, long-term activation of astrocytes within the hippocampus. However, in these preparations, I found significant astrocyte activation in both hemispheres. This spread of activation appeared to be the result of diffusion of

CNTF across the corpus callosum, rather than the spread of the lentivirus infection itself. I came to this conclusion based on β-galactosidase staining in LacZ controls, which showed localized immunofluorescence within the injected hippocampus that did not spread into other regions of the brain (Figure 3.1). Therefore, for subsequent studies I utilized bilateral hippocampal injections of lenti-viral vectors containing either CNTF or LacZ. While this experimental design required more animals to include a full LacZ control set, I was careful to ensure animals were age-matched and interleaved between experimental days. Thus, LacZ and CNTF animals were injected, shipped, housed, fed, and handled in an identical manner to make sure that any variability observed between groups during electrophysiological studies was likely due to changes induced by CNTF expression alone.

5.2.4.2 Effects of astrocyte activation on fEPSPs

Once I had a working model of sustained astrocyte activation, hippocampal slice preparations from CNTF-infected animals were utilized for electrophysiological studies. I observed a significant decrease in excitatory postsynaptic field potentials (fEPSPs) in CNTF preparations when compared with LacZ controls (Figure 3.2). As discussed in detail above, these observed changes in synaptic efficacy were not a result of decreased probability of presynaptic glutamate release (see Section 3.5) based on the results from both my PPF and adenosine A1 antagonist studies.

The decreases in excitatory evoked potentials seen in CNTF animals were quite unlike those observed in a different model of astrocyte activation within the

hippocampus. In those recently-published studies, astrocyte activation was induced by over-expression of eGFP (described above Section 1.4.3.3), and resulted in a significant reduction in both evoked and spontaneous inhibitory postsynaptic currents (IPSCs) with no change in excitatory transmission (Ortinski et al., 2010). Those prior results suggest that decreased inhibitory control may result in neuronal hyperexcitability, which is the opposite of what I observed in my CNTF preparations. The decreases in inhibitory transmission in the eGFP model were attributed to reduced glutamine synthesis in astrocytes, which in turn is required for the production GABA. However, glutamine recycling between astrocytes and neurons is also required to maintain glutamate for excitatory transmission (Bacci et al., 2002). Therefore, it is possible that in our CNTF preparations, astrocyte activation leads to decreased glutamine availability, sufficient to reduce fEPSPs by decreasing vesicular glutamate stores. The reduced glutamine synthesis in the eGFP model of astrocyte activation was attributed to downregulation of glutamine synthase (GS) expression (Ortinski et al., 2010). However, in CNTF preparations, glutamate cleared from the extracellular space by these astrocytes may be metabolized to α-ketoglutarate and enter the TCA cycle, which would also decrease glutamine recycling and contribute to smaller fEPSPs. This hypothesis is supported by previous work in rat striatum with the CNTF model of activation, which has shown these activated astrocytes to have a significant metabolic shift towards a more oxidative phenotype (Escartin et al., 2007).

In mouse models, where astrocyte reactivity was prevented by the double knock out of intermediate filament proteins GFAP and vimentin, there was a significant increase in final infarct volumes following MCAO compared with wild type controls (described above Section 1.4.3.2). It is possible that following ischemic injury, reactive astrocytes reduce glutamate-glutamine recycling, which could be protective by preventing neuronal hyperexcitability and excitotoxicity. However, as observed below (Section 5.3.3), a profound effect of CNTF-astrocyte activation on SD initiation may also be of significant benefit following acute ischemic injuries.

CNTF activation of astrocytes is currently being used in clinical trials for patients with Huntington's disease (HD) (Bloch et al., 2004). HD leads to the degeneration of GABA-ergic striatal neurons, which induces motor disorders and eventually leads to loss of higher brain function resulting in psychiatric disturbances (Peschanski et al., 1995). Current clinical trials are based on previous work showing long-term expression of CNTF by lenti-viral infection protected striatal neurons in an excitotoxic rat model of HD (de Almeida et al., 2001). Therefore, in the context of HD, a reduction in excitatory transmission may be one of the protective effects underlying CNTF astrocyte activation. However, my results raise some concern, since long term effects of fEPSP suppression are not known. It seems important that future behavioral studies be conducted *in vivo* to determine the possible long-term impact of constitutive CNTF expression and astrocyte activation on basic neurological functions, including learning and memory. In the context of chronic diseases such as HD, prolonged expression of

CNTF is likely desirable, but following ischemic injury, where expression of CNTF-activated astrocytes is only required for days to weeks, other methods of inducing activation will likely be more useful than infection with CNTF-expressing vectors.

5.2.4.3 Astrocyte activation and SD propagation rate

As discussed below (Section 5.3.3), exposure to a Na^+/K^+-ATPase inhibitor (ouabain) was needed to reliably initiate SD in preparations containing CNTF-activated astrocytes. With the ouabain stimulus, the rate of SD in CNTF preparations was significantly decreased compared with LacZ controls. At the concentrations used for my studies, inhibition of Na^+/K^+-ATPase activity by ouabain is not astrocyte specific (Basarsky et al., 1998), and likely affects neurons and astrocytes equally. Previous studies utilizing the CNTF model of astrocyte activation in rat striatum showed indirect evidence of increased glutamate clearance by these astrocytes (Escartin et al., 2006), which could account for both the decreased rate of SD propagation and the reduction in excitatory transmission observed in CNTF tissues. However, no significant increase in glutamate clearance was observed CNTF preparations suggesting that enhanced glutamate uptake is not the mechanism underlying my observed effects. This is not unexpected, since in the context of ouabain-SD, inhibition of pump activity will reduce the maintenance of the Na^+ gradient required to drive glutamate uptake. Another possible mechanism could be decreased glutamine recycling, which would reduce glutamate concentrations available for synaptic

vesicular release and could also underlie the increased resistance to SD propagation.

Figure 5.1

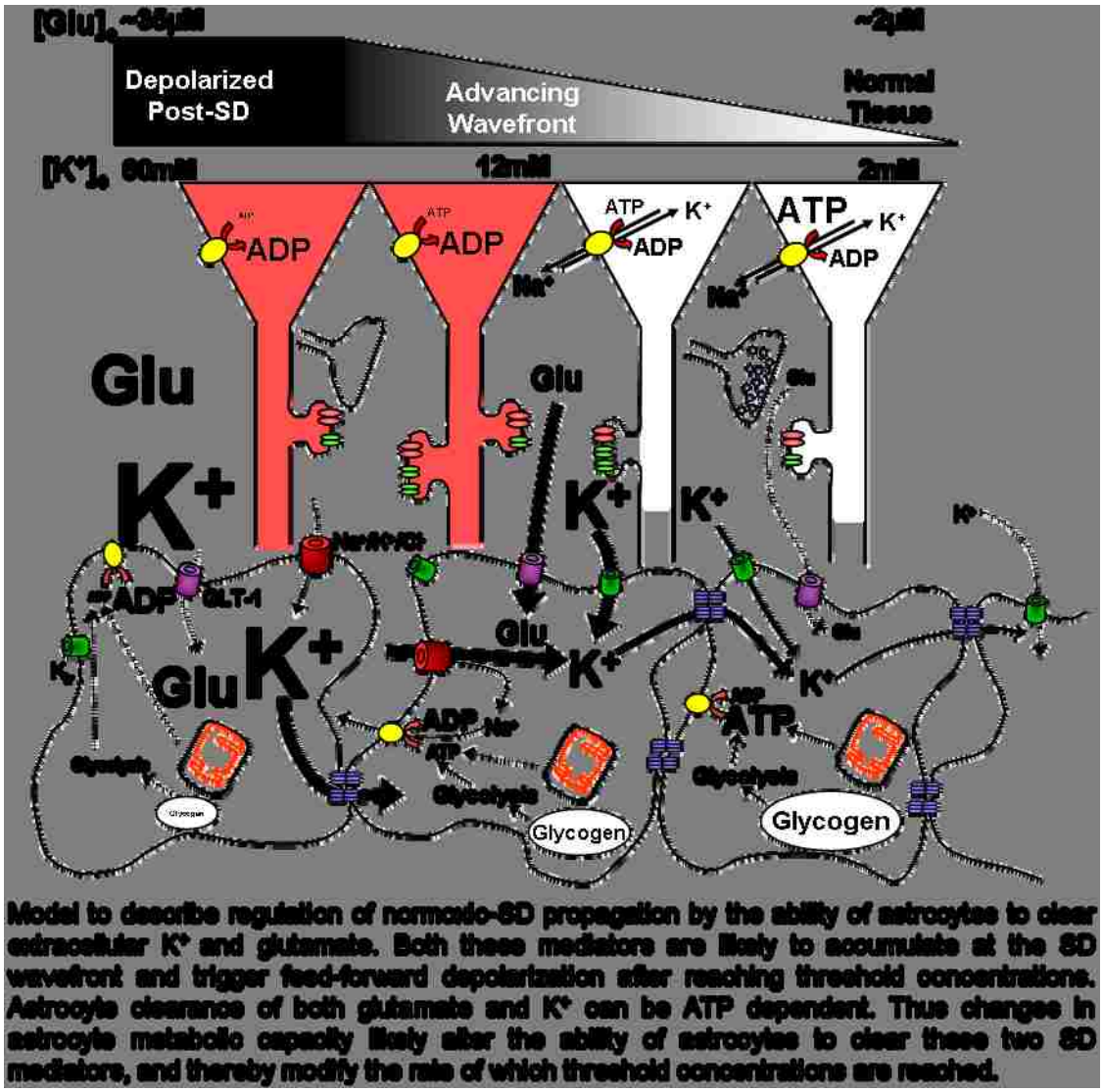

Model to describe regulation of normoxic-SD propagation by the ability of astrocytes to clear extracellular K+ and glutamate. Both these mediators are likely to accumulate at the SD wavefront and trigger feed-forward depolarization after reaching threshold concentrations. Astrocyte clearance of both glutamate and K+ can be ATP dependent. Thus changes in astrocyte metabolic capacity likely alter the ability of astrocytes to clear these two SD mediators, and thereby modify the rate at which threshold concentrations are reached.

5.3 Initiation of SD

5.3.1 SD initiation

5.3.1.1 High K^+-SD

For the studies in this dissertation, SD was induced using either KCl microinjections, oxygen glucose deprivation (OGD), or the Na^+/K^+-ATPase inhibitor, ouabain. KCl microinjections trigger SD by focally raising extracellular K^+ concentrations above threshold levels (Aitken et al., 1998; Bahar et al., 2000; Dietz et al., 2008) resulting in the synchronous depolarization of a group of neurons, which initiate the feed-forward spreading depolarization. Based on my studies, I estimate that the synchronous depolarization of ~20 neurons is required for an SD event to initiate and propagate across a hippocampal slice.

SD threshold could be most effectively evaluated using the high K^+-SD stimulus, and could be finely graded by modifying the duration of the application pressure pulse. With this procedure, I could apply stepwise increases in K^+ volumes to single preparations until the SD threshold was reached. Similar approaches have been used *in vivo* and *in vitro* slice preparations using either graded K^+ applications or electrical stimulation (Ayata et al., 2000; van den Maagdenberg et al., 2004; Ayata et al., 2006; Petzold et al., 2008). One potential drawback of my method is possible variability in the tip size of glass microelectrodes and volumes of K^+ delivered. In all SD threshold experiments, control preparations were interleaved between experimental slices, and the same delivery electrode was used throughout the day. Furthermore, I verified that tip resistance was maintained within a range of 5-8 MΩ. While the exact volume of 1

M KCl injected is not known, microinjection of KCl onto the surface of the slice led to a localized depolarization that was surrounded by normally polarized tissue. From visualization of ejection volumes, I estimated that a 100 ms delivery pulse led to the release of ~3 nL of KCl into the 2 mL bath, implying that these KCl microinjections (usually 30-200 ms) should lead to negligible changes in overall bath K^+ concentrations. This is much different than is seen in threshold studies where SD is induced by bath application of elevated KCl (generally ~25-40mM) (Petzold et al., 2008; Zhou et al., 2010). Under such conditions, SD initiates at a random site, similar to OGD and ouabain-SD, and will likely then propagate through partially depolarized tissue. The focal application method used in my studies had the advantage of known initiation sites, which facilitated threshold tests and examination of both SD initiation and propagation.

5.3.1.2 OGD-SD

SD induced by OGD is a result of metabolic substrate depletion and energy failure, leading to depolarization of neurons that are unable to maintain ionic homeostasis. To generate a spreading depression-like event, a coordinated loss of ionic homeostasis of a population of cells must occur with high spatial and temporal correlation to result in profound depolarization of a tissue volume within a slice. Previous work has shown that during OGD in slice preparations, there is a slow depolarization of CA1 neurons, and reducing the bath temperature resulted in a prolonged delay to the onset of the OGD-induced anoxic depolarization in single cells (Lipski et al., 2006). This effect of decreased temperatures is likely due to reduced metabolic demand in these neurons, which

in turns leads to a longer period of slow depolarization prior to AD threshold. It is assumed that a similar depolarization occurs for the initiation of OGD-SD.

Neurons are usually assumed to be quite homogeneous, with uniform resting potentials and responses to substrate deprivation. However, experiments with OGD show that this may not be the case, since the site of OGD-SD initiation can be at semi-random locations, presumed to be due to sites of relative metabolic compromise (Jarvis et al., 2001). My data is consistent with this view, since OGD-SD showed no consistency in the site of initiation; sometimes propagating through CA1 towards CA3, and sometimes in the opposite direction. This would be expected to underlie some of the variability observed in measurements of the latency to SD onset taken at a single point in mid-CA1, as responses may initiate at a range of distances from the site of the recording electrode.

5.3.1.3 Ouabain-SD

Bath application of ouabain generates SD in a way that is similar to OGD exposures as this agent depolarizes cells, but due to direct Na^+/K^+-ATPase inhibition rather than ATP depletion. Thus, the site of initiation may not be as random as OGD-SD, since depolarization may not be as dependent on regional heterogeneity of metabolic status. Indeed, Basarsky and coworkers argued that ouabain-SD originated at CA1 and propagated towards CA3, because neurons in the initiation site had lower ATPase pump expression levels (Haglund et al., 1985; Basarsky et al., 1998). In my studies, using low power imaging, ouabain-SD events generally initiated in the dentate gyrus (DG) and then moved to the

pyramidal cell layer; spreading from either the CA1 or CA3 (data not shown). Although ouabain is not expected to deplete ATP, it is possible that some of the variability in initiation site could arise because of more rapid ouabain-induce depolarization of already compromised tissue.

I chose to use 100 µM ouabain for my experiments since this concentration was expected to inhibit the major Na^+/K^+-ATPase isoforms found in both neurons and astrocytes (α3 and α2, respectively) (Walz and Hertz, 1982; Watts et al., 1991), and has previously been shown to reliably generate SD in hippocampal slices (Haglund and Schwartzkroin, 1990; Basarsky et al., 1998; Balestrino et al., 1999; Dietz et al., 2008). In primary neuronal and astrocyte culture, 100 µM ouabain resulted in almost complete inhibition of K^+ uptake (Walz and Hertz, 1982). This suggests that neurons will begin to slowly depolarize due to the accumulation of extracellular K^+ that cannot be effectively cleared by astrocytes. Astrocyte membrane potential would be expected to depolarize as well, since astrocyte V_m closely follows K^+ equilibrium potential (Orkand et al., 1966; Amedee et al., 1997). Like OGD-SD, ouabain-SD was exploited for studies of SD latency.

5.3.2 Substrate manipulation on OGD-SD initiation

Previous work has established that depletion of glucose availability (rather than O_2 depletion) is an important determinant for the onset of single-cell depolarizations in *in vitro* ischemia models. This prior work utilized whole cell recordings from pyramidal neurons (Rossi et al., 2000; Hamann et al., 2002;

Allen et al., 2005), and thus, did not evaluate whether these responses were part of propagating SD waves or were instead stochastic anoxic depolarizations that occurred as individual neurons succumbed to substrate deprivation. My initial studies showed that a very similar glucose dependency was also associated with spreading depolarizing events. Removal of glucose from the recording buffer prior to OGD challenge significantly reduced the time to OGD-SD onset, but similar pre-treatments with anoxia were without effect.

Previous studies suggested that depletion of glycogen stores were responsible for the decreased latency in single cell work (Allen et al., 2005). This conclusion was based on the assumption and mathematical modeling that reducing bath glucose concentrations to 2 mM (from 10 mM) would result in glycogen depletion in slice (Allen et al., 2005). I tested this assumption, and found a similar reduction in the latency of SD. However, glycogen levels were not significantly decreased in preparations pre-exposed to 2 mM glucose compared to 10 mM controls. In addition, inhibition of glycogenolysis with DAB/DNJ prior to OGD did not have a significant effect on the latency of SD; suggesting that depletion of glycogen stores within astrocytes does not determine the onset of OGD-SD. There was a trend towards a decrease in slice glycogen content with 2 mM glucose exposures, but there was not complete loss of glycogen as was observed after 20 minute OGD exposures. This suggests that the assumptions made by Allen and colleagues may be partially correct, but it is likely that astrocyte glycogen is more resistant to glucose deprivation than is accounted for by their mathematical model (Allen et al., 2005). In conditions of reduced

glucose, slices were perfused with 95% O_2, and while astrocytes are considered to be primarily glycolytic cells (Wender et al., 2000; Brown, 2004), it is possible that they may shift to an oxidative phenotype to produce ATP more efficiently. This is not unreasonable to consider, since astrocytes have significant numbers of mitochondria and possess all the enzymes required for mitochondrial respiration (Lovatt et al., 2007). Therefore, to significantly deplete glycogen within a slice, either the use of lower glucose concentrations or other challenges will likely be required.

The fact that glucose depletion but not inhibition of glycogenolysis or astrocyte oxidative metabolism affected OGD-SD latency raised the possibility that the availability of glucose within neurons is most relevant. Neurons are known to be more sensitive to metabolic inhibition than astrocytes (Silver et al., 1997), and my studies provide support for the hypothesis that SD is initiated under ischemic conditions when glucose is no longer available to neurons to provide adequate ATP to maintain ionic homeostasis.

In half of the preparations pre-exposed to MSO prior to OGD, SD events were not generated, but signs of neuronal damage were still evident after 20 min OGD exposures. It is possible that single cell depolarizations may have been initiated, but because of enhanced glycogen content, astrocytes had sufficient energy substrates to prevent the accumulation of glutamate and/or K^+ within the extracellular space required for SD initiation. In addition to enhancing glycogen accumulation, MSO is also known to inhibit glutamine-glutamate cycling between astrocytes and neurons (Laake et al., 1995). Therefore, resistance to OGD-SD

onset in MSO could also be due to decreased vesicular glutamate content rather than changes in glycogen concentrations. However, if decreased vesicular glutamate were underlying the effects of MSO, a decrease in the propagation rate during high K^+-SD would be expected as well. Therefore, the significant delay in OGD-SD initiation is likely to be due to the effects of MSO on glycogen concentrations within astrocytes.

5.3.3 Effects of astrocyte activation on SD initiation

For studies on effects of astrocyte activation, SD threshold was determined using graded, localized KCl microinjections, delivered by pressure pulses of increasing duration from a conventional patch electrode. I found that SD could readily be induced in LacZ preparations with 30-100 ms KCl microinjections, but SD could not be induced with KCl in CNTF preparations, even with very prolonged K^+ stimuli (800 ms). Furthermore, elevated bath K^+ concentrations (from 2 mM to 8 mM) did not allow SD generation, as had been described for other relatively SD-resistant tissues (brainstem) (Funke et al., 2009). CNTF and LacZ preparations were interleaved on individual recording days using the same KCl microelectrode and autofluorescence imaging indicated similar degrees of slice activation at the K^+ ejection site. These observations suggested a greatly increased threshold for SD initiation with the K^+ stimulus, or possibly a complete inability of CNTF preparations to allow propagation of SD waves (Section 3.4). This is the first demonstration of changes in SD threshold in conjunction with manipulation of astrocyte phenotype.

Experiments with bath application of ouabain revealed that CNTF tissues do retain the ability to generate SD, albeit with a significantly longer latency to onset than observed in LacZ controls. This confirms that CNTF CA1 pyramidal neurons do retain the appropriate structural and functional properties required for SD. This is an important observation in light of the significant reduction in excitatory transmission (discussed Section 5.2.4), which could be a result of decreased neuronal viability thereby making it difficult to induce SD. As discussed above, ouabain triggers SD by a very different mechanism than does localized K^+ applications, and it leads to a significant impairment in Na^+-dependent glutamate uptake by astrocytes as a consequence of Na^+/K^+-ATPase inhibition (Rose et al., 2009). The increased latency observed in CNTF tissues, may be a result of decreases in the overall glutamate pool, as suggested by the observed reduction of fEPSP in CNTF tissues (discussed in Section 3.5).

The significant resistance to SD, particularly under normoxic conditions, in CNTF tissues may explain some of the neuroprotective effects observed in striatum against excitotoxins (Escartin et al., 2006). It will be of great interest to determine whether these effects on SD threshold are observed in *in vivo* studies as well. For such experiments, CNTF-containing lentivirus would need to be injected into the cortex instead of the hippocampus. Once cortical astrocyte activation was confirmed, SD threshold could be evaluated with high K^+ application to the cortical surface or the measurement of spontaneous SD-like events following focal ischemic injury (Nedergaard and Hansen, 1993; Ayata et al., 2000). Future studies using such models could provide useful additional

insights as to how activation of astrocytes could be targeted during ischemia and migraine. If SDs were significantly limited or even abolished *in vivo*, it would be of particular interest to determine whether ischemic infarct volumes were also reduced.

Figure 5.2

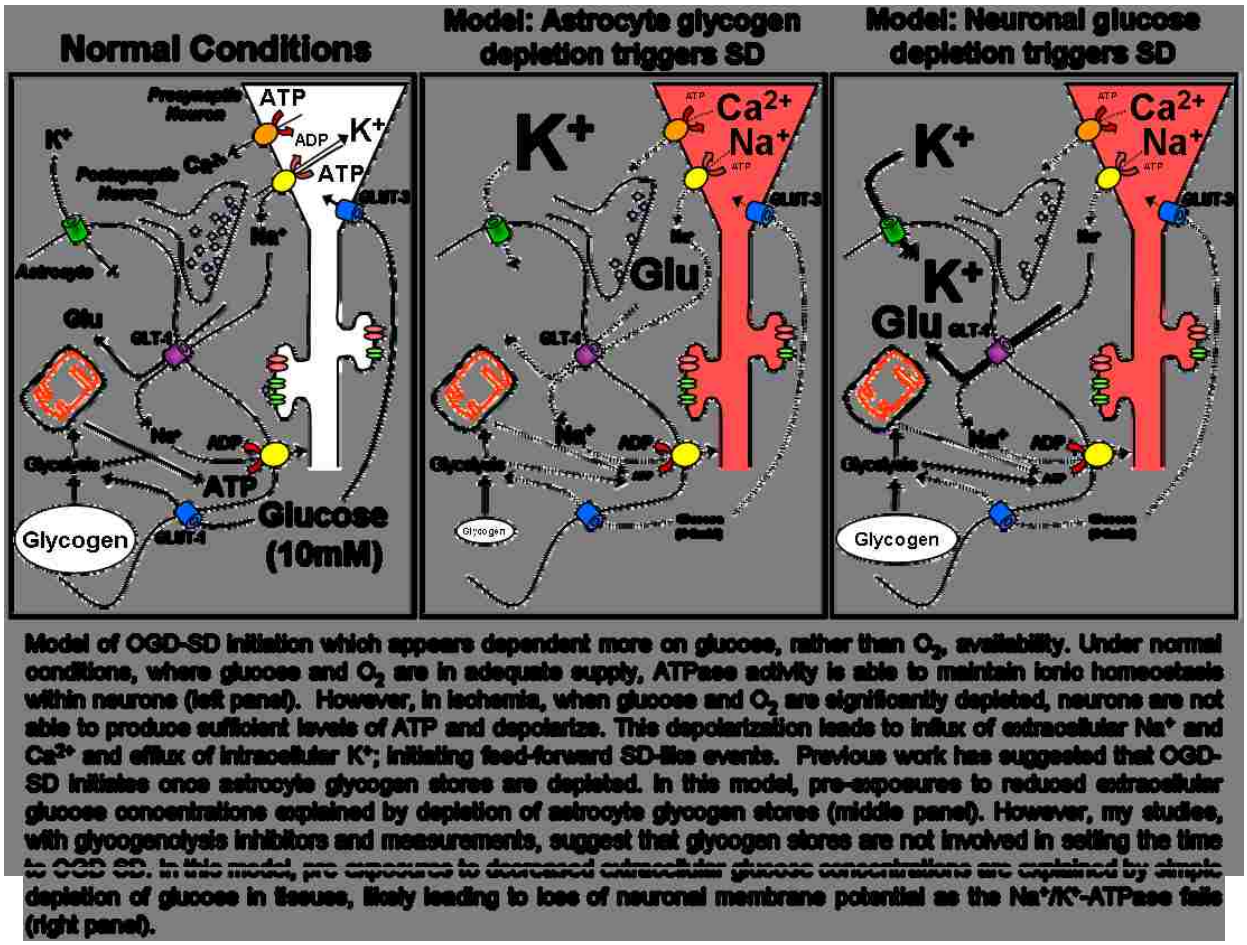

Model of OGD-SD initiation which appears dependent more on glucose, rather than O_2, availability. Under normal conditions, where glucose and O_2 are in adequate supply, ATPase activity is able to maintain ionic homeostasis within neurons (left panel). However, in ischemia, when glucose and O_2 are significantly depleted, neurons are not able to produce sufficient levels of ATP and depolarize. This depolarization leads to influx of extracellular Na^+ and Ca^{2+} and efflux of intracellular K^+; initiating feed-forward SD-like events. Previous work has suggested that OGD-SD initiates once astrocyte glycogen stores are depleted. In this model, pre-exposures to reduced extracellular glucose concentrations explained by depletion of astrocyte glycogen stores (middle panel). However, my studies, with glycogenolysis inhibitors and measurements, suggest that glycogen stores are not involved in setting the time to OGD-SD. In this model, pre-exposures to decreased extracellular glucose concentrations are explained by simple depletion of glucose in tissues, likely leading to loss of neuronal membrane potential as the Na^+/K^+-ATPase fails (right panel).

5.4 Consequences of SD in slice

5.4.1 General consequences of normoxic and ischemic SD

While the mechanisms underlying the initiation of SD during both normoxic conditions (high K^+-SD) and conditions that mimic ischemia (OGD-SD) are

inherently different (discussed above Section 5.2.1), the depolarizing event itself has striking similarities under both conditions (Aitken et al., 1998). Following SD events *in vivo*, energy demands to produce ATP required for the restoration of ionic gradients increase dramatically. This in turn results in significant increases in both blood flow and oxygen consumption (Gido et al., 1994; Piilgaard and Lauritzen, 2009). Normoxic SD is usually considered to be innocuous, as long as it is initiated in healthy tissue and not in metabolically compromised preparations (Nedergaard and Hansen, 1988; Gido et al., 1994). However, in the context of ischemia, SD can lead to neuronal damage, if neurons lack the metabolic capacity to regain ionic homeostasis (Mies et al., 1993; Nedergaard and Hansen, 1993; Hossmann, 1996; Strong et al., 1996). My studies utilizing fEPSPs and MAP2 immunohistochemistry to assess neuronal viability are consistent with these general assumptions. Thus, in preparations where SD was induced with local microinjections of 1 M KCl, these events resulted in no neuronal damage, while SD induced by OGD invariably led to persistent neuronal injury.

5.4.2 NAD(P)H Autofluorescence imaging

5.4.2.1 Combined NAD(P)H and fEPSPs measurements to asses neuronal injury following OGD-SD

Evoked synaptic potentials are a well established method to assess neuronal viability within slice preparations (Rudolphi et al., 1987; Rudolphi et al., 1992; Masino and Dunwiddie, 1999). Previous studies have shown that following OGD there is irreversible damage and persistent loss of fEPSPs (Rudolphi et al., 1992). In my studies, there was an initial loss of fEPSPs, which appeared due to

adenosine activating presynaptic A1 receptors (Figure 2.3), that was completely prevented by addition of an A1 receptor antagonist (DPCPX) (Figure A.1). During continued OGD, following the initial loss of fEPSPs, there was a brief period of hyperexcitability prior to SD onset (see Section 2.5). All synaptic potentials were then permanently abolished at the onset of SD in the context of substrate depletion. On the basis of fEPSPs alone, it is difficult to distinguish between the initial reversible and the secondary irreversible loss of fEPSPs due to neuronal injury (see also (Attwell and Laughlin, 2001). However, imaging NAD(P)H autofluorescence simultaneously with fEPSP recordings allowed such a discrimination.

As described in Section 2.4, there are significant changes in NAD(P)H autofluorescence signals during OGD exposures. NAD(P)H autofluorescence initially increases ~80% above baseline levels due to hypoxia, where it plateaus until the onset of SD. The spread of SD was well tracked by NAD(P)H autofluorescence and the time point at which decreases in NAD(P)H crossed the recording electrode matched very closely the loss of both pre- and post- synaptic components of the fEPSP. NAD(P)H levels then continued to decline below baseline levels, even with the reintroduction of nACSF, which was a hallmark of irrecoverable neuronal damage. This optical decrease is due to swelling (see below) as well as dendritic beading (Obeidat et al., 2000) that accompanies injury.

Neuronal damage was confirmed following OGD-SD using immunohistochemical techniques. Based on previous studies, slices were fixed,

and stained for microtubule associated protein 2 (MAP2) without resectioning to assess neuronal damage (Hoskison and Shuttleworth, 2006; Hoskison et al., 2007). In slices pre-exposed to hypoxia alone, which does not induce SD in our preparations, there was a transient increase in NAD(P)H autofluorescence coincident with a decrease in fEPSPs, both of which returned to baseline levels following reintroduction of nACSF. MAP2 immunohistochemistry was performed on these preparations, where little to no neuronal damage should have been induced, for comparison with OGD-SD preparations (Figure A.2). Consistent with previous work (Hoskison et al., 2007), in healthy slice preparations, neurons expressed MAP2 almost exclusively in dendrites while in preparations where OGD induced SD, there was dendritic beading and significant loss of MAP2 within the dendritic process and an accumulation within the cell soma.

Therefore, when NAD(P)H autofluorescence was above baseline levels and there was a loss of fEPSPs, I could conclude these changes were adenosine-mediated synaptic depression, but when NAD(P)H autofluorescence was below baseline levels and there was a loss of fEPSPs, this was invariably associated with neuronal damage.

5.4.2.2 Metabolic contributions of NAD(P)H signal

NAD(P)H autofluorescence provides a useful method not only to visualize the propagation of SD across the tissue, but it also provides a measure of mitochondrial redox potential during these events. Consistent with previous work (Hashimoto et al., 2000), high K^+-SD induced biphasic NAD(P)H transients in my studies. As noted above, during OGD, NAD(P)H autofluorescence levels are

already elevated prior to OGD onset, and the propagating event is marked by NAD(P)H decreases (Figure 2.3). It has been assumed that autofluorescence excited at 360nm is due primarily to mitochondrial NADH dynamics (Lipton and Whittingham, 1979; Hansen, 1985; Tian and Baker, 2002), and can therefore be used to indirectly assess regional oxygen consumption during SD (Jarvis et al., 2001; Joshi and Andrew, 2001). The rapid decrease in NAD(P)H at the onset of normoxic SD has been attributed to rapid oxygen consumption (Takano et al., 2007; Galeffi et al., 2010), but it is likely that other optical effects contribute to the drop particularly during OGD-SD.

It is well established that NAD(P)H measurements *in vivo* during SD are significantly complicated by blood flow changes (Mayevsky et al., 1974). In slice preparations, blood flow is not a confounding factor, but it remains possible that autofluorescence signals due to redox changes in NADH concentrations can be contaminated by intrinsic signals from the preparation itself (Lipton, 1973). Severe cell swelling is a consequence of SD and provides the bases for intrinsic optical signal (IOS) imaging of SD described above (Section 1.1.2) (Andrew et al., 1999). Therefore, it is possible that changes in cellular volume may significantly contaminate the NAD(P)H autofluorescence signals in the slice. One of my aims was therefore to determine whether 360 nm autofluorescence signals were indeed attributable to mitochondrial dynamics alone. In order to determine which parts of the NAD(P)H signal were in fact due to mitochondrial respiration, near-simultaneous recordings of NAD(P)H and flavoprotein (FP) were performed during both high K^+ and OGD-SD. Changes due to mitochondrial respiration

should result in NAD(P)H increases and matched, but inverted FP fluorescence. Interestingly, I found that the sharp decrease in NAD(P)H was actually matched by a sharp decrease in FP autofluorescence. This strongly suggests that initial NAD(P)H decreases are largely an optical artifact, likely attributable to neuronal swelling, and not a result of rapid oxygen consumption for both high K^+ and OGD-SD (Figure A.3). My results also suggest that the swelling response enhances the prolonged FP decease while masking part of the prolonged NAD(P)H increases following high K^+-SD. In the context of OGD, following SD NAD(P)H levels decline and are matched by FP increases for a time following reperfusion with nACSF. However, NAD(P)H eventually drops below baseline levels and FP starts to decrease as well, suggesting neuronal damage.

In conclusion, my results reemphasize the importance of accounting for cellular swelling when using NAD(P)H optical imaging techniques to assess mitochondrial redox changes. It has been acknowledged previously that this NAD(P)H imaging method does not provide quantitative measurements of NAD/NADH redox changes in ischemia SD studies (Strong et al., 2000). Therefore, rigorous correction for swelling due to SD when interpreting imaging results is required, and studies, which have not accounted for the profound contamination of 360 nm autofluorescence signals following SD may misinterpret changes due to swelling as changes is mitochondrial redox potential (Mayevsky and Rogatsky, 2007).

5.4.2.3 Contribution of different cell types to autofluorescence signals

My work also sheds some light on the possible contributions of different cell types to the autofluorescence signals observed during OGD. Autofluorescence measurements were taken from the stratum pyramidale (*sp*), and therefore are likely to arise from a combination of CA1 dendrites, astrocytes, and interneurons. Following all pre-exposure conditions, which selectively targeted astrocyte metabolism, there were no significant differences in NAD(P)H autofluorescence increases during OGD prior to SD onset. If astrocyte metabolism contributes greatly to the NADH increases due to OGD, then selective inhibition with FA may be expected to reduce increases in autofluorescence, since FA inhibits TCA cycle activity prior to NADH-producing steps. Inhibition of glycogenolysis also did not significantly affect NAD(P)H autofluorescence changes, a finding, which again could be consistent with a primarily mitochondrial basis for these signals (see above) .

Taken together, these studies demonstrate the importance of simultaneous optical and field potential recordings to allow studies of SD mechanism as well as effective tracking of SD propagation. In addition, effects observed that are likely due to metabolic changes appear to be mitochondrial and likely originate predominantly from neurons.

5.5 Implications for migraine

While there are many moderately effective treatments for relieving migraine headaches, the mechanisms underlying many of these drugs are not

well understood (see Section 1.2.2). It is becoming more widely appreciated that SD events may trigger migraine headache, and it is exciting that some of the more effective treatments available have recently been shown to reduce SD events in a dose-dependent manner (Moskowitz, 2008; Ayata, 2010). This strongly suggests that targeting SD may be a promising strategy to prevent the onset of migraine itself. My work raises the possibility that targeting astrocyte metabolism may be useful to inhibit the progression of SD events related to migraine symptoms.

As discussed above, targeting either glycolytic or oxidative metabolism could be useful approaches to retard SD propagation. It is unclear from my studies whether increasing glycogen stores within astrocytes may be protective against SD in the context of migraine. Prolonged 2 mM MSO pre-exposures prior to high K^+-SD slowed the rate of SD propagation, but did not inhibit the event completely. As discussed above (Section 5.2.1), under normoxic conditions, astrocytes appear to have sufficient substrate to clear extracellular K^+ and glutamate at optimal levels. One could speculate however, that in chronic migraine patients, particularly those with FHM, many cellular processes, perhaps including some related to astrocyte metabolism and function, may potentially not be functioning normally. Therefore, it may be of interest to examine effects of astrocyte manipulation in future studies using animal models of FHM. For example, in one form of FHM, increased susceptibility is due to genetic mutations and dysfunction of Na^+/K^+-ATPase (Vanmolkot et al., 2006). It is unclear which cell type(s) these mutations will target and result in disruption of pump activity.

However, in astrocytes, decreased ATPase activity will significantly reduce the driving force for both glutamate and K^+ clearance from the extracellular space, and may contribute to increased excitability. This could be one mechanism underlying the susceptibility of these patients to SD-induced migraine headaches, and perhaps also seizures (Moskowitz et al., 2004).

NO synthesis is known to increase following SD (Read et al., 1997; Petzold et al., 2008), and it is therefore possible that SD could contribute to migraine headache by inducing the production of NO. NO has been proposed as a potential initiator of migraine attacks, likely due to its vasodilatory properties, and inhibition of nitric oxide synthase (NOS) can inhibit migraine headache (Olesen et al., 1995; Lassen et al., 1997). In my work, SD was facilitated by high levels of NO, and it is not yet known whether such actions may contribute to the beneficial effects of NOS inhibition of migraine patients.

Gabapentin is a $Ca_v2.1$ channel antagonist that reduces presynaptic glutamate release, and previous work has shown that this agent produced a significant increase in SD threshold (Hoffmann et al., 2010). In our CNTF studies, activation of astrocytes also led to significant increases in SD threshold in normoxic models of SD, to an extent that propagating events could not be induced even at a stimulus intensity 10X that required for SD induction in control preparations. These results raise the possibility of targeting astrocytes for migraine treatments. It is exciting to consider that therapeutic strategies that mimic these effects induced by CNTF-activation without lenti-viral injections may be protective against SD and prevent migraine onset. It is acknowledged that

repetitive SD leads to astrocyte activation in animal models (Kraig et al., 1991), and it is possible that astrocytes in patients who suffer from recurrent headaches with aura may already be significantly activated. Thus future work to understand the phenotypic changes in astrocytes following migraine will be of great interest.

5.6 Implications for ischemic injury

5.6.1 Ischemic stroke

5.6.1.1 SD events and the expansion of ischemic injury

As described in the Introduction, focal ischemic infarcts can act as a focus for the initiation of depolarizing events, which spread outward through penumbral tissue (see Section 1.3.3). In recent years, exciting evidence has accumulated that these SD-like events very likely contribute to the expansion of ischemic injury volume, and may be important targets for treatment of acute strokes. Within penumbral regions, tissue perfusion can be maintained by collateral flow, but usually at levels below 40% of normal, leading to ATP reductions of about 50-70% of normal levels (Lipton, 1999). Although collateral flow appears to be sufficient for neuronal survival in penumbral tissues in the absence of other metabolic challenges, repetitive SD-like events present a substantial additional metabolic burden due to ionic fluxes which is likely to lead to neuronal damage (Hossmann, 1996). In addition, other factors released by SD may further compound the metabolic burden of ionic disruption. One such factor is NO, and in my work, high levels of NO are sufficient to transform recoverable SD into an event that results in irreversible neuronal damage even in normoxic tissues.

It is important to emphasize that SD-like events are not restricted to the initial formation of the ischemic core, but have been shown to occur repetitively with high frequency after stroke onset in animal models (Hartings et al., 2003), and indeed have been measured electrically many hours after the onset of injury in human patients. Recordings of SD associated with enlargement of infarcts has been made even 5 days following the initial stroke (Dohmen et al., 2008; Lauritzen et al., 2011), suggesting a dramatically larger window of opportunity for therapeutic intervention than is currently possible with tPA (see Section 1.3.2).

Under normoxic conditions, repetitive SD leads to a stepwise depletion of glucose and accumulation of lactate over time (Krivanek, 1961; Hashemi et al., 2008), albeit without inducing obvious neuronal damage. In the context of ischemia, depletion of substrates would be expected to be much more severe with each SD-like event. The extent of depletion would be dependent on 1) distance from the ischemic core and 2) number of depolarizing events that occur. This is a consequence of the fact that across the penumbra, a gradient of energy substrates from the infarct core to outer lying healthy tissue is expected (Lipton, 1999). Once glucose concentrations fall below levels required to recover ionic homeostasis in a region, neuronal death is expected to follow.

Paradoxically, it is well established that hyperglycemia exacerbates ischemic injury in clinical settings (Capes et al., 2001). Insulin has been suggested for use to manage blood glucose in patients, but the efficacy of this approach is unclear and hypoglycemia can become considerable risk factor in this setting (Kansagara et al., 2008). Several mechanisms are thought to underlie

the deleterious effects of hyperglycemia in stroke recovery. Hyperglycemia in the context of brain ischemia can lead to the accumulation of lactate and result in intracellular acidosis (Levine et al., 1988). Furthermore, hyperglycemia increases reactive oxygen species (ROS) and leads to increased oxidative stress by either lipid peroxidation (Siesjo et al., 1985) or other mechanisms, including increasing activity of NADPH oxidase (Suh et al., 2008). It is possible that provision of alternative approaches to sustain metabolic reserves during repetitive SDs may be more effective and lack the deleterious effects of high glucose exposures.

In slice preparation studies, there are few methods, which provide good models for penumbral conditions. Bath application of oxygen and glucose-free solutions are a useful model of ischemia, which can be used to reliably induce SD. However, this only mimics some of the conditions in the ischemic core, and does not include gradients of reduced substrate availability. A recent study has reported an *in vitro* brain slice model of focal ischemia where OGD solution is focally applied to a small region of a cortical slice, while continuing to perfuse most of the preparation in nACSF, in an effort to produce a gradient of substrates (Richard et al., 2010). Future studies utilizing this model may provide additional insights into generation of SD-like events in penumbra, including the potential roles of astrocytes.

It is important to mention that previous clinical studies on the effects of SD following a wide range of insults have focused on the frequency of SD events and the duration of the associated DC shift rather than the rate of the propagating wave across the tissue. There is a large body of work from the

COSBID study group providing evidence that prolonged DC shifts are associated with limited electrocortiographic (ECoG) recovery and poor patient outcome (Dreier et al., 2006; Fabricius et al., 2006; Oliveira-Ferreira et al., 2010). It has yet to be tested whether the rate of propagation contributes to the expansion of injury in a similar manner. One could speculate that accelerating the spread of SD events may lead to an increase in SD frequency and longer DC durations. Thus, serving as an indirect measure of tissue health since, based on studies from this dissertation, improving metabolic status within the tissue slows the depolarization propagation. It will also be of interest in future studies to determine if more rapid propagation rates allow for SD events to invade into tissue they would not normally reach.

5.6.1.2 Targeting astrocyte metabolism post-ischemia

As described in the Introduction, astrocytes are generally less susceptible to ischemic injury than neurons, and may be important and viable targets for stroke therapy. My work suggests, for the first time, that supplementing glycogen stores to fuel astrocyte function may be useful to limit the progression of SD-like events through ischemic tissues. It is suggested that astrocyte glycogen stores could be important in limiting the spread of these events, as well as providing substrate for astrocytes to clear glutamate and K^+ after the depolarization has passed through the tissue. It is not yet known how bolstering glycogen stores in human stroke brains could be best accomplished. In animal models, insulin and insulin-like growth factor (IGF) cause an increase in brain glycogen, but these agents may have complex and even deleterious effects on human subjects (e.g.

severe hypoglycemia with insulin, see above). MSO or similar agents could potentially be considered, but the effects of MSO on glutamate-glutamine recycling between astrocytes and neurons suggest that it may have profound effects on glutamate and maybe even GABA concentrations which may alter normal synaptic activity.

Another possible therapeutic approach may be targeting astrocyte activation and changes in metabolic substrate dependence that accompanies activation of these cells. Previous studies have shown that ischemic preconditioning with SD increased astrocyte GFAP expression and this was correlated with reduced cortical infarct volume following MCAO (Matsushima et al., 1998). A number of other studies have also described astrocyte activation following SD, as demonstrated by strong increases in GFAP immunolabeling in affected tissues (Kraig et al., 1991; Wiggins et al., 2003). In studies of repetitive application of K^+ in otherwise healthy brain, astrocyte activation occurred within 6 hours of SD-events and persisted for at least one week post-SD (Kraig et al., 1991; Bonthius and Steward, 1993; Wiggins et al., 2003). There have been few studies of the consequences of astrocyte activation following SD, but it is noteworthy that a recent preliminary report describes a progressive increase in SD threshold when rats are repetitively challenged by SD (Sukhotinksky et al., 2008). My results with CNTF-activated astrocytes suggest that the SD threshold increase observed following preconditioning with repetitive SD could be a result of astrocyte activation seen in those experiments.

Previous work has shown that astrocytes undergo a profound metabolic shift following activation with CNTF. This leads to reduced glycolysis and increased capacity for ketolysis and β-oxidation (Escartin et al., 2007). Therefore, if ischemia-induced astrocyte activation also induces this metabolic switch, glucose may not be an appropriate metabolic fuel for activated astrocytes *in situ*. One possible treatment strategy could therefore be placing ischemia patients on a ketogenic diet, as this has been shown to be particularly effective for patients suffering from intractable epilepsies (Freeman et al., 2007; Noh et al., 2008), and these fuels may be readily oxidized by reactive astrocytes surrounding ischemic infarcts.

As discussed above, astrocyte activation is not uniform and the phenotypic changes that are associated with reactive astrocytes following brain injury may be significantly different that those induced with CNTF-activation. In the context of ischemia, the actual phenotypic changes that occur in astrocytes when they become reactive are not described well enough to know if the effects I see with my model of astrocyte activation will be directly applicable. In addition, inhibition of SD under all conditions may not be protective. It seems reasonable to consider that SD may provide protection to neurons following injury, by inhibiting neuronal activity for a period of time after the depolarization. However, in the context of ischemia, where metabolic substrates are not available to allow neurons to repolarize, it is likely that SD-like events are primarily neurodegenerative (Lauritzen et al., 2011), and finding targets to block these

events may provide possible new therapeutic treatments that are sorely needed for the majority of ischemic stroke patients.

5.6.2 SD events and subarachnoid hemorrhage (SAH)

As mentioned above (Section 1.3.5.2), NO has been suggested as a potential therapeutic target for SAH therapy. NO is known to increase following SD (Read et al., 1997; Petzold et al., 2008), and may have a wide range of effects due to the ability of NO to diffuse easily throughout the tissue and influence blood vessels, neurons, and astrocytes. As discussed (Section 5.2.3.2), previous work has established that nitric oxide (NO) at basal levels may be protective against SD due to its interactions with both presynaptic P/Q voltage gated Ca^{2+} channels and postsynaptic NMDA receptors to reduce neuronal excitability. However, my work emphasizes that exogenous NO also can lead to inhibition of oxidative metabolism, which, in turn, promotes the spread of SD across the slice preparation, similar to the effects of FA. Increasing NO results in decreased oxygen consumption and ATP production within neurons, which is likely a result of cytochrome oxidase inhibition (Almeida et al., 2001; Almeida et al., 2005). Therefore, considering the concentration of NO delivered in the context of therapeutic intervention is likely to be critical and difficult to manage in SAH patients. This implies that NO itself may not be useful, and alternative agents that maintain the beneficial effects of NO without deleterious effects of cytochrome oxidase inhibition may be more useful. As discussed above (Section 5.2.3.2), the NO donor S-nitrosoglutathione (GSNO) may be a good candidate, and previous studies have shown that early treatment with GSNO following SAH

in rat preserved cerebral microvasculature structural anatomy, inhibited vasoconstriction, and prevented loss of the blood brain barrier (BBB) (Sehba et al., 2007). Effects on SD of this agent are currently unknown.

5.7 Limitations of research

5.7.1 Animal models

The use of animal models, including mouse models for neurodegenerative studies, has come under great scrutiny, in large part due to the fact that relatively few therapeutic treatments that are effective in mice have proven to be clinically useful in subsequent human trials (Lee et al., 1999). This concern has historically been extended into SD studies. One important difference, relevant for SD, is the fact that mice have lissencephalic brains while humans are glyrencephalic. Indeed, there was a great deal of speculation as to whether SD events were even capable of spreading across human brain tissue. As discussed in the Introduction, it is now well established that SD-like events occur in humans patients following many different forms of injury (Dreier et al., 2006; Fabricius et al., 2006; Dohmen et al., 2008; Dreier et al., 2009), and that the characteristics of these depolarizations are strikingly similar to those observed in mice. Therefore, for studying the phenomenon of SD, using mouse models should provide a great deal of information on the mechanisms underlying these events that should be relevant in human clinical settings.

As mentioned in the Introduction, the ratio of glial cells to neurons in the human brain is at least 10 to 1 (Kimelberg and Nedergaard, 2010), while smaller

mammals not only have fewer cells within the brain, but the ratio of astrocytes to neurons also decreases (Nedergaard et al., 2003). This suggests that the significant effects of astrocyte manipulations observed in my studies conducted in mice (with smaller glial/neuron ratios) may be underestimated when translated to humans. It will be of interest in future work to extend studies of astrocyte activation and also manipulation of astrocyte metabolic substrate availability to slices of human tissue. This may be considered with specimens removed from temporal lobe seizure surgeries.

5.7.2 Acute slice preparations

Spreading depression requires tightly packed neuronal networks to initiate and propagate. Therefore, this phenomenon cannot be studied in cell culture and the mechanisms underlying these events are studied either *in vivo* or *in vitro* slice preparations. Hippocampal slice preparations were useful since they possess the neuronal density required for these propagating events (see (Somjen, 2001)) and maintain basic cellular connections which are not possible in culture. Slices are also useful to test the main hypotheses for my studies because manipulation of experimental conditions (including temperature, substrate concentration, and perfusion rate) is accomplished much more easily in slice preparations than in *in vivo* whole brain preparations. However, the most obvious limitation to the *in vitro* slice preparations is their lack of blood perfusion, which may limit the interpretation of some results in the context of human pathological conditions. This may be very important for stroke and migraine, where blood flow is an additional significant contributor. It will be interesting in future studies, to examine

the effects of modifying either astrocyte metabolism or astrocyte phenotype in *in vivo* preparations to determine if the significant effects on SD that were observed in *in vitro* slice preparations are observed in whole brain.

5.7.3 Lenti-viral injections and immunohistochemistry

Lenti-viral injections are useful for inducing long-term expression of a gene of interest. Indeed, in my CNTF studies, activation of astrocytes induced by lenti-viral infection with CNTF remained persistent for at least 10 months. While this was useful for mechanistic studies, this long term infection may also be a potential drawback of this particular method, since gene expression can never be turned off. This makes the use of these viruses likely not ideal for transient neurological disorders such as stroke or SAH where increased gene expression will only be desired for days to weeks, but may be more relevant for chronic pathological conditions such as Huntington's Disease or Parkinson's Disease where the constitutive expression of CNTF may be neuroprotective and required for many years.

I utilized immunohistochemical staining of GFAP to assess significant astrocyte activation in my CNTF slice preparations, and compared activation with both LacZ and non-injected naïve controls. For these studies, I analyzed areas expressing GFAP within a given region of interest for all groups. CNTF preparations had significantly larger areas expressing GFAP than both LacZ and naïve control preparations. These methods do no provide the best quantitative measure, and protein levels of GFAP within the three different conditions may

have provided a more accurate method for quantitative measurement of changes in GFAP expression levels. However, the changes in GFAP were so robust, that we felt quantifying immunohistochemical labeling was sufficient to verify strong astrocyte activation. In addition, cell counts were taken within each region of interest to ensure that the increased area expressing GFAP was a result of increased expression within the resident population of astrocytes rather than progenitor cell proliferation. However, if more quantitative information is required in future studies to assess the degree of astrocyte activation throughout the time course of a neurological disorder, PCR or western blot analysis may be preferable.

5.8 Conclusion

These studies provide support for the hypothesis that astrocytes are important regulators of depolarizing events, which may spread across tissues. My findings with the CNTF-model of astrocyte activation suggest that reactive phenotypes generally induced under many pathological conditions may, in fact, be neuroprotective by preventing SD-like events which are known to contribute to the expansion of injury. Therefore, further studies to investigate the direct mechanism by which astrocytes may stop the spread of these depolarizing events may be of great clinical relevance to a wide range of disorders including migraine and stroke.

Figure 5.3

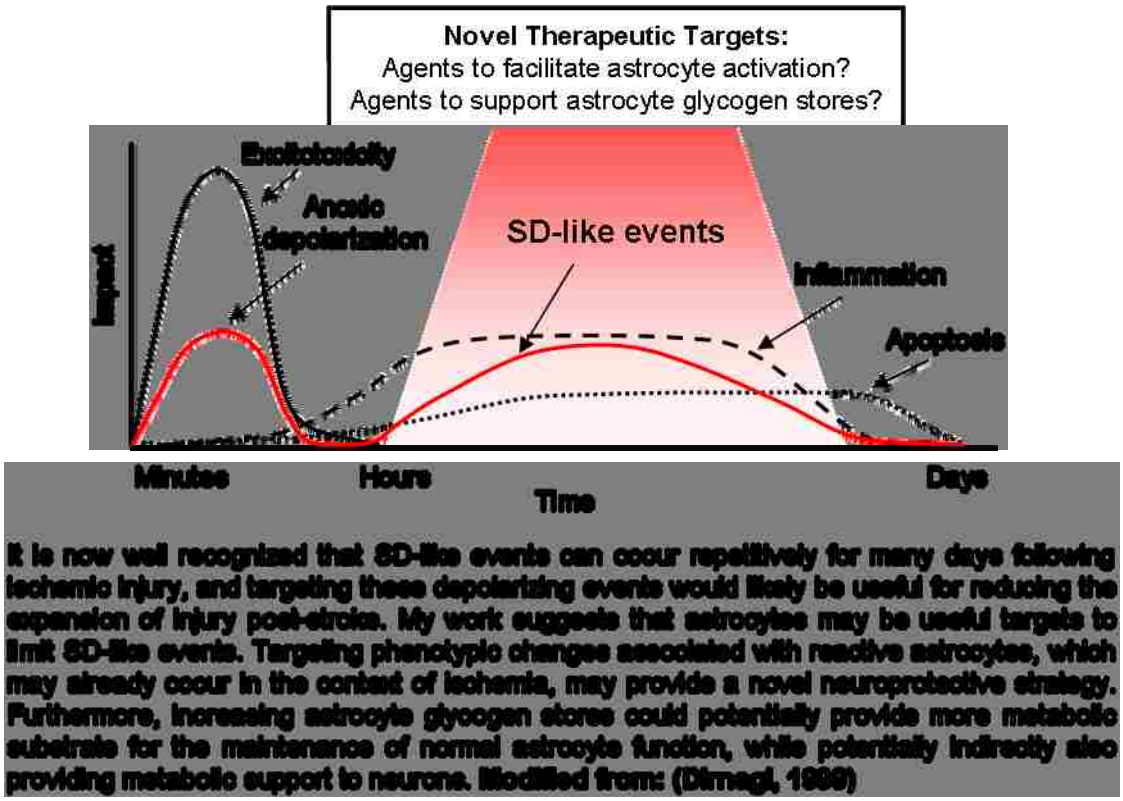

It is now well recognized that SD-like events can occur repetitively for many days following ischemic injury, and targeting these depolarizing events would likely be useful for reducing the expansion of injury post-stroke. My work suggests that astrocytes may be useful targets to limit SD-like events. Targeting phenotypic changes associated with reactive astrocytes, which may already occur in the context of ischemia, may provide a novel neuroprotective strategy. Furthermore, increasing astrocyte glycogen stores could potentially provide more metabolic substrate for the maintenance of normal astrocyte function, while potentially indirectly also providing metabolic support to neurons. [Modified from: (Dirnagl, 1999)]

Appendix A: Supplemental Data

Figure A.1

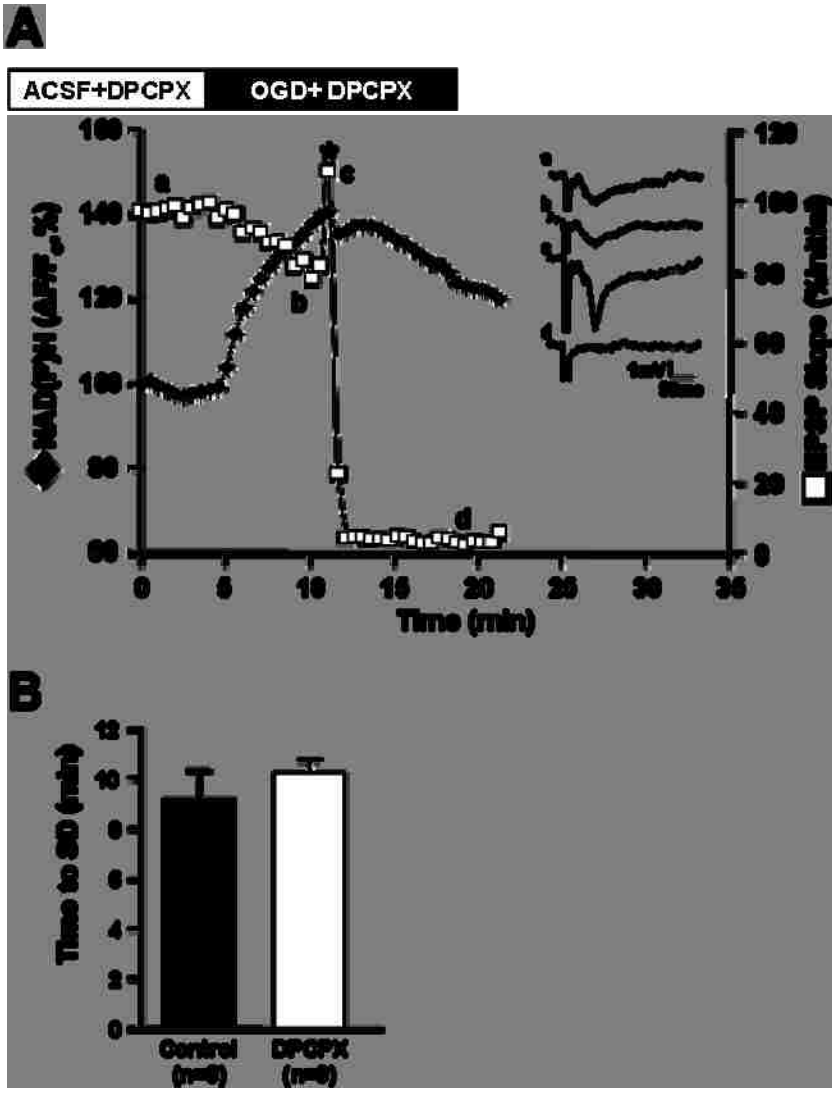

Figure A.1

Effects of A1 receptor antagonist (DPCPX) on OGD-SD. A. Slices were pre-exposed to DPCPX (200nM) for 10 minutes prior to OGD onset. Continued application with OGD showed that although there was some reduction in fEPSPs, it was much smaller than the loss observed in control OGD preparations (see Figure 2.3). fEPSPs were abolished post-SD despite the presence of DPCPX.

B. DPCPX pre-exposures had no effect on mean latency to onset of OGD-SD (n=6).

Figure A.2

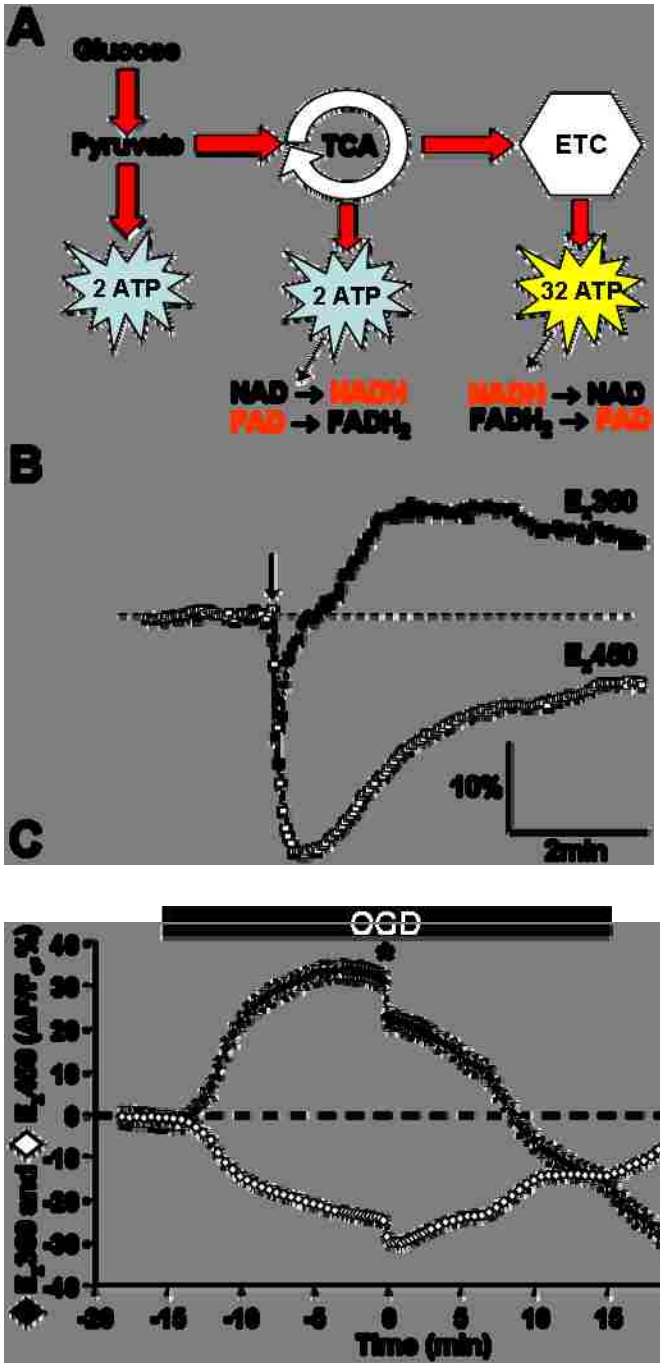

Figure A.2

A. Principles underlying inverted NAD(P)H (E_x360) and flavoprotein (E_x450) autofluorescence signals of mitochondrial origin. In this figure, red species are fluorescent, whereas non-fluorescent species are indicated in black.

B. Near simultaneous autofluorescence imaging of E_x360 and E_x450 during high K^+-SD. SD was initiated at the arrow and slices were ultimately excited at 360nm for 300ms and then 450nm for 150ms. SD resulted in a transient decrease in E_x360 signal followed by a prolonged overshoot. This is typically interpreted as transient NADH oxidation followed by excessive reduction due to inhibition of respiration and/or enhanced TCA cycle activity. However, E_x450 measurements are informative because they imply a prominent optical artifact during the initial phase. This is because no initial E_x450 increase is observed with this time resolution and E_x360 measurements are not inverted with respect to E_x450 signals until late in the response.

C. Near simultaneous autofluorescence imaging of E_x360 and E_x450 during OGD-SD. The same methods used for high K^+-SD were employed during OGD exposures. As described in Section 5.4.2, E_x360 increases prior to SD are likely due to inhibition of mitochondrial respiration due to hypoxia because they are well matched by decreases in E_x450 signals. Like the high K^+-SD responses, initial autofluorescence decreases after OGD-SD onset (asterisk) are largely contaminated by tissue swelling. It is important to note that this does not prevent effective tracking of the SD event with these methods. It does, however, limit the ability to assess mitochondrial function right after SD with these methods.

Figure A.3

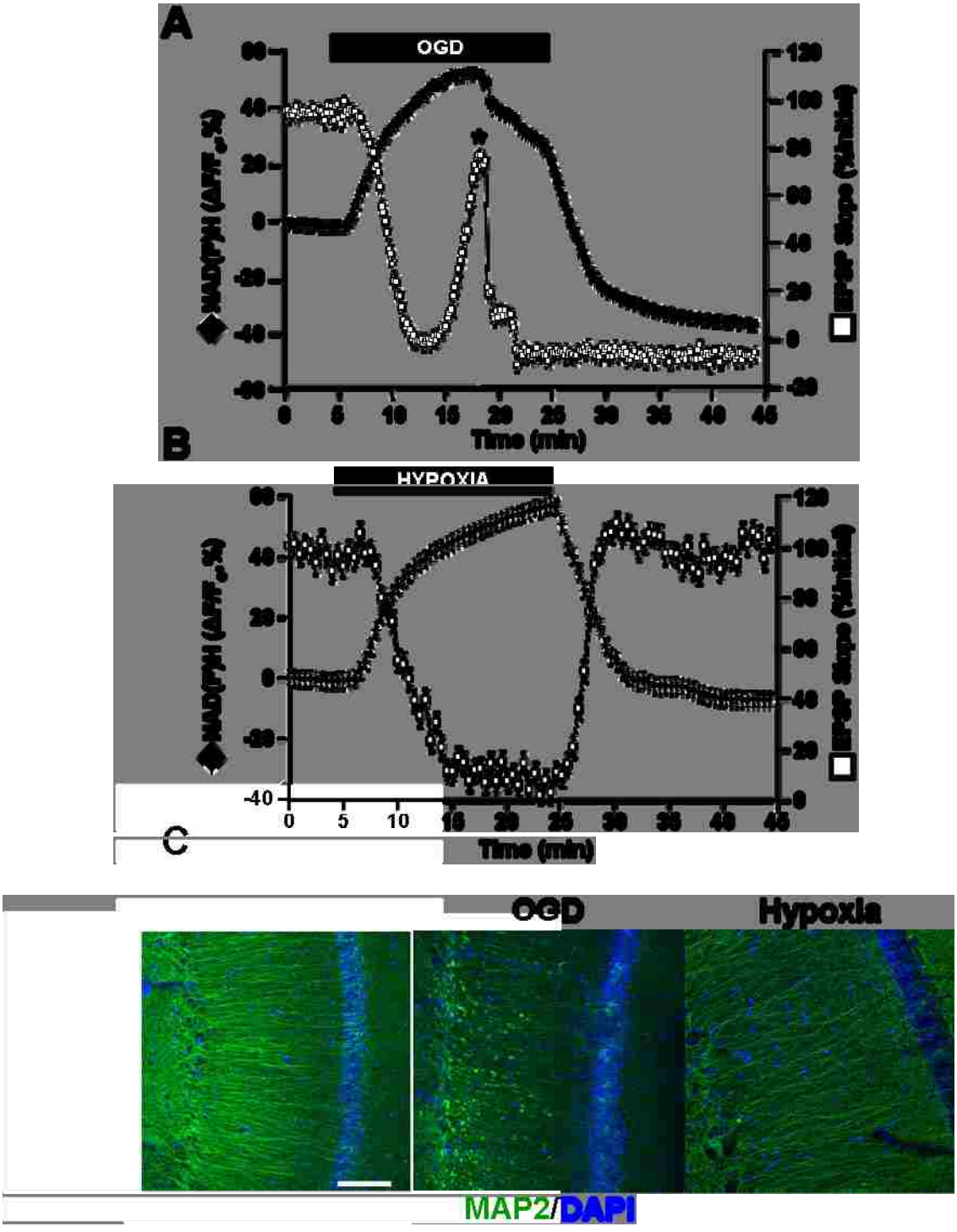

Figure A.3

A. Simultaneous recordings of NAD(P)H and fEPSPs during OGD. Averaged effects of OGD on NAD(P)H autofluorescence and fEPSPs (n=6). As discussed in Section 5.4.2, NAD(P)H increases prior to OGD were a result of mitochondrial inhibition by hypoxia. Coincident with NAD(P)H increases, fEPSPs were suppressed in an A1 receptor-dependent manner. A brief period of hyperexcitability was observed just prior to SD onset, and following OGD-SD, there was a permanent loss of fEPSPs and NADH levels fell significantly below baseline levels (n=6).

B. Simultaneous recordings of NADH and fEPSPs during hypoxia. Similar to OGD exposures, NADH levels increased coincident with a loss of fEPSPs shortly after the onset of hypoxia. However, SD was never generated during 20 minute exposures to hypoxia (95% O_2 replaced with 95% N_2), and following the reintroduction of nACSF, fEPSPs and NADH returned to levels not significantly different from baseline (n=6).

C. Representative examples of MAP2 Immunohistochemistry following hypoxia and OGD exposures. Slices were fixed following electrophysiology experiments and processed for MAP2 immunohistochemistry to assess dendritic damage. No dendritic injury was evident from MAP2 immunohistochemistry in slices exposed to hypoxia when compared with naïve control and MAP2 was localized to the dendrites alone. However, significant damage was observed following OGD-SD, all preparations had severe dendritic beading and accumulation of MAP2 in somata, consistent with substantial rapid injury following SD. (scale bar: 50µms, blue: DAPI nuclear stain, green: MAP2).

Abbreviations Used

ACSF	artificial cerebral spinal fluid
AD	anoxic depolarization
AMPA	α-amino-3-hydroxy-5-methylisoxazole-4-propionic acid
ATP	adenosine triphosphate
CA1	cornu ammonis 1
CNTF	ciliary neurotrophic factor
DAB	1,4-dideoxy-1,4-imino-D-arabinitol
DAPI	4',6-diamidino-2-phenylindole
DNJ	1-deoxynojirimycin
DPCPX	8-cyclopentyl-1-1,3-dipropylxanthine
EPSP	excitatory post-synaptic potential
FA	fluoroacetate
FAD	flavin adenine dinucleotide
FP	flavoprotein
FHM	familial hemiplegic migraine
GLT-1	glutamate transporter 1
GLAST	glutamate-aspartate transporter
IOS	intrinsic optical signals
LacZ	β-galactosidase
MAP2	microtubule associated protein 2
MCAO	middle cerebral artery occlusion
MSO	L-methionine-DL-sulfoximine
NADH	nicotinamide adenine dinucleotide
NADPH	nicotinamide adenine dinucleotide phosphate

NMDA	N-methyl-D-aspartic acid
NO	nitric oxide
OGD	oxygen glucose deprivation
PID	peri-infarct depolarization
SAH	subarachnoid hemorrhage
SEM	standard error of the mean
SD	spreading depression
sp	stratum pyramidale
sr	stratum radiatum
TCA	tricarboxylic acid

References

(2006) Incidence and Prevalence: 2006 Chart Book on Cardiovascular and Lung Diseases. In. Bethesda, Md: National Heart, Lung, and Blood Institute.

(2009) Morbidity and Mortality: 2009 Chart Book on Cardiovascular, Lung, and Blood Diseases. In. Bethesda, Md: National Heart, Lung, and Blood Institute.

Agulhon C, Petravicz J, McMullen AB, Sweger EJ, Minton SK, Taves SR, Casper KB, Fiacco TA, McCarthy KD (2008) What is the role of astrocyte calcium in neurophysiology? Neuron 59:932-946.

Aitken PG, Tombaugh GC, Turner DA, Somjen GG (1998) Similar propagation of SD and hypoxic SD-like depolarization in rat hippocampus recorded optically and electrically. J Neurophysiol 80:1514-1521.

Al-Tamimi YZ, Orsi NM, Quinn AC, Homer-Vanniasinkam S, Ross SA (2010) A review of delayed ischemic neurologic deficit following aneurysmal subarachnoid hemorrhage: historical overview, current treatment, and pathophysiology. World Neurosurg 73:654-667.

Alberts MJ (1998) tPA in acute ischemic stroke: United States experience and issues for the future. Neurology 51:S53-55.

Alberts MJ, Hademenos G, Latchaw RE, Jagoda A, Marler JR, Mayberg MR, Starke RD, Todd HW, Viste KM, Girgus M, Shephard T, Emr M, Shwayder P, Walker MD (2000) Recommendations for the establishment of primary stroke centers. Brain Attack Coalition. Jama 283:3102-3109.

Albrecht PJ, Dahl JP, Stoltzfus OK, Levenson R, Levison SW (2002) Ciliary neurotrophic factor activates spinal cord astrocytes, stimulating their production and release of fibroblast growth factor-2, to increase motor neuron survival. Exp Neurol 173:46-62.

Allen NJ, Karadottir R, Attwell D (2005) A preferential role for glycolysis in preventing the anoxic depolarization of rat hippocampal area CA1 pyramidal cells. J Neurosci 25:848-859.

Almeida A, Almeida J, Bolanos JP, Moncada S (2001) Different responses of astrocytes and neurons to nitric oxide: the role of glycolytically generated ATP in astrocyte protection. Proc Natl Acad Sci U S A 98:15294-15299.

Almeida A, Cidad P, Delgado-Esteban M, Fernandez E, Garcia-Nogales P, Bolanos JP (2005) Inhibition of mitochondrial respiration by nitric oxide: its role in glucose metabolism and neuroprotection. J Neurosci Res 79:166-171.

Amedee T, Robert A, Coles JA (1997) Potassium homeostasis and glial energy metabolism. Glia 21:46-55.

An JH, Su Y, Radman T, Bikson M (2008) Effects of glucose and glutamine concentration in the formulation of the artificial cerebrospinal fluid (ACSF). Brain Res 1218:77-86.

Anderson TR, Andrew RD (2002) Spreading depression: imaging and blockade in the rat neocortical brain slice. J Neurophysiol 88:2713-2725.

Andrew RD, Jarvis CR, Obeidat AS (1999) Potential sources of intrinsic optical signals imaged in live brain slices. Methods 18:185-196, 179.

Attwell D, Laughlin SB (2001) An energy budget for signaling in the grey matter of the brain. J Cereb Blood Flow Metab 21:1133-1145.

Ayata C (2010) Cortical spreading depression triggers migraine attack: pro. Headache 50:725-730.

Ayata C, Shimizu-Sasamata M, Lo EH, Noebels JL, Moskowitz MA (2000) Impaired neurotransmitter release and elevated threshold for cortical spreading depression in mice with mutations in the alpha1A subunit of P/Q type calcium channels. Neuroscience 95:639-645.

Ayata C, Jin H, Kudo C, Dalkara T, Moskowitz MA (2006) Suppression of cortical spreading depression in migraine prophylaxis. Ann Neurol 59:652-661.

Ayata C, Shin HK, Salomone S, Ozdemir-Gursoy Y, Boas DA, Dunn AK, Moskowitz MA (2004) Pronounced hypoperfusion during spreading depression in mouse cortex. J Cereb Blood Flow Metab 24:1172-1182.

Bacci A, Sancini G, Verderio C, Armano S, Pravettoni E, Fesce R, Franceschetti S, Matteoli M (2002) Block of glutamate-glutamine cycle between astrocytes and neurons inhibits epileptiform activity in hippocampus. J Neurophysiol 88:2302-2310.

Bahar S, Fayuk D, Somjen GG, Aitken PG, Turner DA (2000) Mitochondrial and intrinsic optical signals imaged during hypoxia and spreading depression in rat hippocampal slices. J Neurophysiol 84:311-324.

Bak LK, Schousboe A, Waagepetersen HS (2006) The glutamate/GABA-glutamine cycle: aspects of transport, neurotransmitter homeostasis and ammonia transfer. J Neurochem 98:641-653.

Balestrino M, Young J, Aitken P (1999) Block of (Na+,K+)ATPase with ouabain induces spreading depression-like depolarization in hippocampal slices. Brain Res 838:37-44.

Barker FG, 2nd, Ogilvy CS (1996) Efficacy of prophylactic nimodipine for delayed ischemic deficit after subarachnoid hemorrhage: a metaanalysis. J Neurosurg 84:405-414.

Basarsky TA, Duffy SN, Andrew RD, MacVicar BA (1998) Imaging spreading depression and associated intracellular calcium waves in brain slices. J Neurosci 18:7189-7199.

Bates D, Ashford E, Dawson R, Ensink FB, Gilhus NE, Olesen J, Pilgrim AJ, Shevlin P (1994) Subcutaneous sumatriptan during the migraine aura. Sumatriptan Aura Study Group. Neurology 44:1587-1592.

Bentley HR, Mc DE, Whitehead JK (1950) Action of nitrogen trichloride on proteins; a synthesis of the toxic factor from methionine. Nature 165:735.

Blinova K, Levine RL, Boja ES, Griffiths GL, Shi ZD, Ruddy B, Balaban RS (2008) Mitochondrial NADH fluorescence is enhanced by complex I binding. Biochemistry 47:9636-9645.

Bloch J, Bachoud-Levi AC, Deglon N, Lefaucheur JP, Winkel L, Palfi S, Nguyen JP, Bourdet C, Gaura V, Remy P, Brugieres P, Boisse MF, Baudic S, Cesaro P, Hantraye P, Aebischer P, Peschanski M (2004) Neuroprotective gene therapy for Huntington's disease, using polymer-encapsulated cells engineered to secrete human ciliary neurotrophic factor: results of a phase I study. Hum Gene Ther 15:968-975.

Boitier E RR, and Michael R. Duchen (1999) Mitochondria Exert a Negative Feedback on the Propagation of

Intracellular Ca2+ Waves in Rat Cortical Astrocytes. Journal of Cell Biology 145:795-808.

Bon CL, Garthwaite J (2001) Exogenous nitric oxide causes potentiation of hippocampal synaptic transmission during low-frequency stimulation via the endogenous nitric oxide-cGMP pathway. Eur J Neurosci 14:585-594.

Bon CL, Garthwaite J (2003) On the role of nitric oxide in hippocampal long-term potentiation. J Neurosci 23:1941-1948.

Bonthius DJ, Steward O (1993) Induction of cortical spreading depression with potassium chloride upregulates levels of messenger RNA for glial fibrillary acidic protein in cortex and hippocampus: inhibition by MK-801. Brain Res 618:83-94.

Boyle PJ, Conway EJ (1941) Potassium accumulation in muscle and associated changes. J Physiol 100:1-63.

Branston NM, Strong AJ, Symon L (1977) Extracellular potassium activity, evoked potential and tissue blood flow. Relationships during progressive ischaemia in baboon cerebral cortex. J Neurol Sci 32:305-321.

Brookes PS, Bolanos JP, Heales SJ (1999) The assumption that nitric oxide inhibits mitochondrial ATP synthesis is correct. FEBS Lett 446:261-263.

Broome MR, Collingridge GL, Irving AJ (1994) Activation of the NO-cGMP signalling pathway depresses hippocampal synaptic transmission through an adenosine receptor-dependent mechanism. Neuropharmacology 33:1511-1513.

Brown AM (2004) Brain glycogen re-awakened. J Neurochem 89:537-552.

Brown AM, Tekkok SB, Ransom BR (2003) Glycogen regulation and functional role in mouse white matter. J Physiol 549:501-512.

Brown GC, Cooper CE (1994) Nanomolar concentrations of nitric oxide reversibly inhibit synaptosomal respiration by competing with oxygen at cytochrome oxidase. FEBS Lett 356:295-298.

Busch E, Gyngell ML, Eis M, Hoehn-Berlage M, Hossmann KA (1996) Potassium-induced cortical spreading depressions during focal cerebral ischemia in rats: contribution to lesion growth assessed by diffusion-weighted NMR and biochemical imaging. J Cereb Blood Flow Metab 16:1090-1099.

Bush TG, Puvanachandra N, Horner CH, Polito A, Ostenfeld T, Svendsen CN, Mucke L, Johnson MH, Sofroniew MV (1999) Leukocyte infiltration, neuronal degeneration, and neurite outgrowth after ablation of scar-forming, reactive astrocytes in adult transgenic mice. Neuron 23:297-308.

Bushong EA, Martone ME, Jones YZ, Ellisman MH (2002) Protoplasmic astrocytes in CA1 stratum radiatum occupy separate anatomical domains. J Neurosci 22:183-192.

Buzzi MG, Moskowitz MA (1990) The antimigraine drug, sumatriptan (GR43175), selectively blocks neurogenic plasma extravasation from blood vessels in dura mater. Br J Pharmacol 99:202-206.

Canals S, Larrosa B, Pintor J, Mena MA, Herreras O (2008) Metabolic challenge to glia activates an adenosine-mediated safety mechanism that promotes neuronal survival by delaying the onset of spreading depression waves. J Cereb Blood Flow Metab.

Capes SE, Hunt D, Malmberg K, Pathak P, Gerstein HC (2001) Stress hyperglycemia and prognosis of stroke in nondiabetic and diabetic patients: a systematic overview. Stroke 32:2426-2432.

Cataldo AM, Broadwell RD (1986) Cytochemical identification of cerebral glycogen and glucose-6-phosphatase activity under normal and experimental conditions. II. Choroid plexus and ependymal epithelia, endothelia and pericytes. J Neurocytol 15:511-524.

Chan PH (1996) Role of oxidants in ischemic brain damage. Stroke 27:1124-1129.

Chance B (2004) Mitochondrial NADH redox state, monitoring discovery and deployment in tissue. Methods Enzymol 385:361-370.

Chance B, Baltscheffsky H (1958) Respiratory enzymes in oxidative phosphorylation. VII. Binding of intramitochondrial reduced pyridine nucleotide. J Biol Chem 233:736-739.

Chance B, Cohen P, Jobsis F, Schoener B (1962) Intracellular oxidation-reduction states in vivo. Science 137:499-508.

Chebabo SR, Hester MA, Aitken PG, Somjen GG (1995) Hypotonic exposure enhances synaptic transmission and triggers spreading depression in rat hippocampal tissue slices. Brain Res 695:203-216.

Chen Q, Chopp M, Bodzin G, Chen H (1993) Temperature modulation of cerebral depolarization during focal cerebral ischemia in rats: correlation with ischemic injury. J Cereb Blood Flow Metab 13:389-394.

Chen Y, Swanson RA (2003) Astrocytes and brain injury. J Cereb Blood Flow Metab 23:137-149.

Chen Y, Vartiainen NE, Ying W, Chan PH, Koistinaho J, Swanson RA (2001) Astrocytes protect neurons from nitric oxide toxicity by a glutathione-dependent mechanism. J Neurochem 77:1601-1610.

Chever O, Djukic B, McCarthy KD, Amzica F (2010) Implication of Kir4.1 channel in excess potassium clearance: an in vivo study on anesthetized glial-conditional Kir4.1 knock-out mice. J Neurosci 30:15769-15777.

Choi JH, Yoo KY, Lee CH, Park OK, Yan BC, Li H, Moon YS, Hwang IK, Lee YL, Shin HC, Won MH (2010) Transient Cerebral Ischemia Induces Active Astrocytosis Without Distinct Neuronal Death in the Gerbil Main Olfactory Bulb: A Long-Term Analysis. Neurochem Res.

Clarke DD, Nicklas WJ, Berl S (1970) Tricarboxylic acid-cycle metabolism in brain. Effect of fluoroacetate and fluorocitrate on the labelling of glutamate, aspartate, glutamine and gamma-aminobutyrate. Biochem J 120:345-351.

Cleeter MW, Cooper JM, Darley-Usmar VM, Moncada S, Schapira AH (1994) Reversible inhibition of cytochrome c oxidase, the terminal enzyme of the mitochondrial respiratory chain, by nitric oxide. Implications for neurodegenerative diseases. FEBS Lett 345:50-54.

Cloix JF, Hevor T (2009) Epilepsy, regulation of brain energy metabolism and neurotransmission. Curr Med Chem 16:841-853.

Collewijn H, Harreveld AV (1966) Membrane potential of cerebral cortical cells during spreading depression and asyxia. Exp Neurol 15:425-436.

Cruz NF, Dienel GA (2002) High glycogen levels in brains of rats with minimal environmental stimuli: implications for metabolic contributions of working astrocytes. J Cereb Blood Flow Metab 22:1476-1489.

Czeh G, Aitken PG, Somjen GG (1993) Membrane currents in CA1 pyramidal cells during spreading depression (SD) and SD-like hypoxic depolarization. Brain Res 632:195-208.

Danbolt NC (2001) Glutamate uptake. Prog Neurobiol 65:1-105.

Davies JA, Annels SJ, Dickie BG, Ellis Y, Knott NJ (1995) A comparison between the stimulated and paroxysmal release of endogenous amino acids from rat cerebellar, striatal and hippocampal slices: a manifestation of spreading depression? J Neurol Sci 131:8-14.

de Almeida LP, Zala D, Aebischer P, Deglon N (2001) Neuroprotective effect of a CNTF-expressing lentiviral vector in the quinolinic acid rat model of Huntington's disease. Neurobiol Dis 8:433-446.

De Fusco M, Marconi R, Silvestri L, Atorino L, Rampoldi L, Morgante L, Ballabio A, Aridon P, Casari G (2003) Haploinsufficiency of ATP1A2 encoding the Na+/K+ pump alpha2 subunit associated with familial hemiplegic migraine type 2. Nat Genet 33:192-196.

Dichgans M, Freilinger T, Eckstein G, Babini E, Lorenz-Depiereux B, Biskup S, Ferrari MD, Herzog J, van den Maagdenberg AM, Pusch M, Strom TM (2005) Mutation in the neuronal voltage-gated sodium channel SCN1A in familial hemiplegic migraine. Lancet 366:371-377.

Dietz RM, Weiss JH, Shuttleworth CW (2008) Zn2+ influx is critical for some forms of spreading depression in brain slices. In: J Neurosci, pp 8014-8024.

Dijkhuizen RM, Beekwilder JP, van der Worp HB, Berkelbach van der Sprenkel JW, Tulleken KA, Nicolay K (1999) Correlation between tissue depolarizations and damage in focal ischemic rat brain. Brain Res 840:194-205.

Dirnagl U, Iadecola C, Moskowitz MA (1999) Pathobiology of ischaemic stroke: an integrated view. Trends Neurosci 22:391-397.

Djukic B, Casper KB, Philpot BD, Chin LS, McCarthy KD (2007) Conditional knock-out of Kir4.1 leads to glial membrane depolarization, inhibition of potassium and glutamate uptake, and enhanced short-term synaptic potentiation. J Neurosci 27:11354-11365.

Dohmen C, Sakowitz OW, Fabricius M, Bosche B, Reithmeier T, Ernestus RI, Brinker G, Dreier JP, Woitzik J, Strong AJ, Graf R (2008) Spreading depolarizations occur in human ischemic stroke with high incidence. Ann Neurol 63:720-728.

Dreier JP, Woitzik J, Fabricius M, Bhatia R, Major S, Drenckhahn C, Lehmann TN, Sarrafzadeh A, Willumsen L, Hartings JA, Sakowitz OW, Seemann JH, Thieme A, Lauritzen M, Strong AJ (2006) Delayed ischaemic neurological deficits after subarachnoid haemorrhage are associated with clusters of spreading depolarizations. Brain 129:3224-3237.

Dreier JP, Major S, Manning A, Woitzik J, Drenckhahn C, Steinbrink J, Tolias C, Oliveira-Ferreira AI, Fabricius M, Hartings JA, Vajkoczy P, Lauritzen M, Dirnagl U, Bohner G, Strong AJ (2009) Cortical spreading ischaemia is a novel process involved in ischaemic damage in patients with aneurysmal subarachnoid haemorrhage. Brain 132:1866-1881.

Dringen R (2000) Metabolism and functions of glutathione in brain. Prog Neurobiol 62:649-671.

Dringen R, Hamprecht B (1992) Glucose, insulin, and insulin-like growth factor I regulate the glycogen content of astroglia-rich primary cultures. J Neurochem 58:511-517.

Duffy S, Fraser DD, MacVicar BA (1996) Potassium channels. In: Neuroglia (Kettenman H, Ransom B, eds), pp 185-201. New York: Oxford UP.

Dugan LL, Kim-Han JS (2004) Astrocyte mitochondria in in vitro models of ischemia. J Bioenerg Biomembr 36:317-321.

Dunn AK, Bolay H, Moskowitz MA, Boas DA (2001) Dynamic imaging of cerebral blood flow using laser speckle. J Cereb Blood Flow Metab 21:195-201.

Dunwiddie TV, Masino SA (2001) The role and regulation of adenosine in the central nervous system. Annu Rev Neurosci 24:31-55.

Ecker A, Riemenschneider PA (1951) Arteriographic demonstration of spasm of the intracranial arteries, with special reference to saccular arterial aneurysms. J Neurosurg 8:660-667.

Eddleston M, Mucke L (1993) Molecular profile of reactive astrocytes--implications for their role in neurologic disease. Neuroscience 54:15-36.

Eikermann-Haerter K, Dilekoz E, Kudo C, Savitz SI, Waeber C, Baum MJ, Ferrari MD, van den Maagdenberg AM, Moskowitz MA, Ayata C (2009) Genetic and hormonal factors modulate spreading depression and transient hemiparesis in mouse models of familial hemiplegic migraine type 1. J Clin Invest 119:99-109.

Endoh M, Maiese K, Wagner J (1994) Expression of the inducible form of nitric oxide synthase by reactive astrocytes after transient global ischemia. Brain Res 651:92-100.

Escartin C, Bonvento G (2008) Targeted activation of astrocytes: a potential neuroprotective strategy. Mol Neurobiol 38:231-241.

Escartin C, Brouillet E, Gubellini P, Trioulier Y, Jacquard C, Smadja C, Knott GW, Kerkerian-Le Goff L, Deglon N, Hantraye P, Bonvento G (2006) Ciliary neurotrophic factor activates astrocytes, redistributes their glutamate transporters GLAST and GLT-1 to raft microdomains, and improves glutamate handling in vivo. J Neurosci 26:5978-5989.

Escartin C, Pierre K, Colin A, Brouillet E, Delzescaux T, Guillermier M, Dhenain M, Deglon N, Hantraye P, Pellerin L, Bonvento G (2007) Activation of astrocytes by CNTF induces metabolic plasticity and increases resistance to metabolic insults. J Neurosci 27:7094-7104.

Fabricius M, Jensen LH, Lauritzen M (1993) Microdialysis of interstitial amino acids during spreading depression and anoxic depolarization in rat neocortex. Brain Res 612:61-69.

Fabricius M, Akgoren N, Lauritzen M (1995) Arginine-nitric oxide pathway and cerebrovascular regulation in cortical spreading depression. Am J Physiol 269:H23-29.

Fabricius M, Fuhr S, Bhatia R, Boutelle M, Hashemi P, Strong AJ, Lauritzen M (2006) Cortical spreading depression and peri-infarct depolarization in acutely injured human cerebral cortex. Brain 129:778-790.

Fabricius M, Fuhr S, Willumsen L, Dreier JP, Bhatia R, Boutelle MG, Hartings JA, Bullock R, Strong AJ, Lauritzen M (2008) Association of seizures with cortical spreading depression and peri-infarct depolarisations in the acutely injured human brain. Clin Neurophysiol 119:1973-1984.

Feelisch M (1998) The use of nitric oxide donors in pharmacological studies. Naunyn Schmiedebergs Arch Pharmacol 358:113-122.

Fiacco TA, Agulhon C, Taves SR, Petravicz J, Casper KB, Dong X, Chen J, McCarthy KD (2007) Selective stimulation of astrocyte calcium in situ does not affect neuronal excitatory synaptic activity. Neuron 54:611-626.

Fishman P, Black L (1999) Indirect costs of migraine in a managed care population. Cephalalgia 19:50-57; discussion 51.

Folbergrova J (1973) Glycogen and glycogen phosphorylase in the cerebral cortex of mice under the influence of methionine sulphoximine. J Neurochem 20:547-557.

Foster KA, Beaver CJ, Turner DA (2005) Interaction between tissue oxygen tension and NADH imaging during synaptic stimulation and hypoxia in rat hippocampal slices. Neuroscience 132:645-657.

Fowler PA, Lacey LF, Thomas M, Keene ON, Tanner RJ, Baber NS (1991) The clinical pharmacology, pharmacokinetics and metabolism of sumatriptan. Eur Neurol 31:291-294.

Freeman JM, Kossoff EH, Hartman AL (2007) The ketogenic diet: one decade later. Pediatrics 119:535-543.

Fricke MN, Jones-Davis DM, Mathews GC (2007) Glutamine uptake by System A transporters maintains neurotransmitter GABA synthesis and inhibitory synaptic transmission. J Neurochem 102:1895-1904.

Funke F, Kron M, Dutschmann M, Muller M (2009) Infant brain stem is prone to the generation of spreading depression during severe hypoxia. J Neurophysiol 101:2395-2410.

Galeffi F, Somjen GG, Foster KA, Turner DA (2010) Simultaneous monitoring of tissue PO(2) and NADH fluorescence during synaptic stimulation and spreading depression reveals a transient dissociation between oxygen utilization and mitochondrial redox state in rat hippocampal slices. J Cereb Blood Flow Metab.

Gavillet M, Allaman I, Magistretti PJ (2008) Modulation of astrocytic metabolic phenotype by proinflammatory cytokines. Glia 56:975-989.

Gerich FJ, Hepp S, Probst I, Muller M (2006) Mitochondrial inhibition prior to oxygen-withdrawal facilitates the occurrence of hypoxia-induced spreading depression in rat hippocampal slices. J Neurophysiol 96:492-504.

Gibson QH, Roughton FJ (1957) The kinetics of dissociation of the first ligand molecule from fully saturated carboxyhaemoglobin and nitric oxide haemoglobin in sheep blood solutions. Proc R Soc Lond B Biol Sci 147:44-56.

Gido G, Kristian T, Siesjo BK (1994) Induced spreading depressions in energy-compromised neocortical tissue: calcium transients and histopathological correlates. Neurobiol Dis 1:31-41.

Giulivi C (1998) Functional implications of nitric oxide produced by mitochondria in mitochondrial metabolism. Biochem J 332 (Pt 3):673-679.

Goadsby PJ (1999) Advances in the pharmacotherapy of migraine. How knowledge of pathophysiology is guiding drug development. Drugs R D 2:361-374.

Goldstein LB (2007) Acute ischemic stroke treatment in 2007. Circulation 116:1504-1514.

Gordon GR, Choi HB, Rungta RL, Ellis-Davies GC, MacVicar BA (2008) Brain metabolism dictates the polarity of astrocyte control over arterioles. Nature 456:745-749.

Grafstein B (1956) Mechanism of spreading cortical depression. J Neurophysiol 19:154-171.

Haberg A, Qu H, Sonnewald U (2006) Glutamate and GABA metabolism in transient and permanent middle cerebral artery occlusion in rat: importance of astrocytes for neuronal survival. Neurochem Int 48:531-540.

Hadjikhani N, Sanchez Del Rio M, Wu O, Schwartz D, Bakker D, Fischl B, Kwong KK, Cutrer FM, Rosen BR, Tootell RB, Sorensen AG, Moskowitz MA (2001) Mechanisms of migraine aura revealed by functional MRI in human visual cortex. Proc Natl Acad Sci U S A 98:4687-4692.

Haglund MM, Stahl WL, Kunkel DD, Schwartzkroin PA (1985) Developmental and regional differences in the localization of Na,K-ATPase activity in the rabbit hippocampus. Brain Res 343:198-203.

Halassa MM, Fellin T, Haydon PG (2007) The tripartite synapse: roles for gliotransmission in health and disease. Trends Mol Med 13:54-63.

Halassa MM, Fellin T, Haydon PG (2009) Tripartite synapses: roles for astrocytic purines in the control of synaptic physiology and behavior. Neuropharmacology 57:343-346.

Hamann M, Rossi DJ, Marie H, Attwell D (2002) Knocking out the glial glutamate transporter GLT-1 reduces glutamate uptake but does not affect hippocampal glutamate dynamics in early simulated ischaemia. Eur J Neurosci 15:308-314.

Hamby ME, Sofroniew MV (2010) Reactive astrocytes as therapeutic targets for CNS disorders. Neurotherapeutics 7:494-506.

Hamilton NB, Attwell D (2010) Do astrocytes really exocytose neurotransmitters? Nat Rev Neurosci 11:227-238.

Hansen AJ (1985) Effect of anoxia on ion distribution in the brain. Physiol Rev 65:101-148.

Hansen AJ, Zeuthen T (1981) Extracellular ion concentrations during spreading depression and ischemia in the rat brain cortex. Acta Physiol Scand 113:437-445.

Hartings JA, Rolli ML, Lu XC, Tortella FC (2003) Delayed secondary phase of peri-infarct depolarizations after focal cerebral ischemia: relation to infarct growth and neuroprotection. J Neurosci 23:11602-11610.

Hartings JA, Gugliotta M, Gilman C, Strong AJ, Tortella FC, Bullock MR (2008) Repetitive cortical spreading depolarizations in a case of severe brain trauma. Neurol Res 30:876-882.

Hartings JA, Strong AJ, Fabricius M, Manning A, Bhatia R, Dreier JP, Mazzeo AT, Tortella FC, Bullock MR (2009) Spreading depolarizations and late secondary insults after traumatic brain injury. J Neurotrauma 26:1857-1866.

Hashemi P, Bhatia R, Nakamura H, Dreier JP, Graf R, Strong AJ, Boutelle MG (2008) Persisting depletion of brain glucose following cortical spreading depression, despite apparent hyperaemia: evidence for risk of an adverse effect of Leao's spreading depression. J Cereb Blood Flow Metab.

Hashimoto M, Takeda Y, Sato T, Kawahara H, Nagano O, Hirakawa M (2000) Dynamic changes of NADH fluorescence images and NADH content during spreading depression in the cerebral cortex of gerbils. Brain Res 872:294-300.

Haydon PG (2001) GLIA: listening and talking to the synapse. Nat Rev Neurosci 2:185-193.

Hermann DM, Kilic E, Kugler S, Isenmann S, Bahr M (2001) Adenovirus-mediated GDNF and CNTF pretreatment protects against striatal injury following transient middle cerebral artery occlusion in mice. Neurobiol Dis 8:655-666.

Herreras O, Somjen GG (1993) Analysis of potential shifts associated with recurrent spreading depression and prolonged unstable spreading depression induced by microdialysis of elevated K+ in hippocampus of anesthetized rats. Brain Res 610:283-294.

Herreras O, Largo C, Ibarz JM, Somjen GG, Martin del Rio R (1994) Role of neuronal synchronizing mechanisms in the propagation of spreading depression in the in vivo hippocampus. J Neurosci 14:7087-7098.

Hoffmann U, Dilekoz E, Kudo C, Ayata C (2010) Gabapentin suppresses cortical spreading depression susceptibility. J Cereb Blood Flow Metab.

Hopper R, Lancaster B, Garthwaite J (2004) On the regulation of NMDA receptors by nitric oxide. Eur J Neurosci 19:1675-1682.

Hoskison MM, Shuttleworth CW (2006) Microtubule disruption, not calpain-dependent loss of MAP2, contributes to enduring NMDA-induced dendritic dysfunction in acute hippocampal slices. Exp Neurol 202:302-312.

Hoskison MM, Yanagawa Y, Obata K, Shuttleworth CW (2007) Calcium-dependent NMDA-induced dendritic injury and MAP2 loss in acute hippocampal slices. Neuroscience 145:66-79.

Hossmann KA (1996) Periinfarct depolarizations. Cerebrovasc Brain Metab Rev 8:195-208.

Hudgins SN, Levison SW (1998) Ciliary neurotrophic factor stimulates astroglial hypertrophy in vivo and in vitro. Exp Neurol 150:171-182.

Iijima T, Mies G, Hossmann KA (1992) Repeated negative DC deflections in rat cortex following middle cerebral artery occlusion are abolished by MK-801: effect on volume of ischemic injury. J Cereb Blood Flow Metab 12:727-733.

Iijima T, Shimase C, Iwao Y, Sankawa H (1998) Relationships between glutamate release, blood flow and spreading depression: real-time monitoring using an electroenzymatic dialysis electrode. Neurosci Res 32:201-207.

Jarvis CR, Anderson TR, Andrew RD (2001) Anoxic depolarization mediates acute damage independent of glutamate in neocortical brain slices. Cereb Cortex 11:249-259.

Joshi I, Andrew RD (2001) Imaging anoxic depolarization during ischemia-like conditions in the mouse hemi-brain slice. J Neurophysiol 85:414-424.

Kalman M (2004) Glial reaction and reactive glia. In: Non neuronal cells of the nervous system: function and dysfunction (Hertz L, ed), pp 787-835. Amsterdam: Elsevier.

Kansagara D, Wolf F, Freeman M, Helfand M (2008) Management of Inpatient Hyperglycemia: A Systematic Review. In: VA Evidence-based Synthesis Program Reports. Washington DC: Department of Veterans Affairs (US).

Katzan IL, Hammer MD, Hixson ED, Furlan AJ, Abou-Chebl A, Nadzam DM (2004) Utilization of intravenous tissue plasminogen activator for acute ischemic stroke. Arch Neurol 61:346-350.

Keefer LK, Nims RW, Davies KM, Wink DA (1996) "NONOates" (1-substituted diazen-1-ium-1,2-diolates) as nitric oxide donors: convenient nitric oxide dosage forms. Methods Enzymol 268:281-293.

Kelman L (2004) The aura: a tertiary care study of 952 migraine patients. Cephalalgia 24:728-734.

Kimelberg HK, Nedergaard M (2010) Functions of astrocytes and their potential as therapeutic targets. Neurotherapeutics 7:338-353.

Kitahara Y, Taga K, Abe H, Shimoji K (2001) The effects of anesthetics on cortical spreading depression elicitation and c-fos expression in rats. J Neurosurg Anesthesiol 13:26-32.

Kofuji P, Newman EA (2004) Potassium buffering in the central nervous system. Neuroscience 129:1045-1056.

Kraig RP, Dong LM, Thisted R, Jaeger CB (1991) Spreading depression increases immunohistochemical staining of glial fibrillary acidic protein. J Neurosci 11:2187-2198.

Krebs HA (1972) The Pasteur effect and the relations between respiration and fermentation. Essays Biochem 8:1-34.

Krivanek J (1961) Some metabolic changes accompanying Leao's spreading cortical depression in the rat. J Neurochem 6:183-189.

Kunkler PE, Kraig RP (1998) Calcium waves precede electrophysiological changes of spreading depression in hippocampal organ cultures. J Neurosci 18:3416-3425.

Kuriyama C, Kamiyama O, Ikeda K, Sanae F, Kato A, Adachi I, Imahori T, Takahata H, Okamoto T, Asano N (2008) In vitro inhibition of glycogen-degrading enzymes and glycosidases by six-membered sugar mimics and their evaluation in cell cultures. Bioorg Med Chem 16:7330-7336.

Kvamme E, Torgner IA, Roberg B (2001) Kinetics and localization of brain phosphate activated glutaminase. J Neurosci Res 66:951-958.

Laake JH, Slyngstad TA, Haug FM, Ottersen OP (1995) Glutamine from glial cells is essential for the maintenance of the nerve terminal pool of glutamate: immunogold evidence from hippocampal slice cultures. J Neurochem 65:871-881.

Lajtha A, Berl S, Waelsch H (1959) Amino acid and protein metabolism of the brain. IV. The metabolism of glutamic acid. J Neurochem 3:322-332.

Largo C, Ibarz JM, Herreras O (1997a) Effects of the gliotoxin fluorocitrate on spreading depression and glial membrane potential in rat brain in situ. J Neurophysiol 78:295-307.

Largo C, Tombaugh GC, Aitken PG, Herreras O, Somjen GG (1997b) Heptanol but not fluoroacetate prevents the propagation of spreading depression in rat hippocampal slices. J Neurophysiol 77:9-16.

Lashly K (1941) Patterns of cerbral integration indicated by the scotomas of migraine. Arch Neurol Psychiatry 46:259-264.

Lassen LH, Ashina M, Christiansen I, Ulrich V, Olesen J (1997) Nitric oxide synthase inhibition in migraine. Lancet 349:401-402.

Lauritzen M (1985) On the possible relation of spreading cortical depression to classical migraine. Cephalalgia 5 Suppl 2:47-51.

Lauritzen M, Hansen AJ (1992) The effect of glutamate receptor blockade on anoxic depolarization and cortical spreading depression. J Cereb Blood Flow Metab 12:223-229.

Lauritzen M, Rice ME, Okada Y, Nicholson C (1988) Quisqualate, kainate and NMDA can initiate spreading depression in the turtle cerebellum. Brain Res 475:317-327.

Lauritzen M, Dreier JP, Fabricius M, Hartings JA, Graf R, Strong AJ (2011) Clinical relevance of cortical spreading depression in neurological disorders: migraine, malignant stroke, subarachnoid and intracranial hemorrhage, and traumatic brain injury. J Cereb Blood Flow Metab 31:17-35.

Leao A (1944) Spreading depression of activity in the cerebral cortex. Journal of Neurophysiology 7:359-390.

Leao A (1947) Further observations on the spreading depression of activity in the cerebral cortex. J Neurophysiology 10:409-414.

Leao A, Morrison R (1945) Propagation of Spreading Cortical Depression. Journal of Neurophysiology 8:33-45.

Lee JM, Zipfel GJ, Choi DW (1999) The changing landscape of ischaemic brain injury mechanisms. Nature 399:A7-14.

Levine SR, Welch KM, Helpern JA, Chopp M, Bruce R, Selwa J, Smith MB (1988) Prolonged deterioration of ischemic brain energy metabolism and acidosis associated with hyperglycemia: human cerebral infarction studied by serial 31P NMR spectroscopy. Ann Neurol 23:416-418.

Li L, Lundkvist A, Andersson D, Wilhelmsson U, Nagai N, Pardo AC, Nodin C, Stahlberg A, Aprico K, Larsson K, Yabe T, Moons L, Fotheringham A, Davies I, Carmeliet P, Schwartz JP, Pekna M, Kubista M, Blomstrand F, Maragakis N, Nilsson M, Pekny M (2008) Protective role of reactive astrocytes in brain ischemia. J Cereb Blood Flow Metab 28:468-481.

Liang SL, Carlson GC, Coulter DA (2006) Dynamic regulation of synaptic GABA release by the glutamate-glutamine cycle in hippocampal area CA1. J Neurosci 26:8537-8548.

Lin JH, Lou N, Kang N, Takano T, Hu F, Han X, Xu Q, Lovatt D, Torres A, Willecke K, Yang J, Kang J, Nedergaard M (2008) A central role of connexin 43 in hypoxic preconditioning. J Neurosci 28:681-695.

Lipski J, Park TI, Li D, Lee SC, Trevarton AJ, Chung KK, Freestone PS, Bai JZ (2006) Involvement of TRP-like channels in the acute ischemic response of hippocampal CA1 neurons in brain slices. Brain Res 1077:187-199.

Lipton P (1973) Effects of membrane depolarization on nicotinamide nucleotide fluorescence in brain slices. Biochem J 136:999-1009.

Lipton P (1989) Regulation of glycogen in the dentate gyrus of the in vitro guinea pig hippocampus; effect of combined deprivation of glucose and oxygen. J Neurosci Methods 28:147-154.

Lipton P (1999) Ischemic cell death in brain neurons. Physiol Rev 79:1431-1568.

Lipton P, Whittingham TS (1979) The effect of hypoxia on evoked potentials in the in vitro hippocampus. J Physiol 287:427-438.

Lipton RB, Stewart WF, Diamond S, Diamond ML, Reed M (2001) Prevalence and burden of migraine in the United States: data from the American Migraine Study II. Headache 41:646-657.

Lloyd-Jones D, Adams RJ, Brown TM, Carnethon M, Dai S, De Simone G, Ferguson TB, Ford E, Furie K, Gillespie C, Go A, Greenlund K, Haase N, Hailpern S, Ho PM, Howard V, Kissela B, Kittner S, Lackland D, Lisabeth L, Marelli A, McDermott MM, Meigs J, Mozaffarian D, Mussolino M, Nichol G, Roger VL, Rosamond W, Sacco R, Sorlie P, Roger VL, Thom T, Wasserthiel-Smoller S, Wong ND, Wylie-Rosett J (2010) Heart disease and stroke statistics--2010 update: a report from the American Heart Association. Circulation 121:e46-e215.

Lovatt D, Sonnewald U, Waagepetersen HS, Schousboe A, He W, Lin JH, Han X, Takano T, Wang S, Sim FJ, Goldman SA, Nedergaard M (2007) The transcriptome and metabolic gene signature of protoplasmic astrocytes in the adult murine cortex. J Neurosci 27:12255-12266.

MaassenVanDenBrink A, Reekers M, Bax WA, Ferrari MD, Saxena PR (1998) Coronary side-effect potential of current and prospective antimigraine drugs. Circulation 98:25-30.

Maia LM, Amancio-dos-Santos A, Duda-de-Oliveira D, Angelim MK, Germano PC, Santos SF, Guedes RC (2009) L-Arginine administration during rat brain development facilitates spreading depression propagation: evidence for a dose- and nutrition-dependent effect. Nutr Neurosci 12:73-80.

Makar TK, Nedergaard M, Preuss A, Gelbard AS, Perumal AS, Cooper AJ (1994) Vitamin E, ascorbate, glutathione, glutathione disulfide, and enzymes of glutathione metabolism in cultures of chick astrocytes and neurons: evidence that astrocytes play an important role in antioxidative processes in the brain. J Neurochem 62:45-53.

Mares P, Kriz N, Brozek G, Bures J (1976) Anoxic changes of extracellular potassium concentration in the cerebral cortex of young rats. Exp Neurol 53:12-20.

Martin RL, Lloyd HG, Cowan AI (1994) The early events of oxygen and glucose deprivation: setting the scene for neuronal death? Trends Neurosci 17:251-257.

Martinez-Hernandez A, Bell KP, Norenberg MD (1977) Glutamine synthetase: glial localization in brain. Science 195:1356-1358.

Martins-Ferreira H, Ribeiro LJ (1995) Biphasic effects of gap junctional uncoupling agents on the propagation of retinal spreading depression. Braz J Med Biol Res 28:991-994.

Masino SA, Dunwiddie TV (1999) Temperature-dependent modulation of excitatory transmission in hippocampal slices is mediated by extracellular adenosine. J Neurosci 19:1932-1939.

Matsushima K, Schmidt-Kastner R, Hogan MJ, Hakim AM (1998) Cortical spreading depression activates trophic factor expression in neurons and astrocytes and protects against subsequent focal brain ischemia. Brain Res 807:47-60.

Mayevsky A, Rogatsky GG (2007) Mitochondrial function in vivo evaluated by NADH fluorescence: from animal models to human studies. Am J Physiol Cell Physiol 292:C615-640.

Mayevsky A, Jamieson D, Chance B (1974) Oxygen poisoning in the unanesthetized brain: correlation of the oxidation-reduction state of pyridine nucleotide with electrical activity. Brain Res 76:481-491.

McKeon RJ, Schreiber RC, Rudge JS, Silver J (1991) Reduction of neurite outgrowth in a model of glial scarring following CNS injury is correlated with the expression of inhibitory molecules on reactive astrocytes. J Neurosci 11:3398-3411.

Mies G, Iijima T, Hossmann KA (1993) Correlation between peri-infarct DC shifts and ischaemic neuronal damage in rat. Neuroreport 4:709-711.

Mies G, Kohno K, Hossmann KA (1994) Prevention of periinfarct direct current shifts with glutamate antagonist NBQX following occlusion of the middle cerebral artery in the rat. J Cereb Blood Flow Metab 14:802-807.

Milner PM (1958) Note on a possible correspondence between the scotomas of migraine and spreading depression of Leao. Electroencephalogr Clin Neurophysiol 10:705.

Moncada S, Higgs A (1993) The L-arginine-nitric oxide pathway. N Engl J Med 329:2002-2012.

Moskowitz MA (2008) Defining a pathway to discovery from bench to bedside: the trigeminovascular system and sensitization. Headache 48:688-690.

Moskowitz MA, Bolay H, Dalkara T (2004) Deciphering migraine mechanisms: clues from familial hemiplegic migraine genotypes. Ann Neurol 55:276-280.

Muller M, Somjen GG (2000) Na(+) and K(+) concentrations, extra- and intracellular voltages, and the effect of TTX in hypoxic rat hippocampal slices. J Neurophysiol 83:735-745.

Nedergaard M, Astrup J (1986) Infarct rim: effect of hyperglycemia on direct current potential and [14C]2-deoxyglucose phosphorylation. J Cereb Blood Flow Metab 6:607-615.

Nedergaard M, Hansen AJ (1988) Spreading depression is not associated with neuronal injury in the normal brain. Brain Res 449:395-398.

Nedergaard M, Hansen AJ (1993) Characterization of cortical depolarizations evoked in focal cerebral ischemia. J Cereb Blood Flow Metab 13:568-574.

Nedergaard M, Cooper AJ, Goldman SA (1995) Gap junctions are required for the propagation of spreading depression. J Neurobiol 28:433-444.

Nedergaard M, Ransom B, Goldman SA (2003) New roles for astrocytes: redefining the functional architecture of the brain. Trends Neurosci 26:523-530.

Newman E (1995) Glial cells regulation of extracellular potassium. In: Neuroglia (Kettenman H, Ransom B, eds), pp 717-731. New York: Oxford University Press.

Newman EA (2003) New roles for astrocytes: regulation of synaptic transmission. Trends Neurosci 26:536-542.

Newman EA, Frambach DA, Odette LL (1984) Control of extracellular potassium levels by retinal glial cell K+ siphoning. Science 225:1174-1175.

Noh HS, Kim YS, Choi WS (2008) Neuroprotective effects of the ketogenic diet. Epilepsia 49 Suppl 8:120-123.

O'Collins VE, Macleod MR, Donnan GA, Horky LL, van der Worp BH, Howells DW (2006) 1,026 experimental treatments in acute stroke. Ann Neurol 59:467-477.

Obeidat AS, Andrew RD (1998) Spreading depression determines acute cellular damage in the hippocampal slice during oxygen/glucose deprivation. Eur J Neurosci 10:3451-3461.

Obeidat AS, Jarvis CR, Andrew RD (2000) Glutamate does not mediate acute neuronal damage after spreading depression induced by O2/glucose deprivation in the hippocampal slice. J Cereb Blood Flow Metab 20:412-422.

Obrenovitch TP (1999) High extracellular glutamate and neuronal death in neurological disorders. Cause, contribution or consequence? Ann N Y Acad Sci 890:273-286.

Ohta O, Osaka K, Siguma M, Yamamoto M, Shumizu K, Toda N (1983) Cerebral vasospasm following ruptured intracranial aneurysms, especially some contributions of potassium ion released from subarachnoid hematoma to delayed cerebral vasospasm. In: Vascular Neuroeffector Mechanisms (Bevan J, ed), pp 353-358. New York: Raven Press.

Okada YC, Lauritzen M, Nicholson C (1988) Magnetic field associated with spreading depression: a model for the detection of migraine. Brain Res 442:185-190.

Olesen J, Thomsen LL, Lassen LH, Olesen IJ (1995) The nitric oxide hypothesis of migraine and other vascular headaches. Cephalalgia 15:94-100.

Oliveira-Ferreira AI, Milakara D, Alam M, Jorks D, Major S, Hartings JA, Luckl J, Martus P, Graf R, Dohmen C, Bohner G, Woitzik J, Dreier JP (2010) Experimental and preliminary clinical evidence of an ischemic zone with prolonged negative DC shifts surrounded by a normally perfused tissue belt with persistent electrocorticographic depression. J Cereb Blood Flow Metab 30:1504-1519.

Ophoff RA, Terwindt GM, Vergouwe MN, van Eijk R, Oefner PJ, Hoffman SM, Lamerdin JE, Mohrenweiser HW, Bulman DE, Ferrari M, Haan J, Lindhout D, van Ommen GJ, Hofker MH, Ferrari MD, Frants RR (1996) Familial hemiplegic migraine and episodic ataxia type-2 are caused by mutations in the Ca2+ channel gene CACNL1A4. Cell 87:543-552.

Organization WH (2001) The World Health Report 2001. In. Geneva: WHO.

Orkand RK, Nicholls JG, Kuffler SW (1966) Effect of nerve impulses on the membrane potential of glial cells in the central nervous system of amphibia. J Neurophysiol 29:788-806.

Ortinski PI, Dong J, Mungenast A, Yue C, Takano H, Watson DJ, Haydon PG, Coulter DA (2010) Selective induction of astrocytic gliosis generates deficits in neuronal inhibition. Nat Neurosci 13:584-591.

Ouyang YB, Voloboueva LA, Xu LJ, Giffard RG (2007) Selective dysfunction of hippocampal CA1 astrocytes contributes to delayed neuronal damage after transient forebrain ischemia. J Neurosci 27:4253-4260.

Parpura V, Haydon PG (2000) Physiological astrocytic calcium levels stimulate glutamate release to modulate adjacent neurons. Proc Natl Acad Sci U S A 97:8629-8634.

Parpura V, Basarsky TA, Liu F, Jeftinija K, Jeftinija S, Haydon PG (1994) Glutamate-mediated astrocyte-neuron signalling. Nature 369:744-747.

Pekny M, Nilsson M (2005) Astrocyte activation and reactive gliosis. Glia 50:427-434.

Peschanski M, Cesaro P, Hantraye P (1995) Rationale for intrastriatal grafting of striatal neuroblasts in patients with Huntington's disease. Neuroscience 68:273-285.

Peters O, Schipke CG, Hashimoto Y, Kettenmann H (2003) Different mechanisms promote astrocyte Ca2+ waves and spreading depression in the mouse neocortex. J Neurosci 23:9888-9896.

Petzold GC, Haack S, von Bohlen Und Halbach O, Priller J, Lehmann TN, Heinemann U, Dirnagl U, Dreier JP (2008) Nitric oxide modulates spreading depolarization threshold in the human and rodent cortex. Stroke 39:1292-1299.

Piilgaard H, Lauritzen M (2009) Persistent increase in oxygen consumption and impaired neurovascular coupling after spreading depression in rat neocortex. J Cereb Blood Flow Metab 29:1517-1527.

Pluta RM, Afshar JK, Boock RJ, Oldfield EH (1998) Temporal changes in perivascular concentrations of oxyhemoglobin, deoxyhemoglobin, and methemoglobin after subarachnoid hemorrhage. J Neurosurg 88:557-561.

Rader RK, Lanthorn TH (1989) Experimental ischemia induces a persistent depolarization blocked by decreased calcium and NMDA antagonists. Neurosci Lett 99:125-130.

Rae C, Hare N, Bubb WA, McEwan SR, Broer A, McQuillan JA, Balcar VJ, Conigrave AD, Broer S (2003) Inhibition of glutamine transport depletes glutamate and GABA neurotransmitter pools: further evidence for metabolic compartmentation. J Neurochem 85:503-514.

Ramadan NM, Olesen J (2006) Classification of headache disorders. Semin Neurol 26:157-162.

Read SJ, Smith MI, Hunter AJ, Parsons AA (1997) The dynamics of nitric oxide release measured directly and in real time following repeated waves of cortical spreading depression in the anaesthetised cat. Neurosci Lett 232:127-130.

Richard MJ, Saleh TM, El Bahh B, Zidichouski JA (2010) A novel method for inducing focal ischemia in vitro. J Neurosci Methods 190:20-27.

Ridet JL, Malhotra SK, Privat A, Gage FH (1997) Reactive astrocytes: cellular and molecular cues to biological function. Trends Neurosci 20:570-577.

Roitbak AI, Bobrov AV (1975) Spreading depression resulting from cortical punctures. Acta Neurobiol Exp (Wars) 35:761-768.

Rosamond W, Flegal K, Friday G, Furie K, Go A, Greenlund K, Haase N, Ho M, Howard V, Kissela B, Kittner S, Lloyd-Jones D, McDermott M, Meigs J, Moy C, Nichol G, O'Donnell CJ, Roger V, Rumsfeld J, Sorlie P, Steinberger J, Thom T, Wasserthiel-Smoller S, Hong Y (2007) Heart disease and stroke statistics--2007 update: a report from the American Heart Association Statistics Committee and Stroke Statistics Subcommittee. Circulation 115:e69-171.

Rose EM, Koo JC, Antflick JE, Ahmed SM, Angers S, Hampson DR (2009) Glutamate transporter coupling to Na,K-ATPase. J Neurosci 29:8143-8155.

Rossi DJ, Oshima T, Attwell D (2000) Glutamate release in severe brain ischaemia is mainly by reversed uptake. Nature 403:316-321.

Rossi DJ, Brady JD, Mohr C (2007) Astrocyte metabolism and signaling during brain ischemia. Nat Neurosci 10:1377-1386.

Rothstein JD, Dykes-Hoberg M, Pardo CA, Bristol LA, Jin L, Kuncl RW, Kanai Y, Hediger MA, Wang Y, Schielke JP, Welty DF (1996) Knockout of

glutamate transporters reveals a major role for astroglial transport in excitotoxicity and clearance of glutamate. Neuron 16:675-686.

Rouach N, Byrd K, Petralia RS, Elias GM, Adesnik H, Tomita S, Karimzadegan S, Kealey C, Bredt DS, Nicoll RA (2005) TARP gamma-8 controls hippocampal AMPA receptor number, distribution and synaptic plasticity. Nat Neurosci 8:1525-1533.

Rudolphi KA, Keil M, Hinze HJ (1987) Effect of theophylline on ischemically induced hippocampal damage in Mongolian gerbils: a behavioral and histopathological study. J Cereb Blood Flow Metab 7:74-81.

Rudolphi KA, Schubert P, Parkinson FE, Fredholm BB (1992) Neuroprotective role of adenosine in cerebral ischaemia. Trends Pharmacol Sci 13:439-445.

Sadgrove MP, Galeffi F, Turner DA (2008) NADH imaging and glycogen stores during hypoglycemia in rat hippocampal slices. Society for Neuroscience.

Saito R, Graf R, Hubel K, Fujita T, Rosner G, Heiss WD (1997) Reduction of infarct volume by halothane: effect on cerebral blood flow or perifocal spreading depression-like depolarizations. J Cereb Blood Flow Metab 17:857-864.

Sakowitz OW, Kiening KL, Krajewski KL, Sarrafzadeh AS, Fabricius M, Strong AJ, Unterberg AW, Dreier JP (2009) Preliminary evidence that ketamine inhibits spreading depolarizations in acute human brain injury. Stroke 40:e519-522.

Sakowitz OW, Wolfrum S, Sarrafzadeh AS, Stover JF, Dreier JP, Dendorfer A, Benndorf G, Lanksch WR, Unterberg AW (2001) Relation of cerebral energy metabolism and extracellular nitrite and nitrate concentrations in patients after aneurysmal subarachnoid hemorrhage. J Cereb Blood Flow Metab 21:1067-1076.

Saransaari P, Oja SS (2004) Involvement of nitric oxide in adenosine release in the developing and adult mouse hippocampus. Neurochem Res 29:219-225.

Scheckenbach KE, Dreier JP, Dirnagl U, Lindauer U (2006) Impaired cerebrovascular reactivity after cortical spreading depression in rats: Restoration by nitric oxide or cGMP. Exp Neurol 202:449-455.

Scheller D, Heister, U, Kolb, J and Tegtmeier, F (1993) On the role of excitatory amino acids during the generation and propagation of spreading depression. In: Migraine: Basic Mechanisms and treatment (Lehmenkuhler A, Grotemeyer, KH and Tegtmeier, F, ed), pp 355-366. Munchen, Germany: Urban & Schwarzenberg.

Schousboe A (1981) Transport and metabolism of glutamate and GABA in neurons are glial cells. Int Rev Neurobiol 22:1-45.

Sehba FA, Friedrich V, Jr., Makonnen G, Bederson JB (2007) Acute cerebral vascular injury after subarachnoid hemorrhage and its prevention by administration of a nitric oxide donor. J Neurosurg 106:321-329.

Selman WR, Lust WD, Pundik S, Zhou Y, Ratcheson RA (2004) Compromised metabolic recovery following spontaneous spreading depression in the penumbra. Brain Res 999:167-174.

Shih AY, Johnson DA, Wong G, Kraft AD, Jiang L, Erb H, Johnson JA, Murphy TH (2003) Coordinate regulation of glutathione biosynthesis and release by Nrf2-expressing glia potently protects neurons from oxidative stress. J Neurosci 23:3394-3406.

Shin HK, Dunn AK, Jones PB, Boas DA, Moskowitz MA, Ayata C (2006) Vasoconstrictive neurovascular coupling during focal ischemic depolarizations. J Cereb Blood Flow Metab 26:1018-1030.

Shulman RG, Hyder F, Rothman DL (2001) Cerebral energetics and the glycogen shunt: neurochemical basis of functional imaging. Proc Natl Acad Sci U S A 98:6417-6422.

Shuttleworth CW (2010) Use of NAD(P)H and flavoprotein autofluorescence transients to probe neuron and astrocyte responses to synaptic activation. Neurochem Int 56:379-386.

Shuttleworth CW, Brennan AM, Connor JA (2003) NAD(P)H fluorescence imaging of postsynaptic neuronal activation in murine hippocampal slices. J Neurosci 23:3196-3208.

Sickmann HM, Walls AB, Schousboe A, Bouman SD, Waagepetersen HS (2009) Functional significance of brain glycogen in sustaining glutamatergic neurotransmission. J Neurochem 109 Suppl 1:80-86.

Siesjo BK, Bendek G, Koide T, Westerberg E, Wieloch T (1985) Influence of acidosis on lipid peroxidation in brain tissues in vitro. J Cereb Blood Flow Metab 5:253-258.

Silver IA, Deas J, Erecinska M (1997) Ion homeostasis in brain cells: differences in intracellular ion responses to energy limitation between cultured neurons and glial cells. Neuroscience 78:589-601.

Somjen GG (2001) Mechanisms of spreading depression and hypoxic spreading depression-like depolarization. Physiol Rev 81:1065-1096.

Stanfield PR, Nakajima S, Nakajima Y (2002) Constitutively active and G-protein coupled inward rectifier K+ channels: Kir2.0 and Kir3.0. Rev Physiol Biochem Pharmacol 145:47-179.

Steiner TJ (2005) Lifting The Burden: the global campaign to reduce the burden of headache worldwide. J Headache Pain 6:373-377.

Stornelli SA, French JD (1964) Subarachnoid Hemorrhage--Factors in Prognosis and Management. J Neurosurg 21:769-780.

Strong AJ, Venables GS, Gibson G (1983) The cortical ischaemic penumbra associated with occlusion of the middle cerebral artery in the cat: 1. Topography of changes in blood flow, potassium ion activity, and EEG. J Cereb Blood Flow Metab 3:86-96.

Strong AJ, Harland SP, Meldrum BS, Whittington DJ (1996) The use of in vivo fluorescence image sequences to indicate the occurrence and propagation of transient focal depolarizations in cerebral ischemia. J Cereb Blood Flow Metab 16:367-377.

Strong AJ, Fabricius M, Boutelle MG, Hibbins SJ, Hopwood SE, Jones R, Parkin MC, Lauritzen M (2002) Spreading and synchronous depressions of cortical activity in acutely injured human brain. Stroke 33:2738-2743.

Strong AJ, Smith SE, Whittington DJ, Meldrum BS, Parsons AA, Krupinski J, Hunter AJ, Patel S, Robertson C (2000) Factors influencing the frequency of fluorescence transients as markers of peri-infarct depolarizations in focal cerebral ischemia. Stroke 31:214-222.

Strong AJ, Anderson PJ, Watts HR, Virley DJ, Lloyd A, Irving EA, Nagafuji T, Ninomiya M, Nakamura H, Dunn AK, Graf R (2007) Peri-infarct depolarizations lead to loss of perfusion in ischaemic gyrencephalic cerebral cortex. Brain 130:995-1008.

Suh SW, Shin BS, Ma H, Van Hoecke M, Brennan AM, Yenari MA, Swanson RA (2008) Glucose and NADPH oxidase drive neuronal superoxide formation in stroke. Ann Neurol 64:654-663.

Sukhotinksky I, Dilekoz E, Eikermann-Haerter K, Qin T, Moskowitz MA, Ayata C (2008) Chronic daily cortical spreading depression suppress spreading depression susceptibility. In: Society for Neuroscience 2008. Washington D.C.

Swanson RA (1992) Astrocyte glutamate uptake during chemical hypoxia in vitro. Neurosci Lett 147:143-146.

Swanson RA, Choi DW (1993) Glial glycogen stores affect neuronal survival during glucose deprivation in vitro. J Cereb Blood Flow Metab 13:162-169.

Swanson RA, Sagar SM, Sharp FR (1989a) Regional brain glycogen stores and metabolism during complete global ischaemia. Neurol Res 11:24-28.

Swanson RA, Chen J, Graham SH (1994) Glucose can fuel glutamate uptake in ischemic brain. J Cereb Blood Flow Metab 14:1-6.

Swanson RA, Farrell K, Stein BA (1997) Astrocyte energetics, function, and death under conditions of incomplete ischemia: a mechanism of glial death in the penumbra. Glia 21:142-153.

Swanson RA, Ying W, Kauppinen TM (2004) Astrocyte influences on ischemic neuronal death. Curr Mol Med 4:193-205.

Swanson RA, Yu AC, Sharp FR, Chan PH (1989b) Regulation of glycogen content in primary astrocyte culture: effects of glucose analogues, phenobarbital, and methionine sulfoximine. J Neurochem 52:1359-1365.

Swanson RA, Shiraishi K, Morton MT, Sharp FR (1990) Methionine sulfoximine reduces cortical infarct size in rats after middle cerebral artery occlusion. Stroke 21:322-327.

Szatkowski M, Barbour B, Attwell D (1990) Non-vesicular release of glutamate from glial cells by reversed electrogenic glutamate uptake. Nature 348:443-446.

Szerb JC (1991) Glutamate release and spreading depression in the fascia dentata in response to microdialysis with high K+: role of glia. Brain Res 542:259-265.

Tajti J, Pardutz A, Vamos E, Tuka B, Kuris A, Bohar Z, Fejes A, Toldi J, Vecsei L (2010) Migraine is a neuronal disease. J Neural Transm.

Takano T, Tian GF, Peng W, Lou N, Lovatt D, Hansen AJ, Kasischke KA, Nedergaard M (2007) Cortical spreading depression causes and coincides with tissue hypoxia. Nat Neurosci 10:754-762.

Tanaka E, Yamamoto S, Kudo Y, Mihara S, Higashi H (1997) Mechanisms underlying the rapid depolarization produced by deprivation of oxygen and glucose in rat hippocampal CA1 neurons in vitro. J Neurophysiol 78:891-902.

Theis M, Sohl G, Eiberger J, Willecke K (2005) Emerging complexities in identity and function of glial connexins. Trends Neurosci 28:188-195.

Theis M, Jauch R, Zhuo L, Speidel D, Wallraff A, Doring B, Frisch C, Sohl G, Teubner B, Euwens C, Huston J, Steinhauser C, Messing A, Heinemann U, Willecke K (2003) Accelerated hippocampal spreading depression and enhanced locomotory activity in mice with astrocyte-directed inactivation of connexin43. J Neurosci 23:766-776.

Thomas JE, Rosenwasser RH, Armonda RA, Harrop J, Mitchell W, Galaria I (1999) Safety of intrathecal sodium nitroprusside for the treatment and prevention of refractory cerebral vasospasm and ischemia in humans. Stroke 30:1409-1416.

Tian GF, Baker AJ (2002) Protective effect of high glucose against ischemia-induced synaptic transmission damage in rat hippocampal slices. J Neurophysiol 88:236-248.

van den Maagdenberg AM, Pietrobon D, Pizzorusso T, Kaja S, Broos LA, Cesetti T, van de Ven RC, Tottene A, van der Kaa J, Plomp JJ, Frants RR, Ferrari MD (2004) A Cacna1a knockin migraine mouse model with increased susceptibility to cortical spreading depression. Neuron 41:701-710.

van Gijn J, Rinkel GJ (2001) Subarachnoid haemorrhage: diagnosis, causes and management. Brain 124:249-278.

Van Harreveld A (1959) Compounds in brain extracts causing spreading depression of cerebral cortical activity and contraction of crustacean muscle. J Neurochem 3:300-315.

Vanmolkot KR, Kors EE, Turk U, Turkdogan D, Keyser A, Broos LA, Kia SK, van den Heuvel JJ, Black DF, Haan J, Frants RR, Barone V, Ferrari MD, Casari G, Koenderink JB, van den Maagdenberg AM (2006) Two de novo mutations in the Na,K-ATPase gene ATP1A2 associated with pure familial hemiplegic migraine. Eur J Hum Genet 14:555-560.

Viggiano E, Ferrara D, Izzo G, Viggiano A, Minucci S, Monda M, De Luca B (2008) Cortical spreading depression induces the expression of iNOS, HIF-1alpha, and LDH-A. Neuroscience 153:182-188.

Vyskocil F, Kritz N, Bures J (1972) Potassium-selective microelectrodes used for measuring the extracellular brain potassium during spreading depression and anoxic depolarization in rats. Brain Res 39:255-259.

Walls AB, Sickmann HM, Brown A, Bouman SD, Ransom B, Schousboe A, Waagepetersen HS (2008) Characterization of 1,4-dideoxy-1,4-imino-d-arabinitol (DAB) as an inhibitor of brain glycogen shunt activity. J Neurochem 105:1462-1470.

Walz W (2000) Role of astrocytes in the clearance of excess extracellular potassium. Neurochem Int 36:291-300.

Walz W, Hertz L (1982) Ouabain-sensitive and ouabain-resistant net uptake of potassium into astrocytes and neurons in primary cultures. J Neurochem 39:70-77.

Walz W, Hertz L (1984) Intense furosemide-sensitive potassium accumulation in astrocytes in the presence of pathologically high extracellular potassium levels. J Cereb Blood Flow Metab 4:301-304.

Walz W, Hinks EC (1985) Carrier-mediated KCl accumulation accompanied by water movements is involved in the control of physiological K+ levels by astrocytes. Brain Res 343:44-51.

Walz W, Wuttke WA (1999) Independent mechanisms of potassium clearance by astrocytes in gliotic tissue. J Neurosci Res 56:595-603.

Wang M, Obrenovitch TP, Urenjak J (2003) Effects of the nitric oxide donor, DEA/NO on cortical spreading depression. Neuropharmacology 44:949-957.

Waniewski RA, Martin DL (1998) Preferential utilization of acetate by astrocytes is attributable to transport. J Neurosci 18:5225-5233.

Watts AG, Sanchez-Watts G, Emanuel JR, Levenson R (1991) Cell-specific expression of mRNAs encoding Na+,K(+)-ATPase alpha- and beta-subunit isoforms within the rat central nervous system. Proc Natl Acad Sci U S A 88:7425-7429.

Wender R, Brown AM, Fern R, Swanson RA, Farrell K, Ransom BR (2000) Astrocytic glycogen influences axon function and survival during glucose deprivation in central white matter. J Neurosci 20:6804-6810.

Wiggins AK, Shen PJ, Gundlach AL (2003) Delayed, but prolonged increases in astrocytic clusterin (ApoJ) mRNA expression following acute cortical spreading depression in the rat: evidence for a role of clusterin in ischemic tolerance. Brain Res Mol Brain Res 114:20-30.

Wilhelmsson U, Bushong EA, Price DL, Smarr BL, Phung V, Terada M, Ellisman MH, Pekny M (2006) Redefining the concept of reactive astrocytes as cells that remain within their unique domains upon reaction to injury. Proc Natl Acad Sci U S A 103:17513-17518.

Zhang ZG, Zhang L, Jiang Q, Zhang R, Davies K, Powers C, Bruggen N, Chopp M (2000) VEGF enhances angiogenesis and promotes blood-brain barrier leakage in the ischemic brain. J Clin Invest 106:829-838.

Zhao Y, Rempe DA (2010) Targeting astrocytes for stroke therapy. Neurotherapeutics 7:439-451.

Zhou N, Gordon GR, Feighan D, Macvicar BA (2010) Transient Swelling, Acidification, and Mitochondrial Depolarization Occurs in Neurons but not Astrocytes during Spreading Depression. Cereb Cortex.